Ludwig-Maximilians-Universität München

Analyzing and 3D Modelling of Electrical Resistivity Tomography (ERT) data for Archaeological Prospection

Dissertation

zur Erlangung des Doktorgrades

an der Fakultät für Geowissenschaften

der Ludwig-Maximilians-Universität München

Vorgelegt von

Mandana Parsi

München, den 08.03.2022

Erstgutachter/in: Prof. Dr. Jörg Fassbinder

Zweitgutachter/in: Prof. Dr. Christian Grosse

Tag der mündlichen Prüfung: 20.07.2022

Contents

List of Figures

Summary

Archaeological geophysical prospection is a non-destructive method to detect underground structures and features, which is considered as a fundamental requirement for every archaeological research project and is significant for monument protection. In this research, I applied the Electrical Resistivity Tomography (ERT) method over different archaeological sites in several countries to investigate and analyze the results from each of the subsurface structures in detail, which are made of different materials, such as stone, baked-brick and mudbrick. There are some studies regarding the detection of stone and baked-brick structures with the ERT method; however, there was no solid research on the detection of mudbrick features in the surrounding mud with this method, as it was suggested that resistivity values of these anomalies and the periphery soil, which are made of highly similar materials, are the same and not distinguishable, which I tried to rectify in my dissertation. Additionally, I aimed to discover and optimize the limitation of this method for the investigation of different materials in different countries and areas.

The first attempt of detecting a mudbrick feature using the ERT method in this research is in Ur (Chapter 3), where I could detect a probable Neo-Babylonian mudbrick house. Among the inversion methods, smoothness-constrained was proven to be the most suitable choice for this case study. With the information obtained from this discovery, I was able to unveil an Achaemenid mudbrick complex in Eastern Georgia (Chapter 2). In this chapter, I mathematically and practically proved the possibility of the detection of mudbrick features with the ERT method with a focus on the densification of the soil. The excavation of the Southern part of this complex assured the viability of this method for the detection of mudbrick features thus verifying the ERT method as an ideal tool for the investigation of the mudbrick features and structures.

I showed that the ERT method is capable of detecting canals, qanats and harbours. In Ur, I was successful in the detection of a harbour, whose location inside the city was not yet known, however, the ERT method together with the magnetic method proved the presence of it in that area. In Uruk (Chapter 7), by applying different inversion methods, not only was I able to detect the exact shape and depth of the canal, but also I could uncover gradual sedimentation layers in it, which happened over time. In Iraqi Kurdistan (Chapter 5), though I mainly focused on the detection of qanats, I additionally detected two layers of structures, while the magnetometer results clearly only show a single-phase settlement layer from the Neo-Assyrian period. With the ERT results, I revealed another settlement layer beneath it, which later was proven to be from Chalcolithic early Bronze age period.

In Yeha (Chapter 6), I modelled a multi-layered structure made of stone from the Aksumite and Pre-Aksumite period and verified the extension of the ancient city to the south, which was used by the local administration as a proof to call the area a cultural heritage site. In Peiting (Chapter 4), I compared the results of the ground penetrating radar and ERT. Furthermore, I showed the outcome of the different inversion algorithms over the obtained data and the possibility of detecting the position of the removed walls and structures by applying the correct inversion method on the ERT data. This finding can finally lead us to the most accurate archaeological interpretation of the structure, which may not even be obtained by excavation.

1 Introduction

Applied geophysics is the process of taking and analyzing measurements of the Earth's physical characteristics in order to identify subsurface conditions, generally with commercial or scientific goals and it covers a wide range of study areas, from different experiments to research on the fundamental knowledge about the Earth to study and investigate shallow features. Archaeological geophysics is part of the applied geophysics and provides us with a large range of suitable tools of non-destructive methods to trace and map archaeological structures and monuments beneath the ground. Each one of these methods is focused on a specific physical property, based on these properties and the differences between them we can map and model the underground anomalies and features. Modern archaeological and scientific excavation projects start with prior geophysical prospection to minimize destruction and optimize the project. Namely, for UNESCO World heritage sites and Global Consortium for the Preservation of Cultural Heritage, but also for the national archaeological service and the protection of monuments and sites, geophysical methods, as non-destructive methods, play an indispensable role.

For large-scale investigations, archaeological geophysical methods, such as magnetometer surveys, Ground Penetrating Radar (GPR) prospections and Earth resistance surveys, are suitable tools to get information on hidden archaeological features (Scollar et al., 1990; Papadopoulos et al., 2010; Trinks et al., 2013). Each of these methods has its own advantages and disadvantages. The large-scale archaeological prospection methods are considered as faster methods but most of them are focused on the shallower substructure and are not able to detect the deeper features.

For a large scale and extensive prospection, magnetometer survey is one of the most useful methods to get detailed information of archaeological sites beneath the ground. On the other hand, it is a potential field method and, therefore, it is not suitable to locate archaeological features at deeper parts of the ground. It hardly provides us with

exact information on the depth of features or of the stratigraphy and the maximum depth that is visible to interpret by this method is 3 m (Fassbinder & Gorka, 2009).

Occasionally, specifically when we have a change in environmental and geochemical conditions, such as temporary variations of the underground water table, combined with a dissolution of magnetic minerals in sediments and soils, the magnetic contrast of archaeological objects and the adjacent soil fades away and impedes the detection of archaeological structures (Fassbinder, 2015). Magnetic prospecting is a passive method, which measures an existing magnetic field. All other methods (except the gravity method) are active, which generate a physical signal and measure the response to it.

Complementary to magnetometer survey, the GPR method can be used to locate and trace archaeological features as well as its stratigraphic layers, providing precise information about the depth of the underground structures (Conyers, 2013). GPR yields optimum results in presence of stone structures and fundaments, or in presence of clear material contrast between different structures, features and layers. The penetration depth and resolution of the features are restricted by the frequency of the antennas (usually between 200 and 900 MHz) and the conductivity of the material. Although radar prospecting with a low-frequency antenna could be used for deeper features, the method is limited by the abundance of clay minerals in the soil, as due to the high electrical conductivity of the soil, the GPR signal is attenuated and consequently, it prevents us from conducting a successful GPR measurement. Moreover, the result can be affected by moisture and temporary changes in the weather conditions and it needs some specific surface conditions (such as an even surface). Therefore, with the GPR method details inside large or deep features of archaeological sites, like burial mounds, as well as mudbrick features, ditches, irrigation channels and geo-archaeological conditions, remain hidden and unseen beneath the ground.

With the large-scale earth resistance survey method, one can detect the anomalies based on their difference in resistivity values. Although this method is one of the fastest geoelectric methods to apply, the maximum detectable depth with this method,

considering different electrode configurations, is up to ca. 1 m and it hardly provides any depth information about each one of the anomalies.

In between seismic methods, the refraction seismic method has relatively less success compared to the reflection method in archaeological prospection (Carson, 1962; Aitken, 1974). Refraction techniques perform best when the subsurface is undisturbed and have mapping velocities that increase with depth. When there are velocity inversions indicative of human cultural disruption, or 3D artifacts such as burial sites or stone foundations, the approach becomes less effective and interpretation becomes rather complex (Wynn, 1986). On contrary, seismic reflection is useful to detect buried shipwrecks under the water and to detect the cavities, such as the detection of the cavities in Chephren's pyramid at Giza in Egypt (McGhee et al., 1968; Edgerton, 1972; Dolphin, 1981). Moreover, for the detection of underwater objects (e.g. shipwrecks) the Sonar method, an application of acoustic waves, is a very practical method as well.

Due to specific characteristics of the archaeological sites, single or integrated geophysical methods are preferably used (Burkart et al., 2008; Piro et al., 2011).

1.1. Electrical Resistivity Tomography (ERT)

The first application of ERT was in August-September 1912 by Conrad Schlumberger, in which he injected DC current into the ground at Val-Richer Abbey (France) and generated a hand-drawn blueprint from the result (Schlumberger, 1912; Hulin et al., 2018).

ERT is a promising geophysical method to image the deep underground structures in detail and high resolution. It gives us information about the depth of each feature and the material that each one of them had been made of. Moreover, this method can map the vertical stratigraphic layers of the subsurface, which can partially be of archaeological origin.

In recent years, the application of ERT became more and more important to bridge the gap between magnetometer survey and radar prospection methods. Sophisticated computer programs to trigger the multichannel electrodes, combined with inversion and 3-dimensional analysis software, allow tracing the apparent electric resistivity in great detail, even in deeper sections of the ground (Loke et al., 2013).

One of the goals of using the ERT method in archaeological prospection is to uncover the details, which are not accessible by other methods. ERT is an advanced method to determine the underground resistivity distribution (Schmidt, 2013). Clayey materials, which are carrying electrical currents, are good targets to apply ERT on. Therefore, it is the best method for unveiling structures such as the internal layout of kurgans (burial mounds), mudbrick walls and paleo-channels.

First, by conducting large-scale geophysical methods (such as magnetometer surveys) and analyzing their results, suitable targets for ERT prospections are indicated. Alternatively, it is possible to use the traces of old archaeological excavations to find the aforementioned targets.

For ERT measurements, electrodes are arranged along a line with fixed site-specific spacing, which is chosen regarding the depth and size of the features. If the feature is located in greater depth, the spacing will be larger and if the feature is shallow or the size of the target is small, then smaller spacing is used. For archaeological purposes, the best spacing is between 0.5 and 2 m. Moreover, the number of the used electrodes varies according to the size and the depth of the feature; the minimum number for our application is 40 electrodes, but also more electrodes are used, as some of the structures are larger, deeper and/or the size of the target is small and to reach to a good resolution we need to use more electrodes, due to the required small electrode spacing.

In this method, the DC current penetrates into the ground between two electrodes and the voltage is measured by two other electrodes. The penetration depth depends on the type of the electrode array as well. The 2D ERT method has been mostly used to reconstruct some of the subsurface structures, such as groundwater tables, paleo-channels and qanats. The 3D ERT method, however, is more accurate compared to 2D ERT

and hence more suitable to image the buried structures and archaeological features and it indicates with more accuracy promising areas for further investigation (Tsokas et al., 2012; Tsourlos et al., 2014). There are several methods to acquire a 3D map based on ERT results. One of the most used methods is to measure dense parallel 2D survey lines and collate the data afterwards. For this purpose, at least five parallel survey lines are needed; nevertheless, for a detailed image of the subsurface, more lines are necessary.

Figure 1.1 illustrates the different electrode configurations such as dipole-dipole, Wenner and Schlumberger, which are useful for ERT prospection over archaeological sites. Each of these configurations has its advantages and disadvantages. Some factors, such as target structure, sensitivity to background noise, signal to noise ratio and the penetration depth play a role in choosing the suitable configuration (Aber and MeshinChi Asl, 2010). The Wenner and dipole-dipole array have a higher signal to noise ratio, in comparison to other arrays, therefore are the most popular configuration in archaeological geophysics. The dipole-dipole configuration is more sensitive to lateral variation and is suitable to detect features such as walls and cavities. The Wenner array covers a greater depth and is more sensitive to vertical variation (Griffiths and Barker, 1993). Often the best coverage for archaeological purposes is achieved by the combination of Wenner and dipole-dipole. Figure 1.2 shows the schematic view of a survey line in a 4-point configuration.

In case of the existence of topography (e.g. for burial mounds) within the ERT measuring area, one can directly apply the topography in our modelling of 2D and 3D measurements with RES2DINV and RES3DINV software. To have a better visualization of underground features, I used Voxler, which is a graphical program.

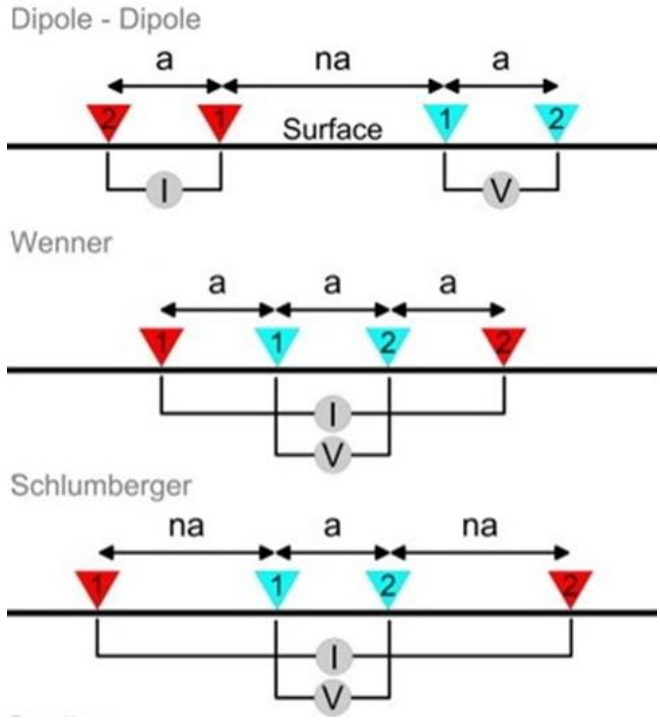

Figure 1.1. The three most important electrode configurations used for ERT in archaeological prospection. Red triangles specify the current emitters and blue triangles show the potential receivers. The distance between electrodes is shown as (n)a (Modified after Carey et al., 2017).

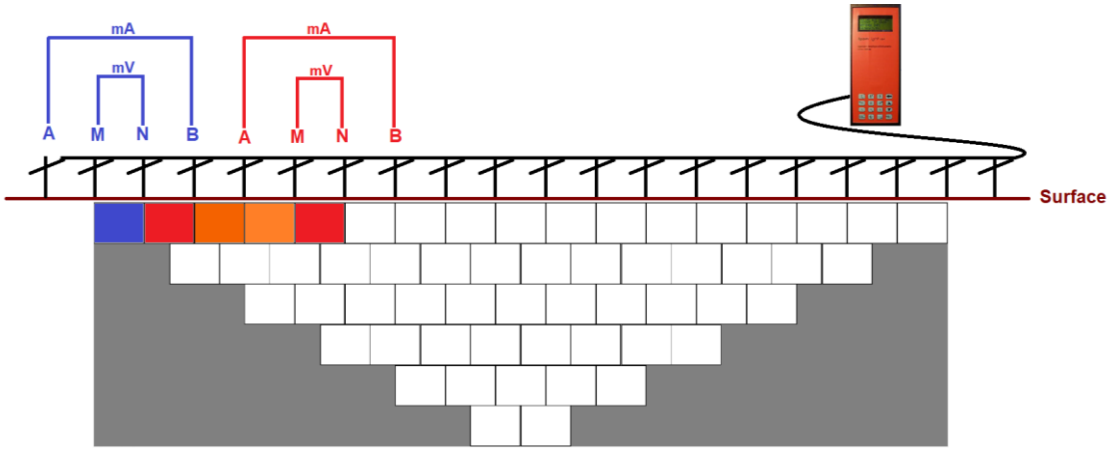

Figure 1.2. Schematic view of the survey line in 4-point configuration.

1.2. Motivations for this Dissertation

Magnetic and GPR methods are the most used methods in the archaeological prospection field. The number of the researches using the ERT method is considerably less compared to these two methods. Especially on certain important archaeological sites, including world heritage sites, the application of the ERT method is underrepresented.

Therefore, in this dissertation, I focused on the ERT method by applying it on different archaeological sites, in different countries over the anomalies made of different materials, to have large and adequate data sets to analyze and compare the results. For this purpose, I have been to several countries to collect data from different areas (each related to a different era) and to provide an adequate amount of data to initiate further researches and projects.

In the detection of archaeological buildings, there were some researches about the detection of stone walls and baked-brick walls with the ERT method, nevertheless, there was no solid research about the detection of mudbrick features with this method. In some reviews, it was even highly discouraged to use the ERT method for the detection of mudbricks, as they argued that it is physically impossible to detect these features based on their resistivity values, due to the mudbrick walls and the periphery soil being made of highly similar material. Despite these negativities, I decided to put part of the focus of this dissertation on the detection of the mudbricks, of which the successful results are shown in detail in chapters 2 and 3.

Another goal of this dissertation was to emphasize the importance of deciding on the correct inversion method for the detection of each one of these structures/features made of different material. Moreover, I aimed to show that in some case studies applying several inversion methods can help to have a better understanding of the subsurface structures and consequently can lead one to a better interpretation of the initial shape of these features and the changes that have happened since then.

The locations I had projects in, for the purpose of this dissertation, were:

a. Gumbati, Saaklemo (Georgia): In this study, which was a joint research project between the institute of Near Eastern Archaeology and the Geophysics institute of LMU (funded by DFG), one of the main goals was to study the influence of the Achaemenid Empire on the monumental architecture in Georgia. With the ERT method, I mainly focused on the detection of mudbrick features with both mathematical and practical approaches. The result of the research in Saaklemo, which is presented in chapter 2 of this dissertation, is one of the most important breakthroughs in the recent researches for the ERT method and it is under review in the Journal of Applied Geophysics.
b. Ur (Iraq): The UNESCO world Heritage site as well as one of the most well-known cities of Mesopotamia served as location for a case study, in which I experimented with the ERT measurement over different archaeological features and for the first time with ERT method with some considerations, I could detect a mudbrick underground structure. The result of this study forms chapter 3 of this dissertation and is published in a peer-reviewed conference journal under the title "Revealing the Hidden Structure of the Ancient City Ur (Iraq) with Electrical Resistivity Tomography" (Parsi et al., 2019). This work was a joint research project between LMU, Stony Brook University and University of Pennsylvania (USA).
c. Germany (with the focus on Bayern, e.g. Peiting, Geibenstetten, Steinfeld, Gochsheim): These researches were all in collaboration with Bayerisches Landesamt für Denkmalpflege (BLfD). One of the most important results with the ERT method was derived from a case study in Peiting over a Roman villa, which was published as a peer-reviewed conference paper under the title "Highlighting the potential of 3D ERT by comparing its results with GPR and the excavation map of a Roman building" (Parsi et al., 2021). In this paper, I compared the results of the GPR and ERT methods and showed the effect of different inversion methods on my results and interpretations. These results are presented in chapter 4 of this dissertation.
d. Kurdistan (Iraq): This study, as a collaboration between the faculty of the History and the Arts and the Geophysics institute of LMU, illustrates the detection of

qanats and two layered of structures with the ERT method in this area. This work is published in a peer-reviewed journal under the title “Remote sensing and sediment analysis in the Bora plain, 2019: The 2019 Electrical Resistivity Tomography (ERT) survey” (Parsi and Fassbinder, 2020). This work is funded by Gerda-Henkel Stiftung.

e. Yeha (Ethiopia): For this case study on the UNESCO world heritage site, I mainly focused on analyzing the ERT results in order to detect the extension of the ancient city of the Aksumite and the Pre-Aksumite period. The results of the study of Yeha formed chapter 6 of this dissertation and it is in the process of publication as an article under the title “Looking beneath Yeha (Ethiopia): A 3D model of a multi-layered substructure with Electrical Resistivity Tomography (ERT)” in Forschungen am nördlichen Horn von Afrika - Research at the northern Horn of Afrika, Archäologische Forschungen in Afrika 2 (from DAI - the estimated year of publication: 2023).) This work was in collaboration with the German Archaeological institute (DAI).

f. Uruk (Iraq): In Uruk, which is the world’s oldest megacity, with the ERT method I focused on the detection of an ancient canal. A part of the result is presented in chapter 7 and is published in a peer-reviewed conference paper under the title “Venice in the desert: Archaeological geophysics on the world’s oldest metropolis Uruk-Warka, the city of King Gilgamesh (Iraq)” (Fassbinder et al., 2019). This work was done in collaboration with the German Archaeological institute (DAI).

g. Shorzha (Armenia): This study was allocated to the detection of the burial mounds with magnetometer survey. I participated to help in the measurement and to find further potential targets for ERT prospection. This work is published in a peer-reviewed journal under the title “The Ecstasy of Gold: Magnetometer Prospection for the Ushkiani Project in Armenia” (Hahn et al., 2021) and it was the collaboration between LMU and Martin-Luther University of Halle.

The data of the below expeditions has been analyzed but not constructed in a form of a paper yet:

h. Kakheti (Georgia): Measurement over the Ananauri IV kurgan to estimate the depth and the size of the burial chamber under this kurgan with ERT method, in collaboration with German Archaeological institute (DAI) and the National museum of Georgia.
i. Karacamirli (Azerbaijan): To study the presence of Achaemenid Empire in this area and to detect the peripheral large gardens of the palaces several ERT measurements have been done in this area. This work was a joint project between the institute of Near Eastern Archaeology and the Geophysics institute of LMU and was funded by DFG.
j. Pasargadae (Iran): To verify the water supplies for the gardens of the palaces belonging to the Achaemenid Empire an ERT prospection was conducted. This work was a joint project between LMU and Lyon University and it was funded by DFG and the Agence National de la Recherche (ANR).

The data sets obtained during the excursions and campaigns provide a large database rich in variety regarding the differences in building material and surrounding soil or geological features. It helps to compare differences in anomalies due to the different resistivity values or contrasts and provides a better understanding of the inversion methods and their application with respect to the different materials.

2 Illuminating Traces of an Achaemenid's Monumental Complex in the Southern Caucasus by Electrical Resistivity Tomography (ERT)

(The following chapter (Parsi et al., in review) is submitted to the Journal of Applied Geophysics and it is under review.)

Abstract

The Achaemenid Empire controlled the Western Asian landmass between ca. 550−300 BC. By some estimates, its subject peoples made up almost 44 % of the world population. In recent years, studies have moved from a consideration of its core region, located in the province of Fars, Iran, to the investigation of imperial rule in the dependent regions. Since Achaemenid centers were often built of mudbrick and thus not easy to recognize by traditional archaeological methods, geophysical methods play an important role in this research. This paper reports the results of an innovative Electrical Resistivity Tomography (ERT) study undertaken at one such center, Saaklemo, in the Kakheti Province, Republic of Georgia and shows the wide impact of the geophysical methods in the detection of the archaeological sites.

In three areas of this ancient site between 2020 and 2021, following archaeological survey and magnetometer prospection, several three-dimensional (3D) ERT measurements, composed of dense parallel two-dimensional (2D) tomographies with dipole-dipole configuration, were carried out. To reconstruct the resistivity distribution of the subsurface, we used the smoothness-constrained inversion method, especially as the substructure was made of mudbrick and thus resistivity values of these anomalies

were close to the background anomaly. Therefore, with smoothness-constrained inversion, we could detect the slight resistivity differences, which were partly due to density differences, and hence this method was capable of detecting these anomalies.

In area1, for the first time with ERT method, we were successful in discovering an extensive mudbrick (partly burnt) substructure at a depth of 40 cm to 1 m. After analyzing the magnetic data and a 3D model of this substructure based on the ERT data, a large excavation was conducted and a mudbrick substructure with six in-situ bell-shaped column bases was discovered, which was destroyed by conflagration. The size and the architectural techniques used for this building prove that this excavated structure was an administrative building and served for representative purposes. Further presumed mudbrick structures were detected in the other two areas with the ERT method, but they have not yet been excavated.

2.1. Introduction

2.1.1. Historical and Geological Background

The Achaemenid Empire (ca. 550 - 330 BC) was an ancient Persian Empire founded by Cyrus the Great. It extended from the Balkans to the Indus Valley and may, according to some estimations, in its heyday have ruled over 44 % of the world's population. Historical information on the empire's development is mostly derived from Greek authors, who perceived their eastern neighbors as a threat and celebrated its destruction by Alexander the Great in 330 BC. These reports were, therefore, single-sided and far from being objective or independent.

For a long time, archaeologists concentrated on the splendor of imperial residences at Pasargadae and Persepolis in their treatment of the Achaemenid period. However, their architecture and the iconography of its imagery constituted a departure from tradition, most notably in the use of elaborate stone masonry for the construction of monumental buildings. These techniques, ultimately derived from Ionian masonry, did not take root in the provinces so the Achaemenid Empire was infamously labelled as an "elusive" Empire (Sancisi-Weerdenburg, 1990). Only through careful fieldwork and

under the deployment of diverse archaeological and geophysical methods, the extent of Achaemenid impact in its dependent territories can be gauged more accurately.

The excavation of a mudbrick (also known as mudstone and adobe) palace in Karacamirli (Rep. of Azerbaijan) built to the exact dimensions of Persepolis' buildings constituted a new departure for Achaemenid studies in the Southern Caucasus (Knauß et al., 2013). In the wake of this discovery, extensive studies were also initiated in neighboring Georgia, combining archaeological and geophysical methods.

The country Georgia is dominated by the Caucasus Mountains. Georgia's climate is diverse, since it is located in the subtropical zone, at the boundary of the Aral-Caspian arid region and continental highland Caucasian. Eastern Georgia, which is the research area for this project, has a dry subtropical climate (Gamkrelidze, 1997b). Historical evidence shows that the Alazani area had no water shortage and was not susceptible to drought (Melikadze et al., 2014). The artesian springs (aquifers) and water canals provided a perfect condition for famed Achaemenid palaces and their associated gardens. Similar geographical conditions can be observed in Pasargadae and Karacamirli (Knauß, 2000; Fassbinder et al., 2021).

Already in 1994, the excavation of the remains of a monumental mudbrick building in eastern Georgia, on the 5th century BC site of Gumbati, had produced some evidence for an Achaemenid presence in Georgia (Knauß, 2006). In 2018, archaeological investigations were restarted at Gumbati and later extended to the newly discovered site of Saaklemo, 2 km to the north, in the framework of a German - French joint project entitled "Achaemenid residences and their paradises" that was funded for three years by the Deutsche Forschungsgemeinschaft (DFG) and the Agence National de la Recherche (ANR).

This project aims to focus on the cultural, historical and political developments of Georgia and the effect of the Achaemenid Empire on the monumental architecture in this region in the first millennium BC. Technically, it centered on the interoperation of archaeological survey work, geophysical prospection and subsequent excavation, to validate results and assist in the development of geophysical methodologies.

2.1.2. Geophysical Background

Archaeological geophysics provides excellent non-destructive tools to acquire information related to archaeological monuments and features beneath the ground and use this information to map and model these structures. Moreover, by these methods, we obtain information about the environmental conditions in ancient times. In modern archaeology, geophysical methods are widely used, usually preceding excavation, to precisely target further fieldwork and to minimize the destruction through invasive excavation and enhance the results of the project (Scollar et al., 1990; Papadopoulos et al., 2010; Sarris, 2012; Fassbinder, 2017; Parsi et al., 2019).

Among a wide range of geophysical methods, which have been developed for this purpose, magnetic prospection, Ground Penetrating Radar (GPR) and resistivity methods are the most frequently used. These three methods are designed for a large-scale prospection to provide information about the underground substructures (Trinks et al., 2013; Parsi et al., 2021). In addition, we use Electrical Resistivity Tomography (ERT) in 2D and/or 3D to obtain detailed information such as accurate location, depth and the material of each one of the features. Moreover, in complex cases, distinguishing the archaeological and geological layers is more likely with ERT.

ERT is a prominent method for archaeological geophysics to receive a detailed image of the subsurface electrical resistivity distribution, which helps us to detect the substructure features (Chambers et al., 2006; Günther et al., 2006; Papadopoulos et al., 2006; Tsokas et al., 2012; Schmidt, 2013; Thiesson et al., 2014). For this purpose, the application of ERT became more and more important to bridge the gap between magnetometry and GPR prospection methods in particular as the wet and clayey soil attenuates the signal and makes the radar prospecting utterly impossible.

Different geological parameters and soil conditions such as porosity, hydraulic permeability, soil moisture content and soil temperature are the factors that affect the underground resistivity. The final image is created with reconstruction algorithms based on the solution of the forward and inverse resistivity problem (Loke and Barker, 1996a; Loke and Barker, 1996b).

The combination and comparison of the results of different methods provide a better understanding of the subsurface and enhances the certainty of the final interpretation as the archaeological features have more variety in shape in comparison to the conventional geological structures and each feature can be located in different depths (Scollar et al., 1986; Sarris, 2012).

In the framework of the Paradise project (2017 - 2021), the German team conducted extensive magnetometer prospections and ERT measurements in Iran (Pasargadae), Azerbaijan (Karacamirli) and Georgia (Gumbati and Saaklemo) in search of traces of the Achaemenid Empire in these regions. In this paper, we describe the results of the Saaklemo geophysical survey with a focus on the ERT method and the effect of specific physical properties on the ERT measurement results.

2.2. Materials and Methods

2.2.1. Magnetic Data Acquisition and Processing

Since 1956, magnetic prospection is one of the most used methods in large-scale archaeological geophysics prospection to find features and ancient activities (Aitken, 1958; Scollar et al., 1990; Fassbinder, 2017). For the purpose of this project, we used Scintrex Smartmag SM4G-Special and the Geometrics G-858 caesium magnetometers in the so-called duo-sensor configuration to attain a maximum speed of prospection and the highest possible sensitivity (Becker, 1999; Fassbinder, 2015). To gain a high spatial resolution combined with the highest possible sensitivity of a total field caesium magnetometer we used a sampling rate of 0.1 s and a traverse interval of 50 cm. By resampling and interpolation, we generated a grayscale image with 25 x 25 cm resolution. We fixed the probes on a nonmagnetic frame and carried the probes around 30 cm above the ground in a 40 x 40 m grid.

In the short time for the measurement of one grid (ca. 25-30 min), we assume the diurnal variation to be linear and the solar activity was negligible. Therefore, we reduced the diurnal variation to the mean value of all data of each grid and if necessary, we apply the deslope function to remove a linear trend within a grid of data (Fassbinder and Gorka, 2009). This allows us not only to measure the magnetic anomalies in

the full range but also gives us information on the deeper parts of the soil. It is worth mentioning that magnetic prospection allows visibility to a maximum investigation depth of around 3 m without information on the depth of features (Fassbinder, 2015).

2.2.2. ERT Data Acquisition and Processing

The ERT instrument used for this project is a 4-point light 10 W, by Erich Lippmann (Lippmann Geophysikalische Messgeräte, Germany), which allows an electrode spacing from 25 cm up to 5 m. The two electrode configurations, w hich were used for this research, are dipole-dipole and Wenner arrays. While the dipole-dipole array is sensitive to lateral variation, the Wenner array is more sensitive to vertical variation (Griffiths and Barker, 1993). The main inversion method for this project is the smoothness-constrained inversion method and the forward resistivity calculations were based on the finite-element method (Loke and Dahlin, 2002; Constable et al., 1987).

For this work, after choosing target areas based on the results of the magnetometer prospection, we employed this method and produced multiple 3D modelling images based on the ERT data. To reduce the time and power required for the 3D inversion by 50 %, as a replacement for the conventional 3D inversion, we used the combination of the dense parallel 2D tomographic data and processed the data by 3D schemes (Papadopoulos et al., 2006).

2.3. Results and Discussion of the Data

In Georgia, large-scale magnetic prospection has been conducted in Gumbati, Murakebis, Didi Gora, and Saaklemo. For ERT prospection, however, we focused on Gumbati and Saaklemo, as in Gumbati (1978) several column base fragments were discovered on the surface in a rescue excavation (Wesenberg, 1971; Furtwängler et al., 1995; Furtwängler et al., 1996; Thiesson et al., 2019; Fassbinder et al., 2021) and in Saaklemo one column base with Achaemenid carvings was found by a local farmer. Figure 2.1 shows the prospection areas in the Alazani valley, in east Georgia, with the picture of two of these column bases with respect to their discovery locations.

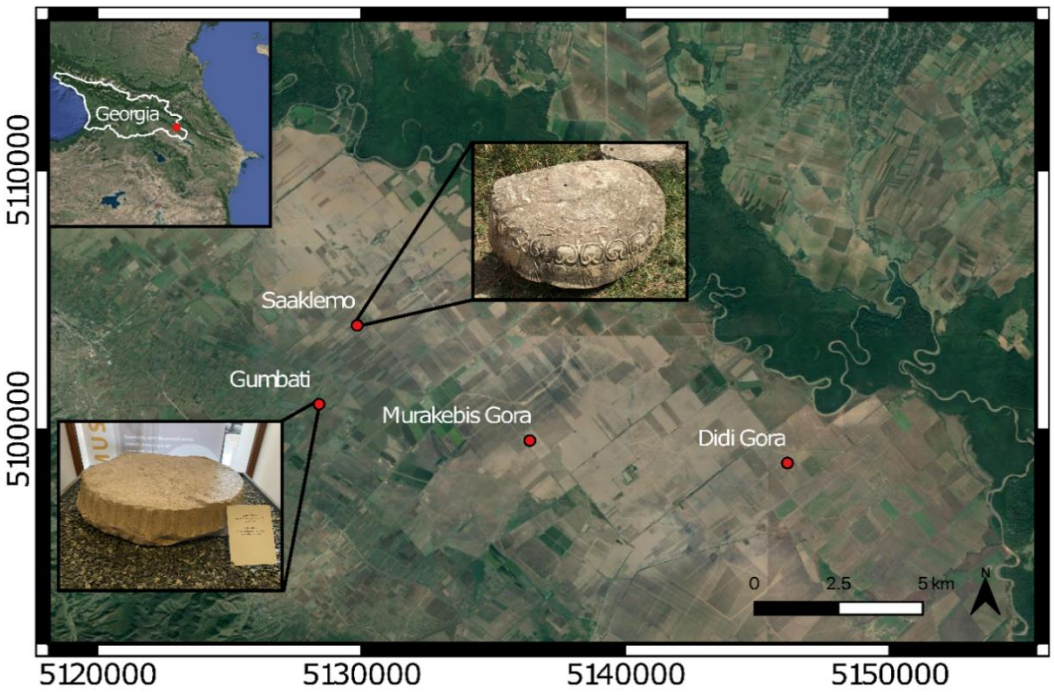

Figure 2.1. Prospection areas in east Georgia. Areal map of the Alazani valley, in east Georgia, with pictures of two of the Achaemenid column bases.

Saaklemo is located at ca. 2000 m north of Gumbati. This field became our area of interest after the discovery of a bell-shaped column base by a local farmer and the pottery, which were found during an archaeological survey and were dated to the Achaemenid period. After this discovery, a large-scale magnetometer prospection was carried out (ca. 360 x 400 m). Figure 2.2 illustrates part of the magnetogram of this area.

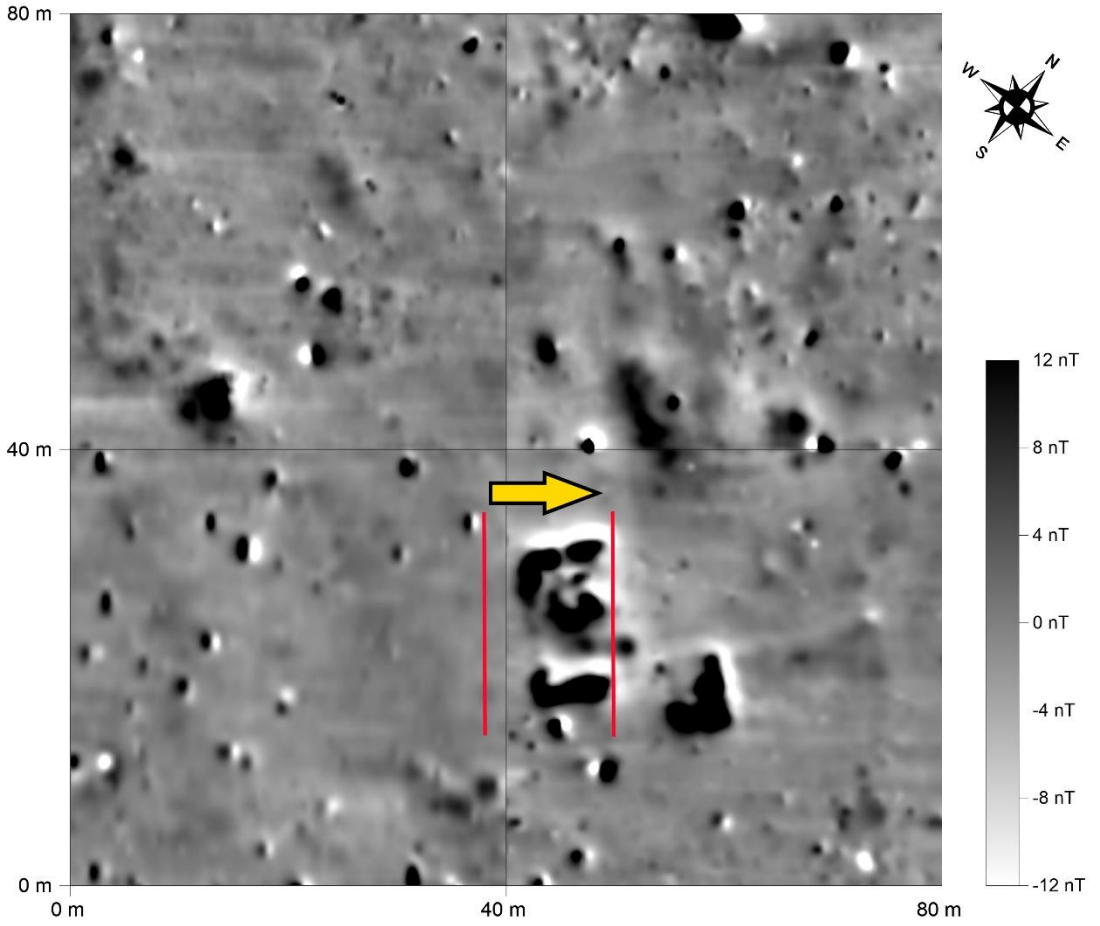

Figure 2.2. Part of the magnetogram of Saaklemo. The cutout part of the magnetogram of area 1 for the ERT prospection. The left red line is the first profile and the right red line is the last profile. The yellow arrow shows the direction of the extension of the parallel survey lines.

According to the magnetometer results, we suggested the probability of the existence of an underground substructure, made of mudbrick. Detailed architecture, which is normally easy to detect by magnetometer prospecting, is almost invisible in the magnetogram. The only parts clearly detectable are the burned parts, which create a high magnetic contrast, while the magnetic susceptibility contrast between the mudbricks and the adjacent soil was understandably almost negligible or extremely low (Fassbinder et al., 2021).

To obtain more insight and detailed information on this structure, we measured some parts of this area with ERT. In contradiction to opposing suggestions that detecting mudbrick walls in the surrounding mud with ERT is not possible, as they are made of

highly similar material, we had mathematical and practical approaches to prove the possibility of detecting them with resistivity prospection.

The relationship between resistivity and the porosity of the rocks was published by Archie (1942) as follows:

$$R_t = a\, R_w\, \varphi^{-m} S_w^{-n} \qquad \textit{Equation 1}$$

In which R_t is the resistivity of the rock with fluid inside, R_w is the resistivity of the fluid itself, a is the tortuosity factor, φ is the porosity and S_w is the fluid saturation. Moreover, m is a constant related to the cementation of the rock (usually in the range 1-3) and n is a parameter that is determined experimentally, which is usually a number close to 2 (Archie, 1942).

This equation shows that with the decrease of porosity the resistivity has the tendency to increase.

From the definition of the porosity, we know

$$\varphi = 1 - \frac{V_p}{V_b} \qquad \textit{Equation 2}$$

In which, V_p is the volume of the particle (compressed volume) and V_b is the volume of the bulk, with the same mass. Therefore, by substituting the volumes using the definition of density, we will consequently reach this equation:

$$\varphi = 1 - \frac{\rho_b}{\rho_p} \qquad \textit{Equation 3}$$

In which the ρ_b is the bulk density and ρ_p is the particle density ($0 < \rho_b \leq \rho_p$). According to this equation, the porosity and bulk density have an inverse relation.

Finally, by comparing equations 1 and 3 we deduce that resistivity and density have a direct relationship, with increasing density, the resistivity increases. This relationship shows us the possibility of the detection of the mudbrick walls in the surrounding mud. Even if they are made of highly similar materials, as with the soil compaction the bulk density increases, the resistivity increases.

Based on the magnetic results of this area, the position of the first area for the ERT measurement has been chosen. We measured several parallel 2D survey lines to form a 3D model based on the ERT data, as the three-dimensional inversion gives a better and more reliable result in comparison to the two-dimensional ones. Twenty-four northwest-southeast parallel survey lines with 40 electrodes for each line with 0.5 m electrode spacing, 0.5 m Y-spacing have been measured in a total of seven days. The dipole-dipole configuration was used and resulted in obtaining a set of 776 data points per survey line (a total of 18,624 data points for the 3D data set), which were inverted with smoothness-constrained inversion method to reconstruct the resistivity distribution of the subsurface. In Figure 2.2, on the top of the magnetogram, we illustrated the position of the first ERT prospection area.

Figure 2.3 shows a few selective results of the 3D modelling in horizontal (X – Y planes) depth slices, vertical (X - Z planes) panels and the interpretation based on these results. In the horizontal view, each section represents a specific depth level and in the vertical view, each panel represents a different survey line from the side view. In Saaklemo, the aerial and environmental situation was suitable for ERT measurement and we had proper contact resistance for electrodes and rather high soil moisture percentage, which is an important soil factor for this method. These conditions lead us to acquire a high-quality ERT result. For this data set the RMS error rate was quite low (maximum of 5.52% for five iterations). After considering the ploughing line, which is around 20 cm in this area, we can deduce that this structure is located from around 40 cm below the surface and is visible up until around 1 m; however, we can observe some anthropogenic anomalies up to 2 m.

The resistivity values of these anomalies are in a wide range (between 12 - 80 Ωm) and the anomalies are in an almost perpendicular orientation with respect to each

other. As in some parts the resistivity values of this structure are close to the periphery soil (the background resistivity value is between 6 - 10 Ωm), we can deduce that the substructure is made of almost the same material but more compact (with more density) compared to the periphery soil. However, the resistivity values are varying dramatically in different parts, e.g. at some parts the resistivity values are around 20 Ωm and at other parts around 80 Ωm. Analyzing these anomalies reveals that these changes in the resistivity values do not have a specific pattern of distribution and are happening rather in a random sequence. This can bring up the argument that the building was not built with baked-bricks but rather was the result of a burn by secondary fire. Therefore, based on this information we suggest that the structure is made of mudbricks but with different degrees of burning in different parts, which has happened due to a conflagration. In spite of this, at the deeper parts of this substructure, we observe the pattern of a slightly different structure, which is presumably the floor of this building, which is based on the resistivity values less affected by the fire.

Based on this 3D model, we sketched a possible interpretation of this substructure (Figure 2.3). This 3D model indicates that the buried structure is a part of a bigger complex and has a high probability of continuation in all directions with regard to this measurement area.

In addition, we measured the moisture, temperature and conductivity of the topsoil over two consecutive days in this area to monitor the stability of these soil characteristics on different days. In these two days, the maximum change in the soil moisture was 6.29 %, the maximum change in the soil temperature was 0.1 °C and the maximum conductivity change of the topsoil was 0.85 dS/m. As small changes will not affect the results, we can be assured by the consistency of the data.

Based on our geophysical results, an ongoing excavation has been started in 2019 (with total coverage of 275 m^2 up to this point). Figure 2.4 shows a drone photo of the excavated area and the reconstruction of this structure over it. The excavation trench confirmed the geophysical interpretation and revealed the remains of a partly burnt mudbrick monumental building with six bell-shaped column bases in situ. One of these column bases shows the relief decoration and for the others, the limestone was

heavily burnt and the decoration probably flaked off. A small deep trench (ca. 2.90 m) has been made at the southwest of the excavation, which showed that the lower limit of the Achaemenid period building in this part was reached at around 80 cm.

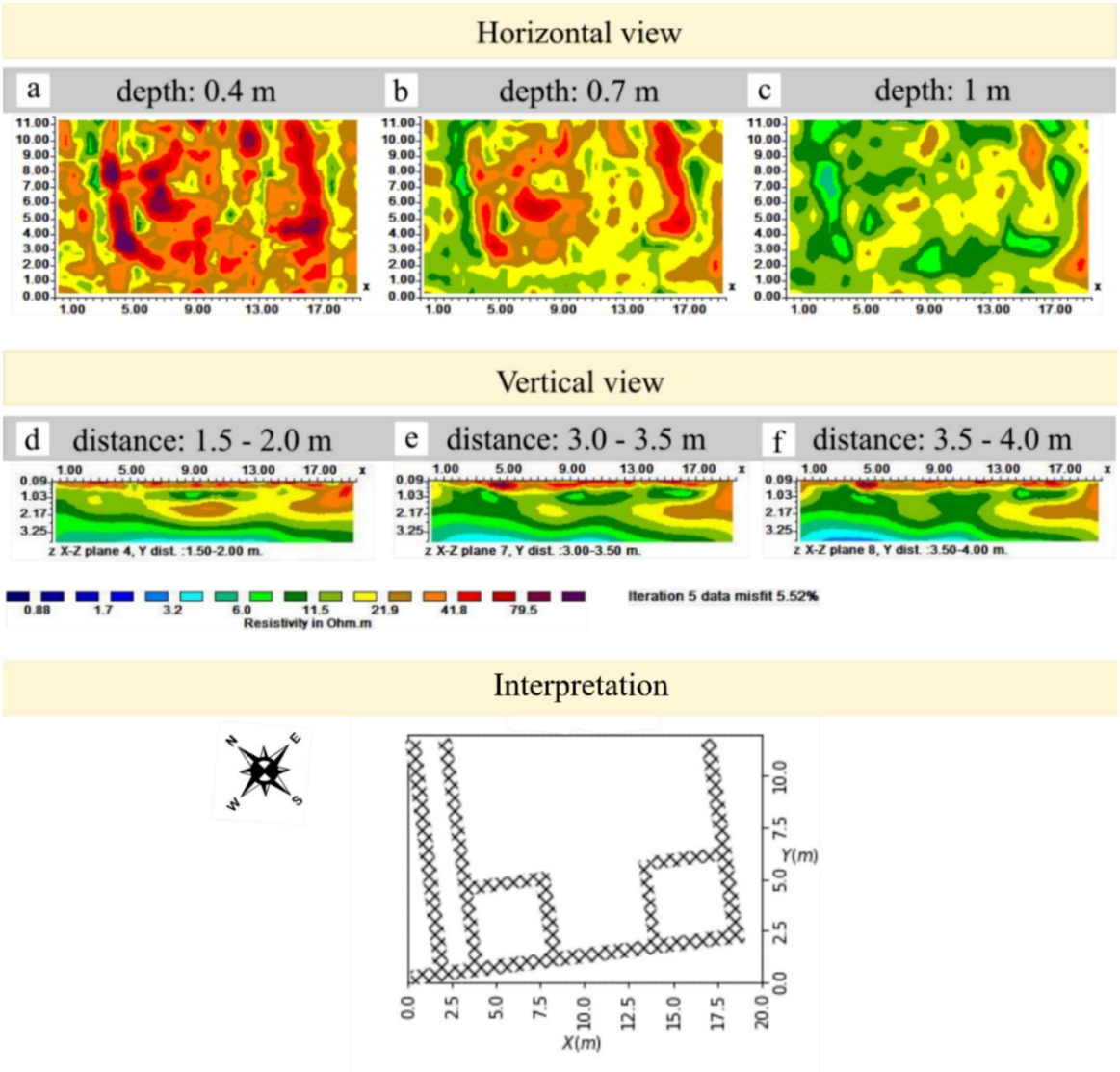

Figure 2.3. ERT results and the interpretation based on ERT data of area 1. Horizontal and vertical views of the 3D model based on the ERT data of this monumental building. In the horizontal view, each rectangle shows an X - Y plane of the map in different depths and the vertical view shows slices in the X – Z planes. This Figure represents the mudbrick walls in different depths (some parts partly burned). The panels chosen for this figure show the clearest view of this monumental substructure.

We overlapped the interpretation based on ERT over the reconstruction of this structure (Figure 2.5). Some of the walls (shown in blue) were detected by resistivity results but were not discovered in the excavation. There can be two reasons for the detection of these anomalies as walls in ERT results and not in the excavation. It can be either because the anomalies initially belonged to the ceiling and after the fire, it collapsed and formed in a way that in resistivity anomalies we see them as walls, or the walls were not detected in the excavation.

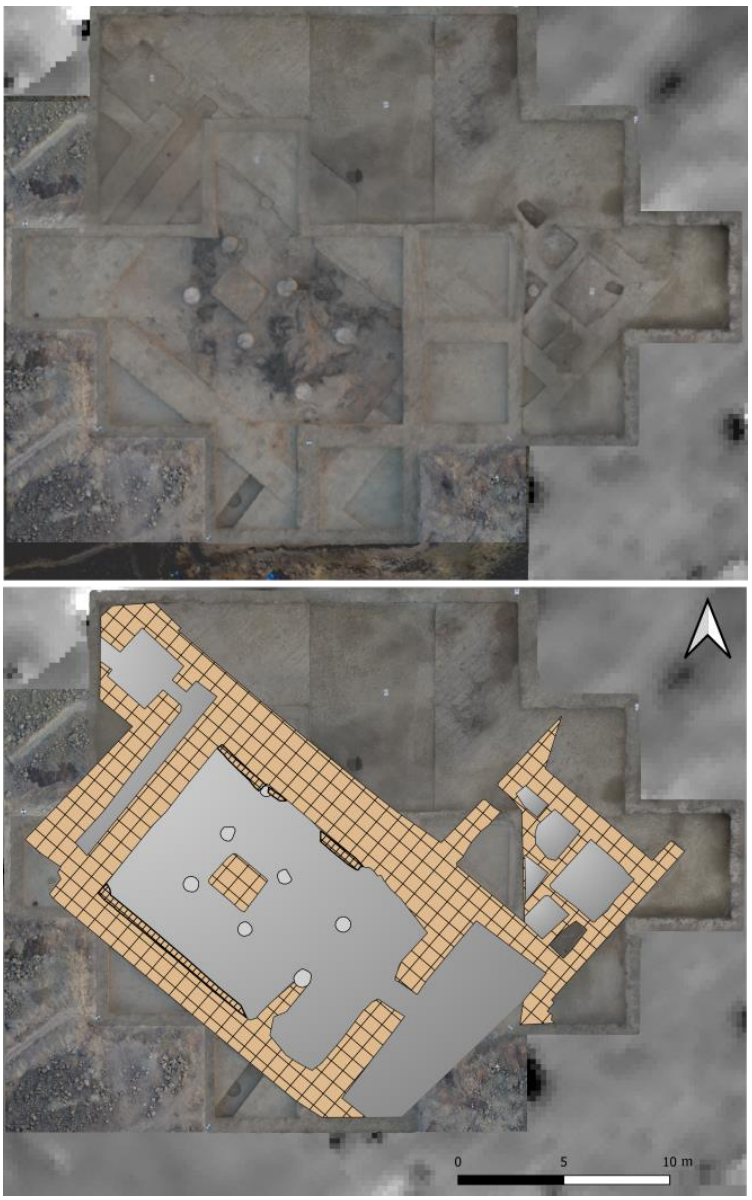

Figure 2.4. A drone picture of the excavation in Saaklemo and the reconstruction of the excavated structure. (© LMU, Saaklemo Project)

Figure 2.5. Interpretation based on ERT results overlapped on the reconstruction of the structure. The red lines illustrate the walls detected in both ERT results and the excavation and the blue lines show the walls observed by ERT results and not in the excavation.

As a final point for this data set, we overlaid a depth layer of the ERT result over the magnetogram and finally the reconstruction of the substructure over it (Figure 2.6). By comparing the reconstruction model with the geophysical results, in the magnetogram, we just observe highly burned parts of the substructure, whereas, in the ERT result, by applying different types of data processing and comparing the results we are able to detect the entire structure.

The excavation of a deep profile beneath the monumental building's mudbrick wall gives us more information about the subsoil and subsurface geological strata. We split the whole profile into 10 x 10 cm grids for the in-situ kappa measurements and measured magnetic susceptibility in the center of each grid using the portable SM30 kappa meter (Figure 2.7). The result indicates that mudbricks were initially made of clay

from the same underlying and neighboring material, and hence cannot provide significant contrast for magnetic prospection (Fassbinder et al., 2021).

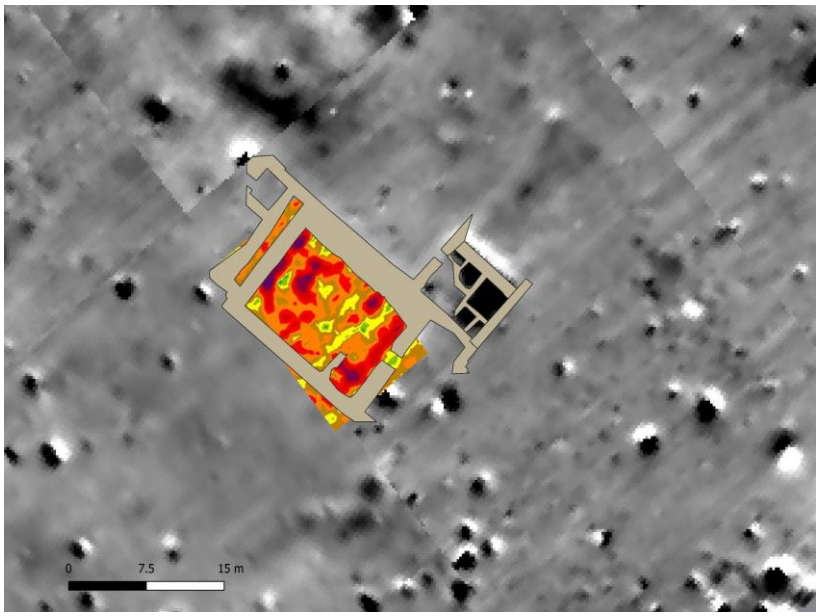

Figure 2.6. Reconstruction of the excavated walls overlaid on the ERT 0.5 m depth layer and the magnetogram (with the dynamics of ±8 nT).

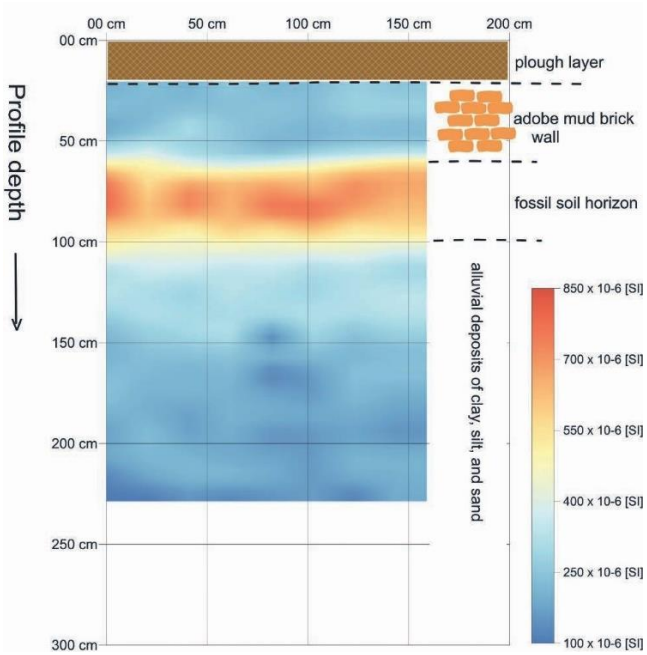

Figure 2.7. Magnetic susceptibility measurement. Magnetic susceptibility measurement of a deep trench of area 1 (Fassbinder et al., 2021).

To continue the investigation, we chose a second area for further ERT prospection, based on the magnetic interpretation of the presence of a partly burnt structure. Figure 2.8 shows part of the magnetogram indicating the position of the area 2 for the ERT prospection. To form a 3D model based on ERT data, we measured Thirty one south-east-northwest parallel survey lines with 0.5 m X-spacing and 1 m Y-spacing with dipole-dipole configuration in a total of four days. These measurements resulted in obtaining a set of 776 data points per survey line (24,056 data points for the 3D data set) and all were inverted by smoothness-constrained inversion method.

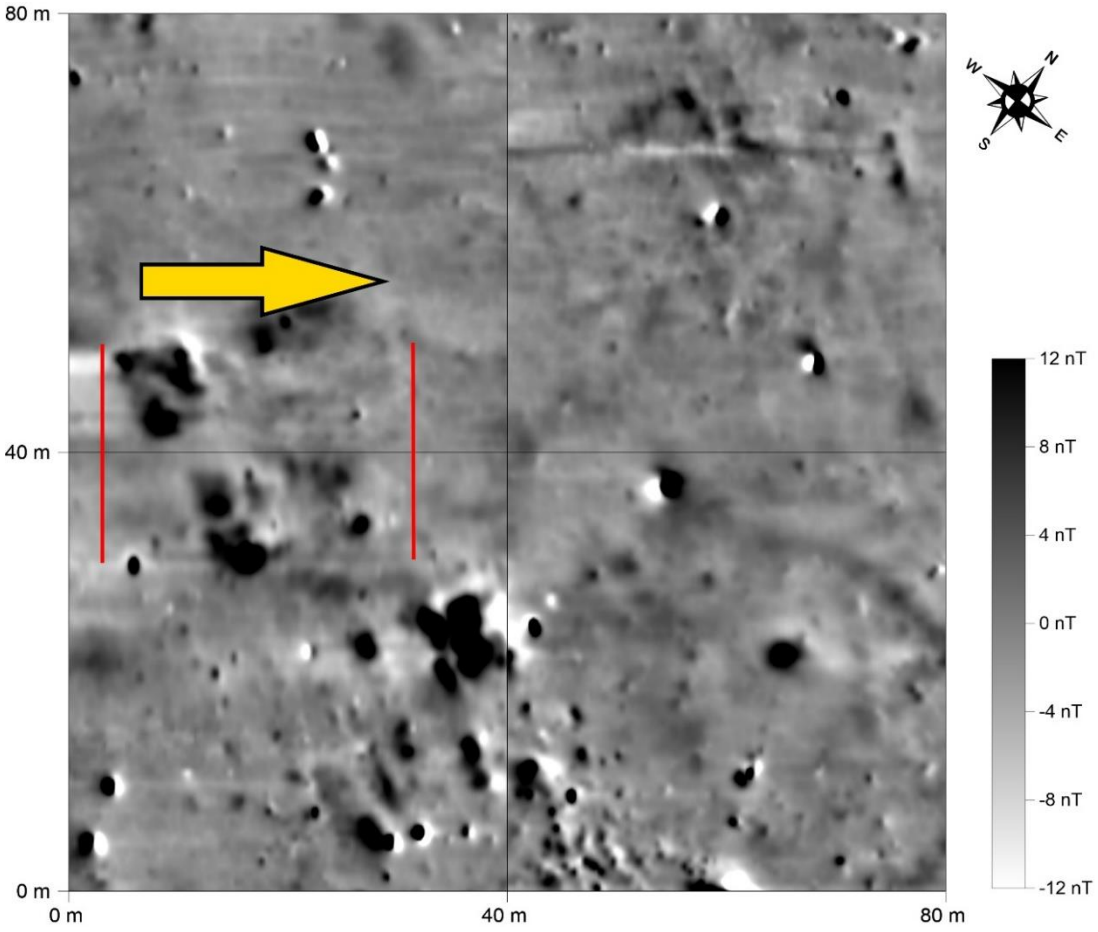

Figure 2.8. The cutout part of the magnetogram of area 2 for the ERT prospection. The left red line is the position of the first profile and the right red line is the position of the last profile.

Figure 2.9 illustrates several depth layers of the 3D model based on the ERT data in area 2. From around 0.3 m until 1.4 m depth, we observe the presence of a substructure

with resistivity values in the range between 10 to 30 Ωm. In comparison to the area 1, this part is mainly made of pure mudbrick and was less exposed to fire. For this reason, we mostly see values of resistivity anomalies close to background resistivity values, except the very shallow part with higher resistivity, which might have been burnt. Presumably, based on the values and the orientation of the anomalies in the magnetogram, this shallow substructure is the same feature visible in the magnetogram. Moreover, all of the walls in this area are mostly in the same orientation with respect to each other except for the very shallow part.

The shallower substructure (from 0.3 m), which is the anomaly observed in the magnetogram, is slightly in a different direction and has a moderately higher resistivity. This brings us to two hypotheses: Either it belongs to a different building, which can explain the different orientation and the resistivity, or all walls belong to one building but the shallower part is partly burnt, which explains the changes in the resistivity. However, in the shallower part, not all walls are in the same orientation, but the values are almost the same. Overall, considering all information, we suggest that we have one substructure, with two different orientations, partly burned. To draw an interpretation, we compared several types of processed data and drew our interpretation of this substructure (Figure 2.9).

In the first 12 parallel survey lines starting from around 0.9 m depth, we can observe a square-shaped anomaly up to until 2.2 m depth. Based on the resistivity values we suggest the presence of a highly resistive anomaly, which is assumed as a layer of stones. We cannot exclude the possibility of the geological origin of this anomaly; however, based on the shape and the orientation of this anomaly, which is aligned with the substructure, we highly suggest that it has an anthropogenic origin.

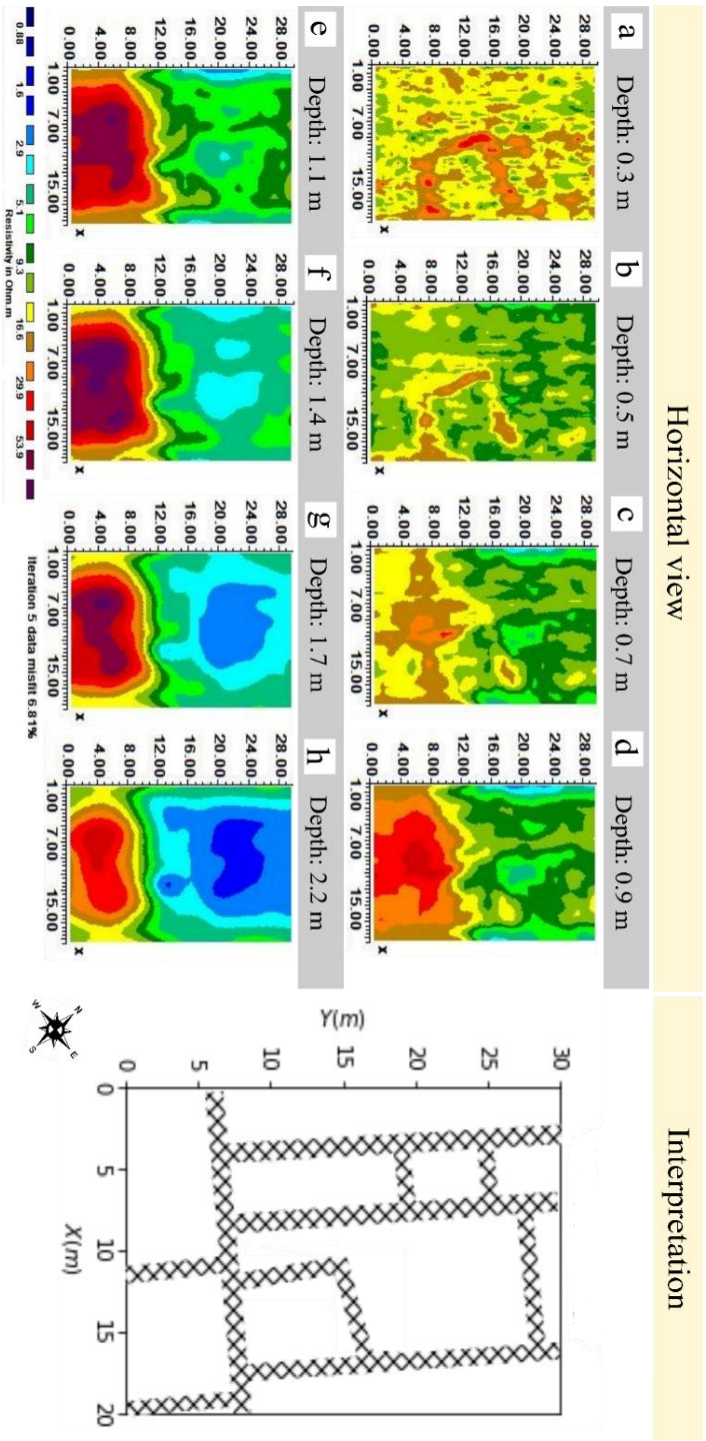

Figure 2.9. ERT results and the interpretation based on ERT data of area 2. Depth layers of the 3D model based on the ERT data for area 2. This Figure represents the mudbrick walls in different depths (at some positions partly burnt).

The third area chosen for the ERT prospection is shown over the magnetogram in Figure 2.10. Based on the magnetic results, we observed the possibility of the presence of a few parallel walls in the rectangular structure.

In this area, for the ERT survey, we measured twenty-four northwest-southeast parallel survey lines with 0.5 m electrode spacing and 1 m Y- spacing with dipole-dipole configuration, which resulted in obtaining 776 data points per line (18,624 data points for the 3D data set) and were inverted with smoothness-constrained inversion method.

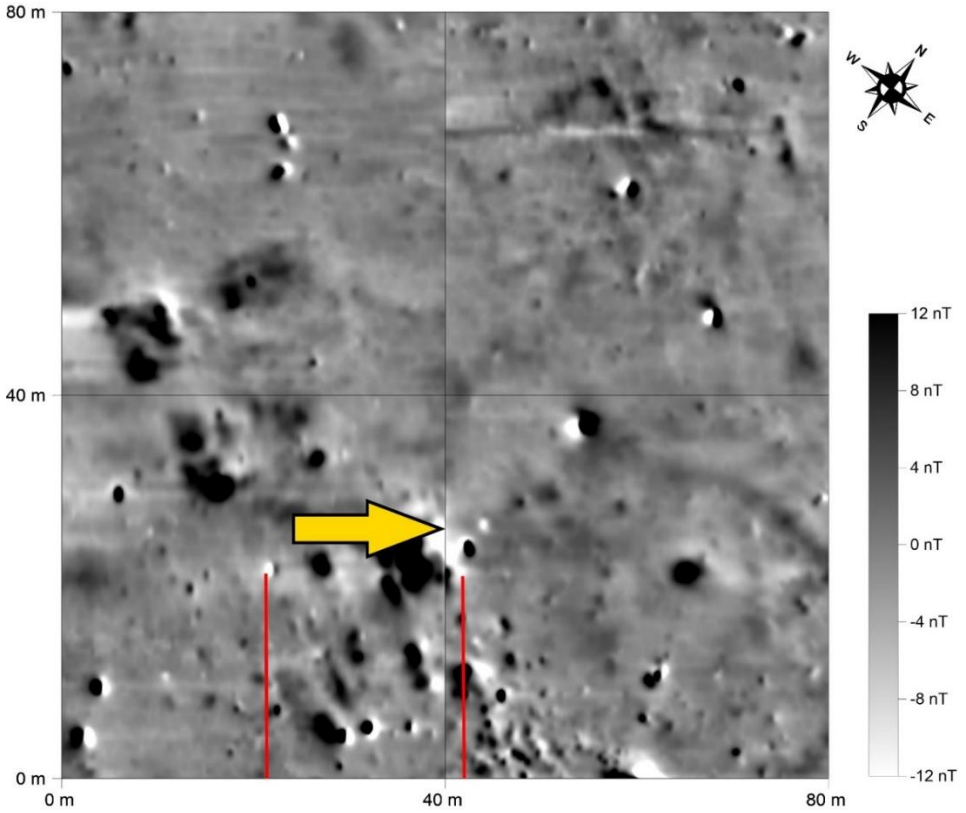

Figure 2.10. The cutout part of the magnetogram of area 3 for the ERT prospection. The left red line is the first profile and the right red line is the last profile. The yellow arrow shows the direction of the extension of the parallel survey lines.

Figure 2.11 illustrates a few depth layers of this data set, in which we can detect the traces of some substructures. Based on the resistivity values (between 10 - 20 Ωm) we can deduce the possibility of the presence of mudbrick walls at the depth between around 0.5 m and 1.3 m with no resistivity anomaly variation that we could interpret

as a burnt part with a secondary fire. Therefore, drawing the interpretation for this data set was more challenging compared to the other ones, as the resistivity value of the substructure is quite close to the resistivity value of the periphery soil. Moreover, we could observe some noisy data, which could either be due to the presence of some disturbances in the measuring area, which was not visible on the surface, or there were some measuring mistakes.

For this purpose, to obtain as much results as possible, we applied both robust and smoothness-constrained inversion methods and for the robust inversion, we used different cut-off factors and finally we compared all results. The final interpretation for this substructure is illustrated in Figure 2.11.

As a final part, we overlaid all three results over the magnetogram to get an overview of the results and their orientation with respect to each other (Figure 2.12). For each area, we chose a different depth layer, as we aimed to show the best depth layer with the most possible visible substructures. Based on the results, we observed that the orientation of these substructures is the same. In the area 1, the resistivity is higher and there are more signs of damaging fire compared to area 2 and 3. In area 2, we observed some anomalies that we can deduce as burned material.

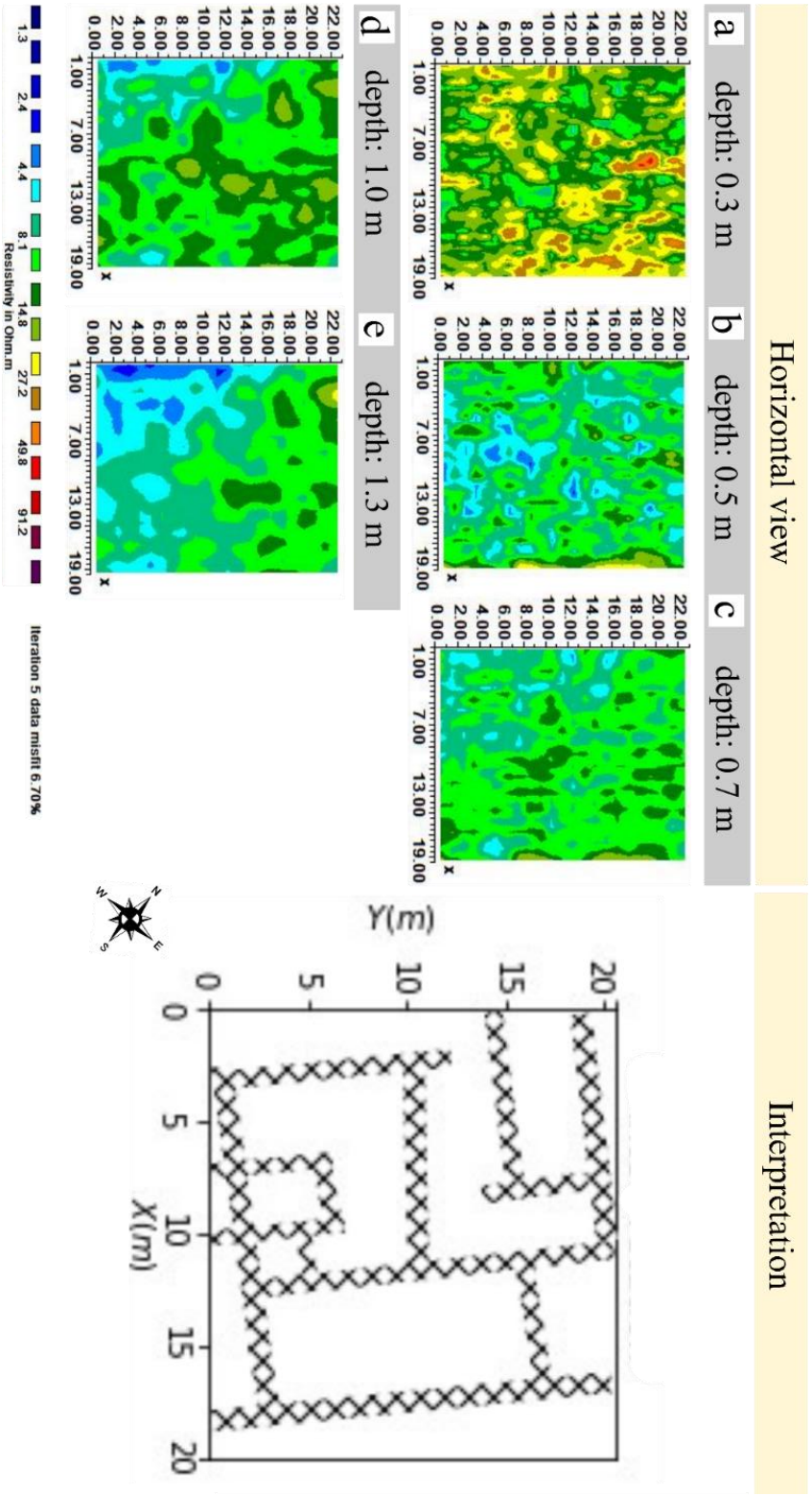

Figure 2.11. Depth layers of the 3D model based on the ERT data for area 3 and the interpretation. This Figure represents the possibility of the presence of the mudbrick walls in different depths.

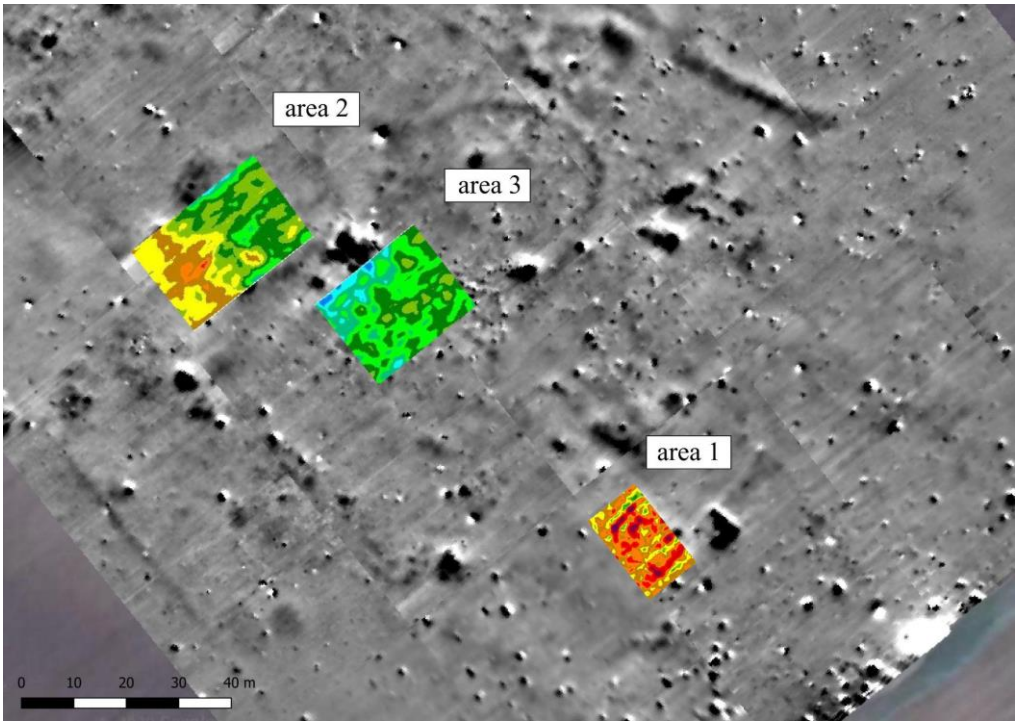

Figure 2.12. ERT depth layers of area 1 (0.4 m), 2 (0.7 m) and 3 (1 m) over magnetogram (dynamics ±12 nT and north is on top).

Based on these results and considering the excavation result of the first area, we suggest that these anomalies belong to a big complex. Resistivity values and the variation of these values, which can be a sign of different degrees of burn over the building, reveal that in this complex, the south part was more affected by the fire compared to the north part. Further excavations for area 2 and 3 are planned for the near future.

2.4. Conclusion

Although magnetic prospection is one of the most used methods in archaeological geophysics prospection and has several advantages, it can hardly detect traces of the underground mudbrick features. Moreover, it cannot provide information about the depth of the substructure. Therefore, using a second method is an essential way to obtain the best and the most accurate results. For this purpose, we chose to use the ERT method in this project.

In Saaklemo, the underground structure comprises of the remnants of a buried building made of mudbricks. The mudbrick wall and its surrounding soil were mostly made of the same material. Therefore, in order to detect these mudbrick walls with the ERT method, we applied several different types of data processing and focused on the density differences of these underground features, as density can affect the resistivity values. For detecting these mudbrick features, the smoothness-constrained inversion method was the most helpful method, as it shows the smooth variations of the resistivity anomalies. The result of the Saaklemo measurements emphasize the importance of applying different types of data processing to analyze the data in more advanced forms.

The underground structure in area 1 was partly burnt and the resistivity values of the burnt material at some parts were dominating the resistivity values of the mudbrick walls. However, with some considerations, we were able to detect and model this monumental building. This result indicates that the buried structure located at a depth between 0.4 and 1 m and formed part of a bigger complex and has a high probability to continue in all directions in our measurement area.

The excavation results show the presence of mudbrick walls and burnt debris at the depth below around 40 cm and six bell-shaped column bases partially in situ. The size, architectural techniques and ornaments used in this building confirm that it was an official building the nature of which could not be clarified due to a nearly complete lack of findings. The most probable hypothesis is that the building must have been a representative building, either a palace or an extended administrative center and that the main excavated part with several column bases could have been used as a meeting hall. The building was destroyed in a conflagration, which ascertains the reason for different burn-percentage, which was observed by the ERT result.

We measured two more areas in Saaklemo. Similar to area 1, in these two areas we detected some underground mudbrick structures, both at the depth between around 0.3 and 1.4 m. However, in these two areas the structures are not burned (area 3) or just slightly burnt (area 2). The comparison of the orientation and the resistivity values between these two structures with the underground structure in area 1, suggests that

these anomalies all belong to an immense complex. In both area 1 and 2, due to the higher resistive anomaly and the shape of them, we suggest the possibility of the existence of an anthropogenic stone layer.

The detection and evaluation of this monumental mudbrick structure with ERT method is one of the most important breakthroughs in recent researches. The results regarding mudbrick structures and the followed-up excavation in area 1 of this monumental building can start a new chapter in the prospection of mudbrick features with this method. These results indicate that for the study of Achaemenid buildings, especially in the Southern Caucasus, ERT is an ideal tool even when these anomalies are located in the surrounding mud made of highly similar materials, as based on the mathematical proportion proved in the paper, the production process of mudbrick increases the bulk density and consequently the resistivity values will increase.

Acknowledgment

The German team in “Achaemenid residences and their paradises” project was funded by the Deutsche Forschungsgemeinschaft (DFG – German Research Foundation) under FA 338/2-1 and KA 2288/5.

Moreover, Mandana Parsi greatly appreciates the funding of her short-term scientific mission (STSM) in the Institute for Mediterranean Studies-FORTH in Greece by the European Cooperation in Science and Technology (COST) under the number CA17131.

3 Revealing the Hidden Structure of the Ancient City Ur (Iraq) with Electrical Resistivity Tomography

(The following chapter (Parsi et al., 2019) is in slightly altered form published on New global perspectives on archaeological prospection: International Conference on Archaeological Prospection, 13: 206-208.)

3.1. Historical Background

Ur, the city of moon god and "Home of Abraham" was founded by settlers in the 4th millennium BC (Figure 3.1). The remains of the site are located 345km south of Baghdad and 257km away from the Persian Gulf. It is one of the most prominent cities in Mesopotamia (Wooley 1934-1976). There is evidence that the occupation was ended by a flood, formerly attributed to the flood described in Genesis. Although the city is much smaller than Uruk, in the next (Early Dynastic) period Ur became the capital of southern Mesopotamia under the Sumerian kings of the 1st dynasty of Ur (25th century BC). The last king, who left his traces both at Ur and Uruk, was the Achaemenian Cyrus the Great, whose inscription on bricks was found in recent excavations. The cities survived until the reign of Artaxerxes II. It was perhaps at this time that the Euphrates changed its course. With the breakdown of the whole irrigation system of Ur, its fields reduced to a desert and were finally abandoned.

3.2. Field Survey

In spring 2017 and 2019, we applied large scale magnetometer prospection to uncover the city plan of Ur (Fassbinder et al. 2019). Due to the salty and clayey soils, radar prospecting is non-applicable to receive information on the depth of adobe mudbrick

walls, canals or the harbour. One of most suitable methods turned out to be Electrical Resistivity Tomography (ERT). Here we show for the first time that ERT is a robust geophysical method to detect and image shallow and deep underground structures made from sundried mudbricks in the adjacent mud in detail and considerable resolution, by determining the underground resistivity distribution (Schmidt 2013). In recent years, the application of ERT became more and more important to bridge the gap between magnetometer and ground-penetrating radar prospection, in enhancing, completing and integrating the information context retrieved by these methods. Sophisticated computer programs to trigger the multichannel electrodes, combined with inversion and three-dimensional (3-D) analysis software, allow for the tracing of apparent electrical resistivity in substantial accuracy, illustrating the stratigraphic composition of underground layers (Tsokas et al. 2012). For the ERT measurements, we applied the Earth resistivity meter 4-point light 10W (Lippmann Geophysikalische Messgeräte, Germany). The design of the active electrodes (ActEle) allows spacing of 0.5 to 5m, together with short, thin and easy to repair cables and a lightweight readout unit of only 750g, the instrument is easy to transport and suitable for archaeological prospection.

Figure 3.1. Ziggurat, the temple for the God of the moon in Ur, (Iraq).

3.3. Results

The first objective of this work was to compile a 3-D representation of the subsurface resistivity related to an area hosting a buried house (neo-Babylonian period) that is traditionally made from adobe bricks. In total 25 parallel ERT profiles were acquired with a profile and electrode spacing of 0.5m in a specific area covering almost half of the house. Figure 3.2 shows the horizontal depth slices extracted by the 3-D resistivity inversion model over the area of the house. The light blue lines have been drawn to visualize the outer walls of the house. The map shows two full rooms on the right side and a bigger room on the left side. According to the resistivity of the walls, we can deduce that the walls have been made from mudbricks. The analysis of the magnetometer measurement reveals a "negative" anomaly for the walls of the house, which is also an indicator for mudbrick. The top of the house's walls are at 1 m depth and they reach approximately 2m downward. This is one of the first studies that detected mud-brick walls by ERT method.

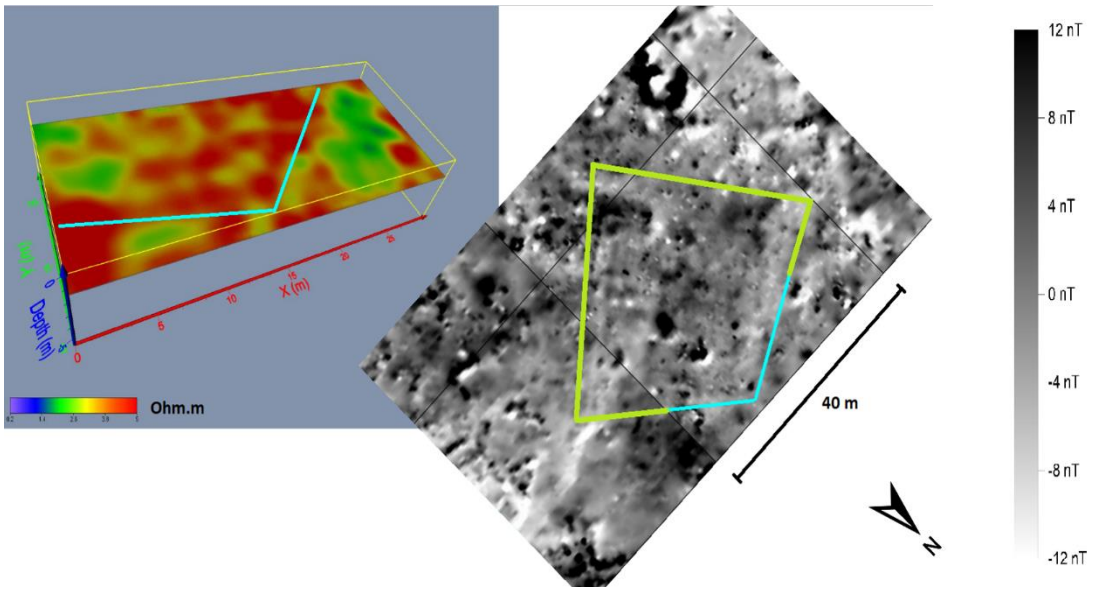

Figure 3.2. The left picture shows a 3-D model of the house. The light blue lines indicate the outer walls of the house (ERT instrument 4-point light 10W, electrode spacing 0.5m x 0.5m). On the right, a magnetogram of the same area is shown.

The light blue lines indicate the walls of the house that are shown in the 3-D model and the green lines are continuations of the walls of the house (magnetogram: Caesium magnetometer, Geometrics G-858 in Duo-sensor configuration spatial resolution 25cm x 50cm).

One other objective of the geophysical survey in Ur was, to map the horizontal extent of the city wall, its vertical dimensions and to acquire information related to the stratigraphic layering between the two main wall structures. An ERT profile was laid out perpendicular to the direction of the wall, which had already been revealed through magnetometer prospection conducted prior to the ERT survey.

The 2-D vertical resistivity inversion section shows the location of the city wall. It has a height of around 1m, which corresponds to the archaeological information retrieved by Woolley (1934-1976). The width of the inner and outer wall is around 4m and 2m respectively (see Figure 3.3a; the black circles show the position of these walls). Moreover, the right part of the Figure 3.3a outlines the refilled archaeological trench from the 19th century mentioned by Woolley. It has comparable depth extent to the respective wall and it is marked with a black rectangle. The middle walls between the main walls are displayed with pink circles.

The water content in the soil is a limiting factor that potentially could affect the interpretation of the results. The moisture content was monitored with repeated ERT measurements over the same profile for a whole day and the tomographic data were also supported by the collection of direct soil moisture, of temperature and conductivity measurements over the city wall with a Time Domain Reflectometry (TDR) instrument. The preliminary results show a maximum moisture content change of about 10 %.

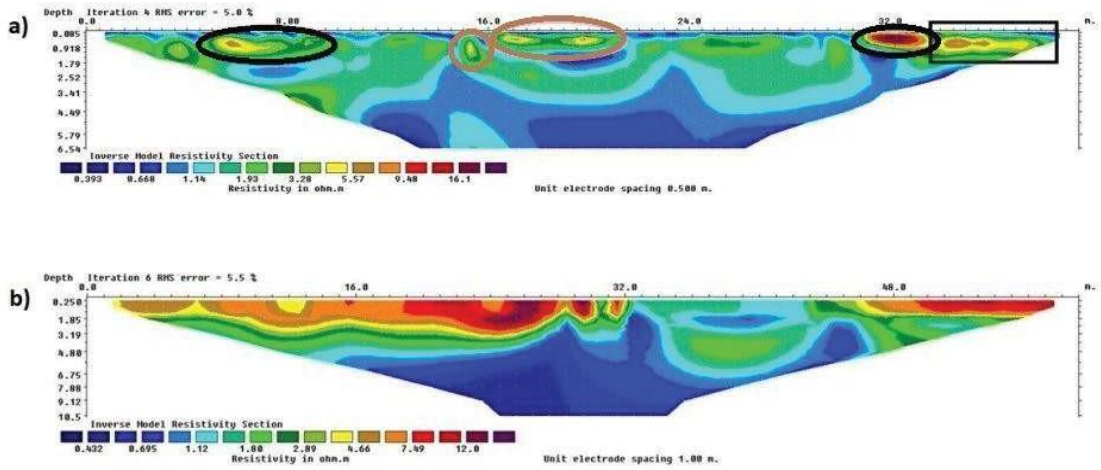

Figure 3.3. (a) ERT profile over the city wall in Ur (electrode spacing 0.5m, dipole-dipole configuration). The black circles indicate inner and outer wall, the pink circles show the walls in between and the black rectangle indicates Woolley's excavation, which was refilled afterwards. (b) 2D map of the harbor (1m electrode spacing, Wenner configuration).

An ERT survey, consisting of several profiles with different electrode spacings, was completed over the location of the harbour to verify its existence, which was originally mapped through the magnetometer survey. The left side of the map in Figure 3.3b shows the wall. The width of the harbour is around 15m and its depth about 8m. Moreover, we can observe the sedimentation in it and the final depth of the usage, which was around 3m. According to the result of the ERT, the wall is made out of baked-bricks and this information matches the archaeological evidence that exists for Ur. Further interpretations will be added to this study, after receiving the soil analysis from our American colleagues.

3.4. Conclusion

ERT measurements turned out to provide a suitable complementary prospection method. It delivers not only reliable information on the depths of archaeological features that are situated in clayey, salty and waterlogged soils, but also depicts a prospecting method that can detect adobe bricks in the adjacent clay and mud.

Acknowledgements

I greatly appreciate the funding of my short-term scientific mission (STSM) in the Institute for Mediterranean Studies-FORTH in Greece by the European Cooperation in Science and Technology (COST) under the number CA17131 and thank the IMS-FORTH lab for being a great host. The work is partly funded by the DFG-Project: “Achaemenidische Residenzen und ihre Paradiese”. Special thanks to Adelheid Otto (LMU), Elisabeth Stone and the University of Pennsylvania group.

4 Highlighting the potential of 3D ERT by comparing its results with GPR and the excavation map of a Roman building

(The following chapter (Parsi et al., 2021) is published on Revue d'archéométrie: 45, 183-186.)

4.1. Historical Background

The villa rustica near Peiting (Bavaria, Germany) is situated on a plateau 1 km east above the Lech river, which is followed in the west by a Roman road called Via Claudia. The first known document concerning the existence of an archaeological site is a letter from 1837. Until 1957, boulders above the field indicated subsurface stone buildings and led the Bavarian State Dept. of Monuments and Sites to excavate parts of the site. Later the excavation was refilled and covered by topsoil.

In the framework of road construction in 1990 and the construction of a gas pipeline, further excavations of the bathhouse were undertaken. The excavations revealed that the villa was first built in the 2nd century AD, before it was destroyed and rebuilt in the middle of the 3rd century AD.

The site, like all typical Roman villa complexes, consists of the main building with a layout more common for central Italy, a bathhouse, several further buildings and storage houses in the near environ and a courtyard wall. The bath building was equipped with a Roman heating system, the hypocaust. The villa rustica was abandoned in the 4th century AD when the Romans left the province Raetia (Leicher, 2018).

4.2. Field Survey

Jörg Fassbinder conducted the first geophysical prospection (resistivity mapping with Geoscan-RM15) in this area in 2002. In summer 2020, we revisited the site and applied further prospection methods. We started the large-scale prospection with ground penetrating radar (GPR). Due to some disturbances such as pipeline, electrical power cable and the presence of two main streets next to the measuring area, magnetic prospection was not an option for us. For a detailed result, we decided to choose a part of the main building for a survey with 3D ERT.

In this paper, we focus on GPR and ERT prospection. The instruments we used in this research are GSSI SIR 4000 with a 400 MHz antenna for GPR and Lippmann 4-point light 10 W for ERT. The purpose of this research is to compare the capabilities of these two methods. Furthermore, we aimed to verify the 3D ERT result with respect to the excavation map and to discover the accuracy and the precision, hence the potential of this instrument.

Moreover, to monitor the soil temperature, moisture and conductivity during our survey, we employed a portable Time Domain Reflectometry (TDR) device.

4.3. Results

For GPR measurement, we used a 400 MHz antenna to obtain a good balance between resolution and penetration in an 80 x 80 m grid in the north and east of the Roman bath. The GPR result shows significant substructures made of stone that belong to the main building of the Roman villa. Figure 4.1 illustrates a part of the measurements in this area. Based on the GPR results, we chose a suitable area to continue the prospection with 3D ERT.

In the ERT method by emitting the DC current, we measure the voltage to derive the resistivity distribution of the subsurface (Schmidt, 2013). To proceed with 3D ERT, we decided to measure several parallel 2D profiles and collate the data. To obtain the

most accurate result, we used both robust and smoothness-constrained inversion and the forward resistivity calculations were based on the finite-element method.

For this purpose, within two days we measured 33 parallel west to east profiles with dipole-dipole configuration and 20 m length. In each profile, the spacing between electrodes was 0.5 m. Furthermore, for a better 3D resolution, we chose to assign the spacing between the parallel profiles to 0.5 m as well. Figure 4.2 illustrates three ERT depth layers and the corresponding GPR depth slices.

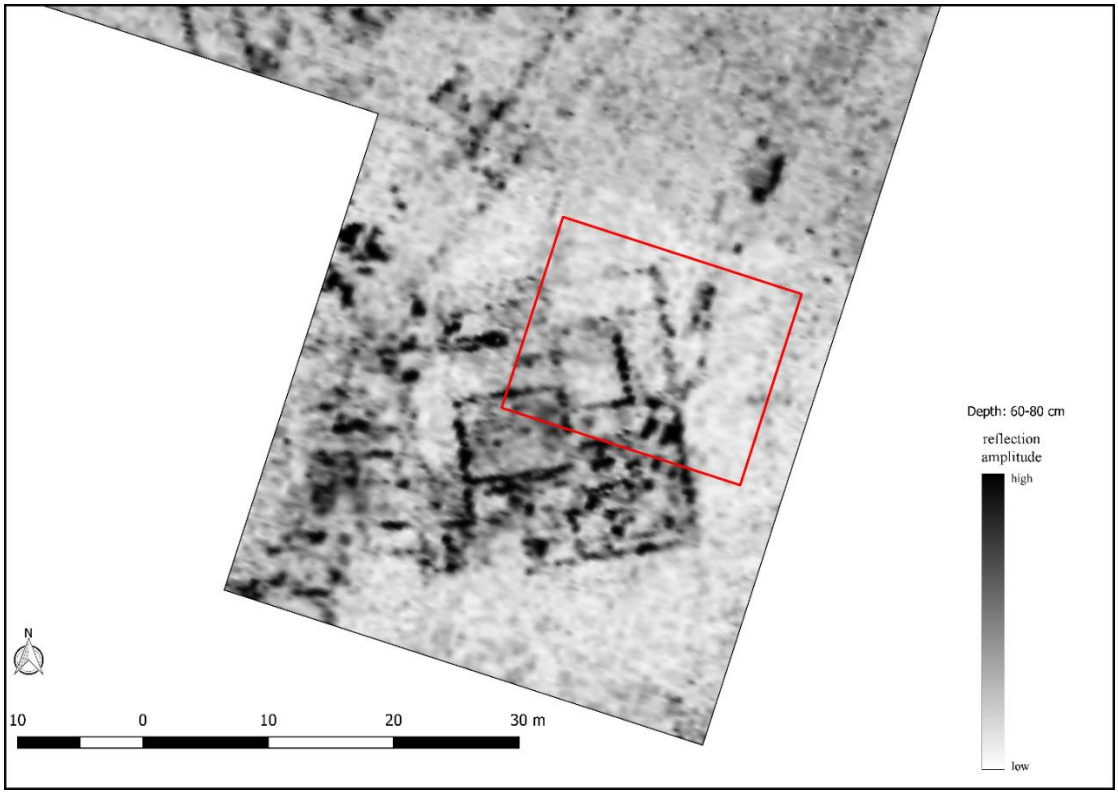

Figure 4.1. GPR depth slice of the Roman building, depth layer 60-80 cm. The red rectangle shows the chosen area for ERT prospection. GSSI SIR 4000 with 400 MHz antenna, sample interval 6x50 cm, interpolated to 25 x 25 cm.

Both instruments show walls and part of the floor of a rectangular substructure made of stone in each depth layer. These walls are located between 30 and 90 cm depth. We applied two different types of data processing to the ERT data. At first, we applied

robust inversion (L1 norm), as we were expecting sharp boundaries for the anomaly. The absolute error for this type of inversion for this data set with five iterations was 1.26 %. Moreover, to detect the smooth variation of resistivity values, we applied smoothness-constrained inversion (L2 norm). The RMS error for this inversion with three iterations was 3.78 %. Latter helped to detect the changes in soil density, which are compressed by the walls. Therefore, although some walls were destroyed, we were able to detect their remnants by this method.

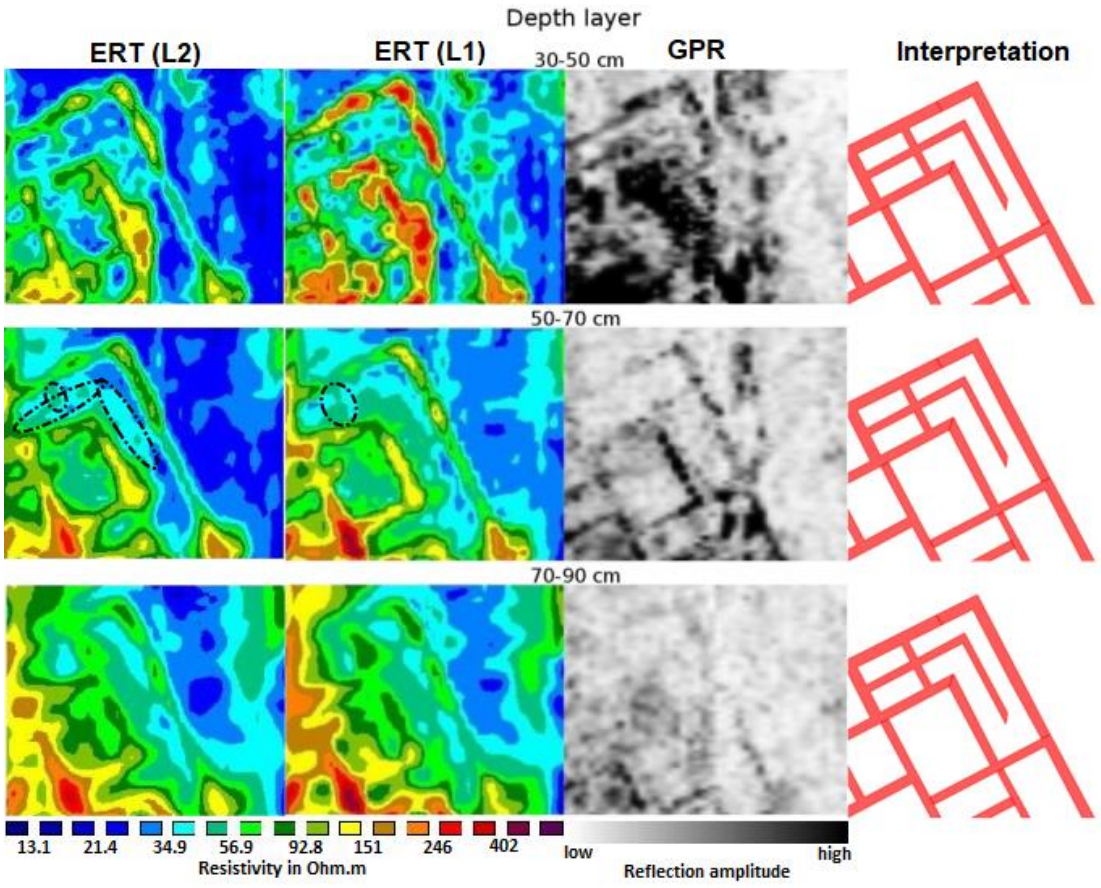

Figure 4.2. Comparison of the depth layers of GPR and 3D ERT. Lippmann 4-point light 10 W in dipole-dipole configuration, sample interval 50 x 50 cm. ERT (L1) is the result of the robust inversion and ERT (L2) is the result of the smoothness-constrained inversion. RES3DINV software was used for the calculation of inversions. Dashed lines illustrates the soil compressions due to previous walls (removed or destroyed ones) in ERT results. The last column illustrates the combined interpretation based on geophysical data and excavation.

Moreover, as some soil characteristic changes can play an important role in both GPR and ERT prospection, we monitored additionally the topsoil moisture, temperature and conductivity with the TDR instrument. The soil moisture percentage was in the range of 37 % with the maximum change of 0.62 %, the maximum soil temperature change was 2.4 °C and the topsoil conductivity was stable with the maximum change of 0.33 dS/m.

Figure 4.3. Final interpretation of the substructure. Red lines show the general interpretation lines, color blue illustrates the part, which are only mapped during excavations (partly detected their remnants by geophysical methods) and color green represents the substructures, which have been detected by RM15 in 2002, as they lay outside of the GPR grid and it was measured outside of the 3D ERT area.

Figure 4.3 shows the final interpretation based on the initial shallow excavation in 1957, GPR, RM15 and ERT prospection results. In this Figure, red lines are the general interpretation lines of the substructures, blue lines show some parts that are partly

detected by geophysical methods, they were destroyed after the excavation by construction work or are outside of the survey areas and green lines illustrate the substructures detected by RM15.

4.4. Discussion and Conclusion

3D ERT provides the same excellent result as GPR prospection in this area. Therefore, in some areas that due to the field circumstances an application of GPR is not possible, 3D ERT is a trustable substitution.

Both instruments have some limitations in field surveys. GPR is a great instrument to detect stone-made features, but its signal will be dampened dramatically in case of the presence of clayey soil. ERT is a reliable instrument to map the underground substructure in detail; nevertheless, it is time consuming to apply 3D ERT. Moreover, by a lack of soil moisture, the ERT electrodes sometimes have a high contact resistance; therefore, the measurement cannot be conducted efficiently.

Consequently, a TDR measurement is important, as we can monitor the moisture percentage during the ERT measurement. In this research, TDR results show a stable and suitable soil condition during the day.

The results of both instruments illustrate a rectangular stone-made substructure with some inner rooms. This underground feature is located from 30 to 90 cm depth. Some walls were destroyed or removed during the first excavation and we can just observe the remnant of their pressure over the soil beneath it, as they are denser compared to the periphery soil. These remnants are called “ghost features”, since they most likely remain overlooked in the normal practice of an excavation (Schleifer, 2004).

In the data processing for ERT, these features are mostly visible by smoothness-constrained inversion. This fact proves the necessity of applying different data processing methods for one data set.

As in an excavation “ghost features” cannot be detected, to model the initial shape of substructures (especially when they are only partly preserved), operating the combination of different geophysical methods is necessary.

5 Remote sensing and sediment analysis in the Bora plain, 2019: The 2019 Electrical Resistivity Tomography (ERT) survey

(The following chapter (Parsi and Fassbinder, 2020) is in slightly altered form published as a chapter of the Remote sensing and soil analysis in the Peshdar Plain Project Publication, 5: 24-37.)[1]

5.1. Introduction

Between April 19 and May 5 2019, an Electrical Resistivity Tomography (ERT) survey was conducted in the Bora Plain with two main goals. The first goal was to continue the investigation of the qanat system, the underground irrigation system that was first identified on the surface in 2015 and further investigated in 2016-2018 (Altaweel, 2017). The second goal was to investigate at a greater depth the archaeological features of the Dinka Settlement Complex which became visible after the magnetic surveys conducted in 2015-2017 by Jörg Fassbinder and his team (Fassbinder and Asandulesei, 2016; Fassbinder et al., 2017; Fassbinder et al., 2018).

In the following sections, we will present the methodology, results and the interpretation of the data, after a brief introduction about qanats in the Middle East.

[1] The authors would like to thank Marion Scheiblecker, Hero Salih Ahmed, Cajetan Geiger and Andrea Squitieri for their tireless help with setting-out, hammering and laying out the ERT electrodes.

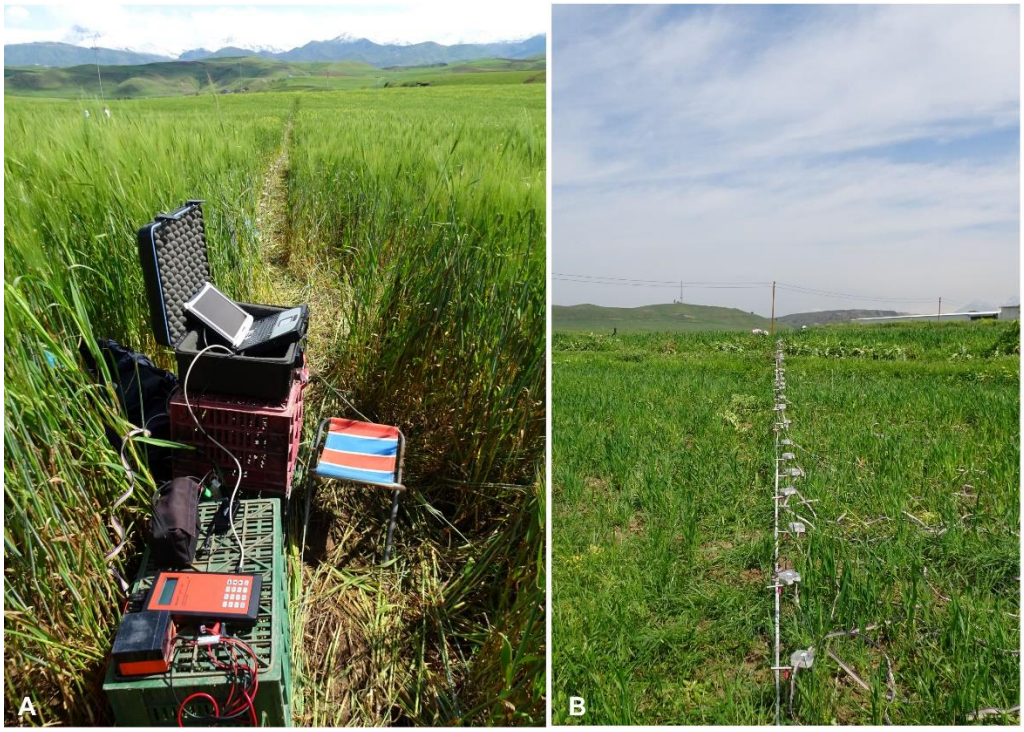

Figure 5.1. The ERT 4-point light 10W instrument (a) and the chain of electrodes (b) used during the 2019 spring campaign. The instrument was deployed and designed by Erich Lippmann (Schaufling, Germany; https://www.l-gm.de/). Photos by Jörg Fassbinder.

5.2. Methodology

Electrical Resistivity Tomography (ERT) is an effective method for archaeological geophysicists to receive detailed information not only from an archaeological feature but also about the depth of the underground structures in a non-destructive way (Schmidt, 2013). For this purpose, the application of ERT became increasingly important to bridge the gap between magnetometry and radar prospection methods in particular when wet and clayey soil conditions makes GPR prospecting utterly impossible (Parsi et al., 2019).

Sophisticated computer programs to trigger the multichannel electrodes, combined with inversion and 3-dimensional analysis software, allow tracing the apparent electric resistivity in detail, even in deeper sections of the ground. For this work, after

choosing the target area from our magnetograms, we employed this method and produced multiple 2D and 3D modelling images of ERT (Loke et al., 2013; Tabbagh, 2017).

Figure 5.2. Bing satellite image of the Bora Plain, overlaid by the magnetograms of the Lower Town and Qalat-i Dinka generated by J. Fassbinder and his team. White squares show the zones targeted by the ERT survey, with yellow lines showing ERT profiles. Prepared by Andrea Squitieri.

Different geological parameters or archaeological features affect the underground resistivity. Porosity, hydraulic permeability, moisture content and soil temperature are also the factors that affect resistivity. The resistivity prospecting method is based on Ohm's law. This law explains the relationship between current, voltage and resistance. There are two different methods used with this instrument, self-potential (SP) and induced-polarization (IP). Both methods are suitable for geological purposes. For archaeological purposes, IP is the main method. Electrode configurations are different

arrangements of electrodes, which help us to focus on different aspects and to be more efficient in surveys. The main configuration that we use for archaeological geophysics are dipole-dipole, Wenner and in some cases Schlumberger. In each measurement with these arrays four electrodes are involved, A and B as emitters and M and N as receivers.

In dipole-dipole configuration, the emitters are at one side with the electrode spacing of "a", the receivers are at the other side with the separation of "a" and the distance between former and latter is "n a". This configuration helps us to have a more detailed information of the shallower substructures. In Wenner and Schlumberger configurations, emitters are the two outer electrodes and receivers are the two inner electrodes. In the Wenner configuration, the electrode spacing between all of the electrodes are "a" and in Schlumberger only the electrode separation of the receivers are "a" and the rest are" n a". The Wenner configuration helps us to have good detail from the deeper parts and with Schlumberger configuration, we generally get information from the geology of the subsurface.

For measuring a longer profile with a specific amount of electrodes and cables, we use the so-called "Roll-on" technique. In this method, after measuring the profile, we use the first set of electrodes and cables at the end of the existing profile and we will measure again. We can repeat this process as much as we cover the area. With data processing, we are able to combine the data to produce a large profile from our measurements.

For the 2019 survey, we used the ERT 4 point light 10V instrument shown in Figure 5.1a, while Figure 5.1b shows the chain of electrodes that were fixed in the ground with the electronic boxes on top of them. Figure 5.2 shows the general map of the surveyed area with the magnetograms and the positions of the 2019 ERT profiles (yellow lines).

During the measurement, we use Geosoft software, which gives us the apparent resistivity values of the underground. Afterward, for data processing, we use Geotomo's

RES2DINV and RES3DINV software. These software programs calculate the resistivity distribution of underground. Resistivity is a relative value, therefore, each range of resistivity values represent one or more features. Based on different facts and evidence we can decide what type of the features exists in the subsurface and which material it is made of.

5.3. Qanats in the Middle East

Qanats occur mainly in the Middle East but they are also present in Nasca (Peru) and probably in many other dry areas of the world. They provide an irrigation system for agriculture but also drinking water for humans and animals. The construction of qanats consists of tunnels from a relatively higher elevation, either taping underground aquifers or bringing water from other specific sources (Figure 5.3). In some areas, they are several kilometers long tunnels with shafts along it in distances of 10-20 meters (e.g. Pasargadae in Iran). These were used during their construction but served the same time as wells and as an entrance to clean and foster the tunnels. Around the shafts, the builders deposit the excavated sediment – which makes these holes easily visible on the ground and when destroyed and removed they are very often still visible on satellite or aerial photographs.

Using gravity flow, the tunnels transport the water to a settlement but another very positive side effect prevents the water effectively from evaporation and pollution. If not anymore in use, these qanats and shafts will soon collapse or clog and then refilled by sediments and remain hidden in the underground. To detect such features by ERT seems at first sight an easy attempt but turned out as a challenge since it is difficult to know if the tunnels or shafts collapsed and refilled with no water flow or the water still flows through the stones. The ERT data can then also resemble the results of paleo-channels, hence, the interpretation is not always very clear and leave space for discussion.

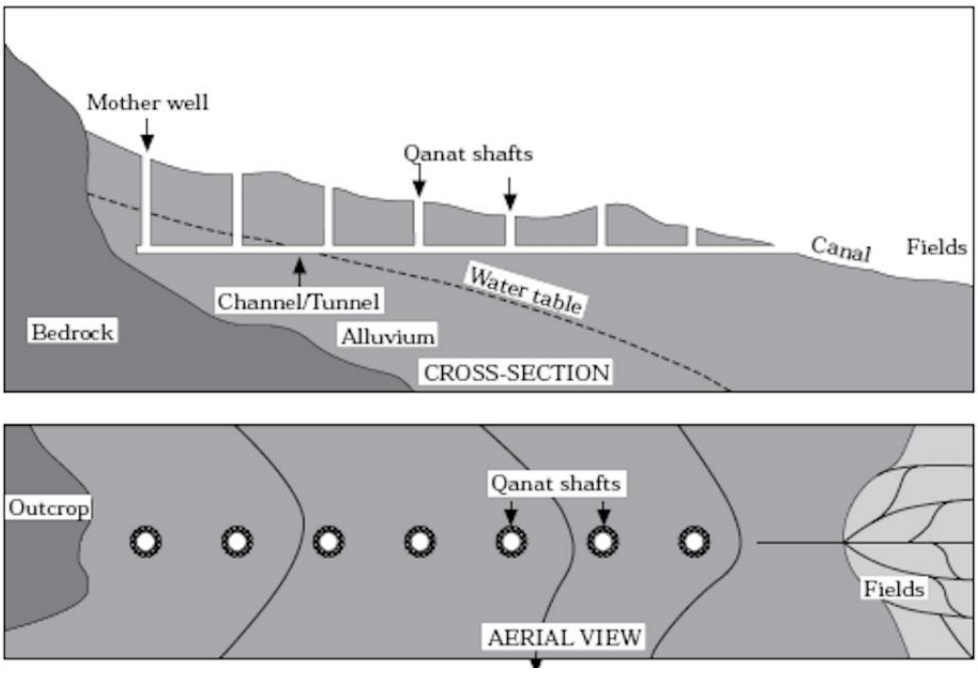

Figure 5.3. Schematic view of a typical qanat system, with the cross section above and the aerial view below (After Lightfoot, 1996, Fig 1).

5.4. ERT surveying in the southeastern part of the Bora Plain

This section deals with the measurements that were applied on the already known traces of the qanats located in the south-eastern part of the Bora Plain, about 1.5 km south of the Lower Town of the Dinka Settlement Complex (Figures 5.2 and 5.4). This qanat system was identified by the Peshdar Plain Project team in 2015 through satellite images and ground-truthing as some of the qanat shafts' openings are still visible today on the surface today (Altaweel and Marsh, 2016). Subsequently, ERT measurements were first conducted in this area in autumn 2016 and spring 2017 by a team from the Sulaymaniyah University's Geology Department (under the supervision of Prof. Bakhtiar Qader Azir) a team from the University College London (under supervision of Dr. Mark Altaweel). Their results highlighted a possible qanat running almost parallel to the river in a northwest-southeast direction, intersecting another qanat running in an east-west direction (Altaweel, 2017). At the point where the two qanats meet, modern fish ponds are present today (Figure 5.4).

Figure 5.4. Bing satellite image of the southeastern area of the Bora Plain where the openings of qanat shafts are still visible today. The yellow lines show the positions of the ERT profiles (note that profiles 10-11 and 7-8 were very close to one another so they appear as a single line in the image). The label "fish ponds" shows the location of fish ponds that were created after the satellite image had been taken; they were already in use in 2015 when PPP started work in the region. Prepared by Andrea Squitieri.

In spring 2019, 10 ERT profiles (Figure 5.4: yellow lines) were measured in this area using the three configurations Wenner, Schlumberger and dipole-dipole. For our purpose, the most effective configuration proved to be the dipole-dipole array. Figure 5.5 illustrates the ERT result of profile 8, which is the only profile in this area that yielded significant results. The direction of this profile is southwest-northeast. As the feature was located in a shallow subsurface, we chose the dipole-dipole configuration results for our interpretation. The electrode spacing is 0.5 m and the length of the profile is 30 m. In Figure 5.5, the horizontal line shows the x-direction (length of the profile) and vertical direction illustrates the depth of the measurement. Each color represents

a specific resistivity value (the color scale located at the lower left of the profile describes the correspondence value of each color). In this profile, we detected two types of anomalies. Ellipsoidal-shaped features that are filled with water (black rectangles in Figure 5.5) and an ellipsoidal-shaped feature filled with materials such as clay, gravel and sand (black circle in Figure 5.5). The black circle shows an anomaly that could be caused by the remains of a collapsed shaft at a depth of around 1.7 m, located at the middle of the profile. Other interpretations are possible, however, as this may also be the remains of a refilled paleo-channel. The black rectangle beneath it illustrates the possible active qanat tunnel with water inside of it, and on the left of it traces of a water table, both at a depth of around 3.5 m. On the left side of the profile, towards the top, we detected some features that can be interpreted as small shafts, which could bring water to the surface. We have to mention that since the spacing of our electrodes is 0.5 m, we could not document features smaller than this size. We also measured and processed all the profiles of this area by using a Wenner configuration and an electrode spacing of 0.75 m and 1 m to get information from the deeper parts of the subsurface. By increasing the electrode separation, we filtered automatically the features that are smaller than the spacing. The outcomes, however, did not show further relevant results and therefore, they are not presented here.

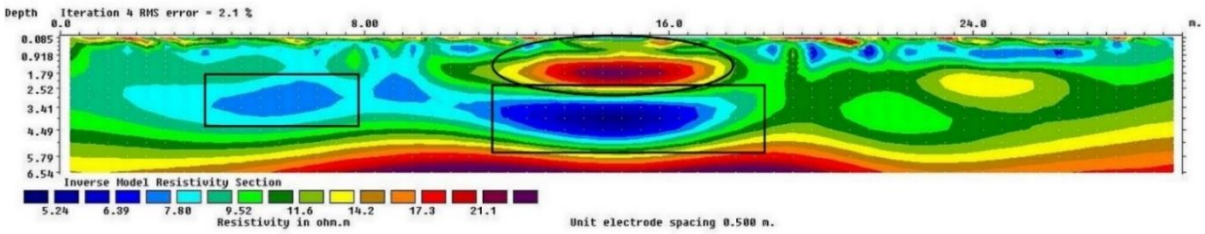

Figure 5.5. ERT Profile 8. Direction: southwest-northeast. The black circle shows an anomaly that may be the remains of a collapsed qanat shaft at a depth of around 1.7 m. The black rectangle beneath it illustrates the possible active qanat tunnel with water inside of it. While the black rectangle on the left shows traces of a water table at a depth of around 3.5 m. Prepared by Mandana Parsi.

5.5. ERT surveying near the Lower Town of the Dinka Settlement Complex

Moving closer to the Lower Town of the Dinka Settlement Complex, we measured 6 profiles to the south-east of the Lower Town magnetogram. These are profiles 1-4 and 18-19 (Figures 5.6 and 5.7). The aim was to understand whether we could find traces of qanats close to the Lower Town that may have provided water to the settlement or further traces of the continuation of the settlement in this direction.

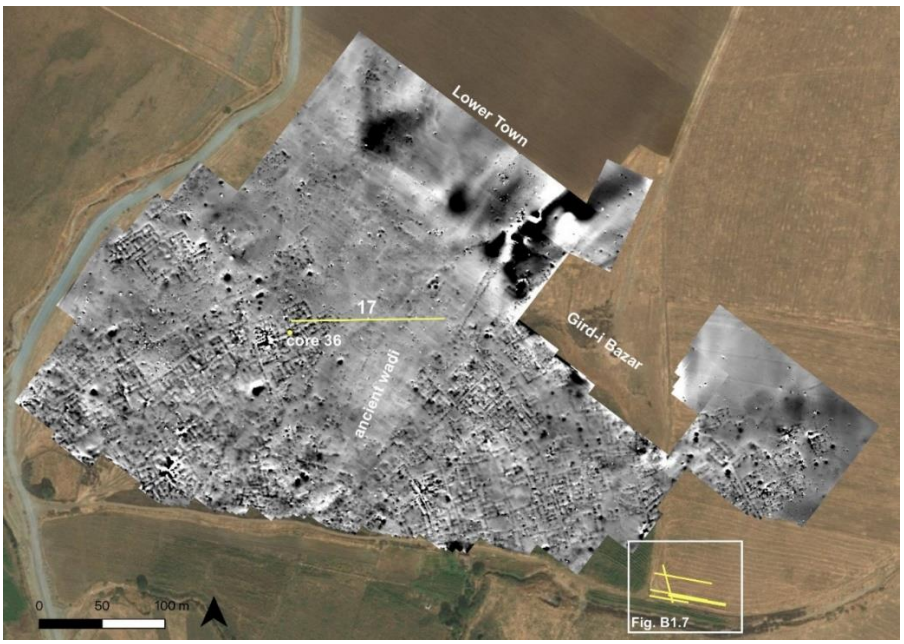

Figure 5.6. Bing satellite image overlaid by the magnetogram of the Lower Town of the Dinka Settlement Complex showing with yellow lines the locations of the ERT profiles and with a yellow dot the location of Core C36. Note the ancient wadi crossing the settlement. Prepared by Andrea Squitieri.

Figure 5.7. Close-up image showing the location of the ERT Profiles 1-4, 18, and 19 to the south-east of the Lower Town. Prepared by Andrea Squitieri.

In Figure 5.7, the three parallel profiles 1, 2 and 3 show the presence of some anomalies, with the first two profiles running parallel to each other and having the same extension, while the third extends more to the west than the previous two. Figures 5.8 and 5.9 show the results from profiles 1 and 2, respectively. The distance between the two profiles is 1 m. Both profiles were laid out in the west-east direction, with 0.75 m electrode separation, a total length of 45 m and measured in a dipole-dipole configuration.

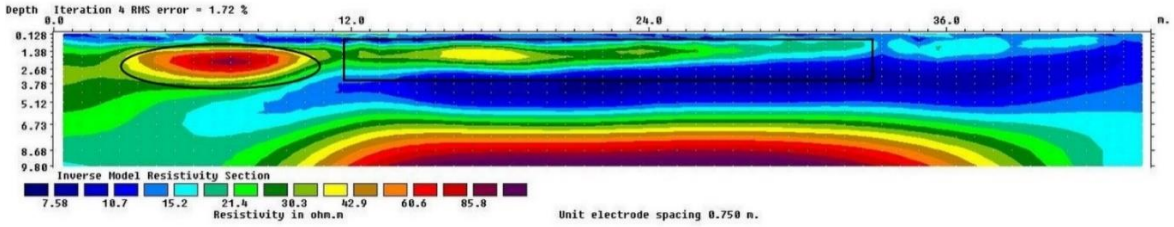

Figure 5.8. ERT Profile 1. Direction: west-east. The black circle shows the presence of an artificial anomaly; while the black rectangle shows possible accumulations of coarse gravel, perhaps coming from a pavement or a floor. The feature showing in blue is a geological formation. Prepared by Mandana Parsi.

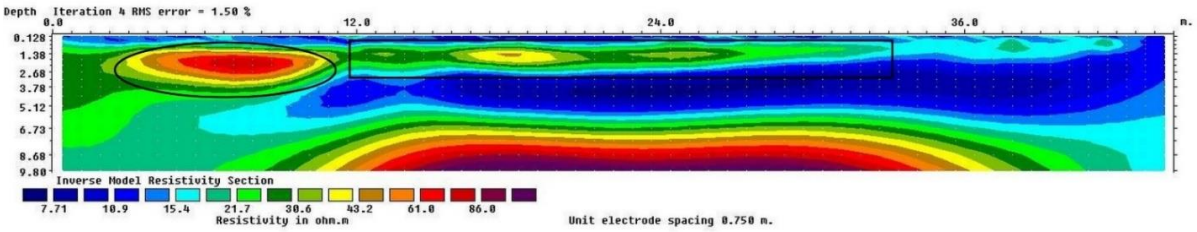

Figure 5.9. ERT Profile 2. Direction: west-east. This profile shows the same results as Profile 1. Prepared by Mandana Parsi.

The black circle in Figure 5.8 (profile 1) show an anomaly that occur around 1.5 m deep and it goes down to around 4 m. The width of this anomaly is hard to estimate, as we do not know the exact direction of the profile in respect to it. Further measurements are required to obtain precise information about the true diameter. According to the resistivity values, we suggest that this anomaly represents artificial elevated structure next to some lower features. The lower anomalies could be the accumulation of coarse gravel, which can be interpreted as pavement or floor (shown in black rectangular). Due to their shape, it is not clear if they can be interpreted as buildings. The large anomaly in blue located below the three black circles in the figure represents a geological formation, perhaps what remains of an alluvium accumulation. Profile 2 (Figure 5.9) yielded the same results as profile 1. Figure 5.10 illustrates the results from profile 3, which was slightly shifted to the west compared to profiles 1 and 2. It shows the same anomalies, as visible in the previous profiles, shifted to the right side of the profile and below them the alluvium accumulation in blue. Profile 4 (Figure 5.11) was nearly parallel to the profiles 1-3 but located ca. 15 m north of them. It only revealed geological formations with no anomaly indicating artificial structures. That means that here we could not detect any continuation in this profile of the features we traced in profiles 1-3.

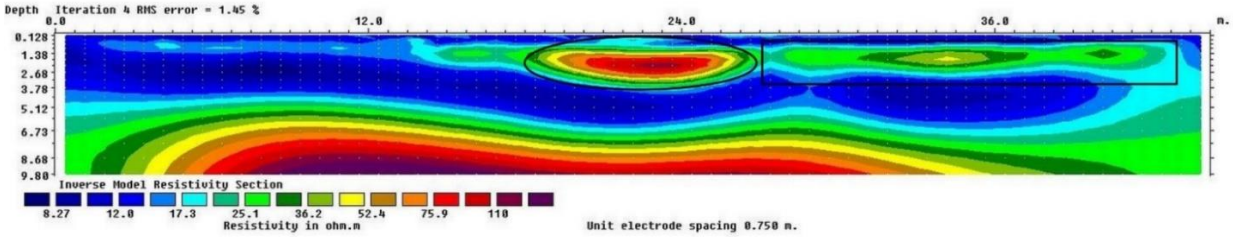

Figure 5.10. ERT Profile 3. Direction: west-east. This profile shows the same results as Profiles 1 and 2. Prepared by Mandana Parsi.

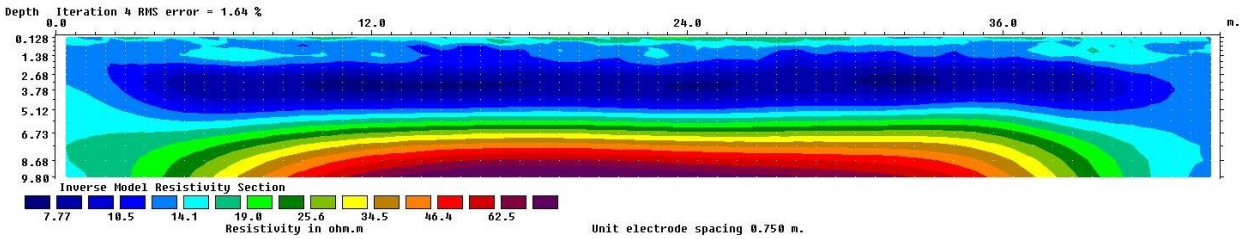

Figure 5.11. ERT Profile 4. Direction: west-east. This profile shows only geological features. Prepared by Mandana Parsi.

To the south of profile 1, we measured profile 18, whose results are shown in Figure 5.12. This is a west-east profile, 30 m length with dipole-dipole configuration and 0.5 electrode separation. Features are shown with black circles and rectangular. The width of the anomaly to the right is around 2-2.5 m, the width of the middle anomaly is around 3.5-4 m. The depth of all of them is around 1.5 m and the deepest (the middle one) goes down to around 3.5 m. The exact size of the anomaly cannot be estimated, as we need more information about the direction of the ERT profile with respect to the feature. As in the previous profiles 1-3, we suggest that these anomalies are not geological formations but possible accumulations of coarse gravels (shown in black rectangular) and some elevated stone features (shown in black circles). As above, due to the shape of these anomalies, it is not clear if they can be interpreted as buildings.

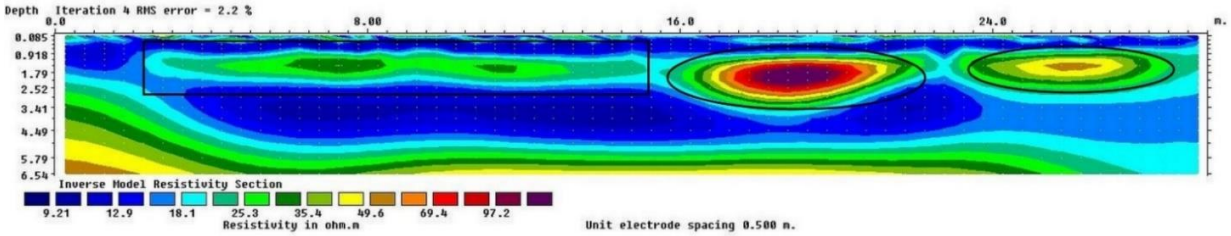

Figure 5.12. ERT Profile 18. Direction: west-east. Black circles showing the presence and positions of artificial anomalies. The anomaly shown in the rectangle can be a pavement or floor. Prepared by Mandana Parsi.

The last profile measured in this area is profile 19, set in such a way to intersect the previous profiles. The results from this profile are illustrated in Figure 5.13. This is a northwest-southeast profile with 0.5 electrode spacing, dipole-dipole configuration and a total length of 30 m. The black circles show the position of the artificial features, which are connected to one another and they are around 1-3 m deep. They also showed up in profiles 1 to 3. The black rectangles below them show anomalies that based on their resistivity values may contain water inside. These anomalies are also inter-connected and they are between 3 to 5 m deep.

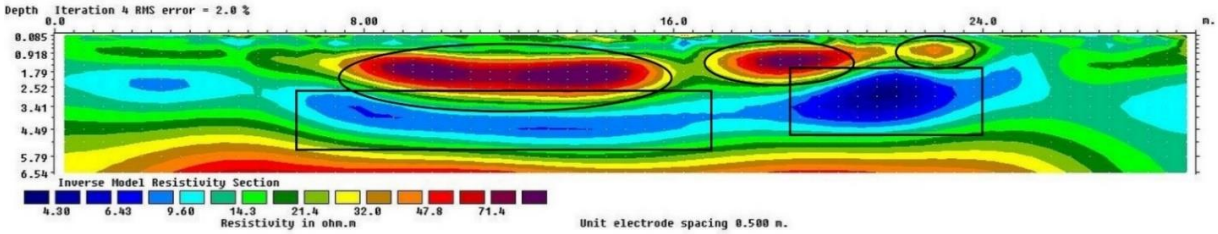

Figure 5.13. ERT Profile 19. Direction: northwest-southeast. The black circles show the positions of three artificial anomalies while the black squares show features saturated with water. As in previous profiles the anomalies in the circle can be interpreted as a wall. Prepared by Mandana Parsi.

5.6. Investigating the Lower Town of the Dinka Settlement Complex

The second goal of the 2019 ERT survey was to further investigate the archaeological features of the Dinka Settlement Complex, which can be seen in the magnetograms produced by the magnetometer surveys conducted by J. Fassbinder and his team in 2015-2017 (Fassbinder and Asandulesei, 2016; Fassbinder et al., 2017; Fassbinder et al., 2018).

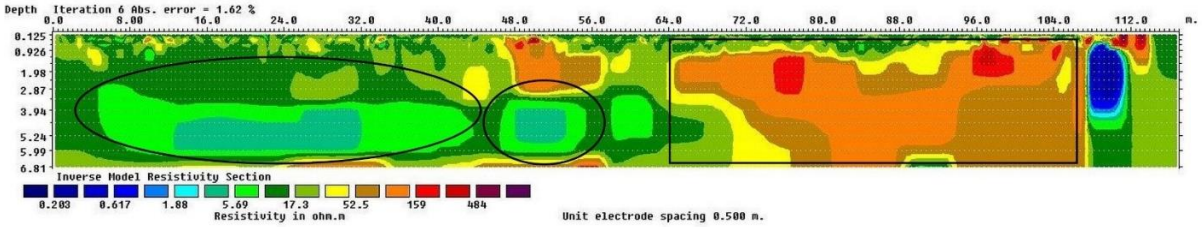

Figure 5.14. ERT Profile 17. Direction: west-east. On the right, the black rectangle shows the bed of the ancient wadi once crossing the Lower Town; on the left, the two black circles show a possible mudbrick building located below the Iron Age structures, which appear as smaller anomalies on the top left. Prepared by Mandana Parsi.

In the Lower Town, a 120 m long profile called profile 17 was measured (position is shown on the Figure 5.6). For measuring this profile, we used the Roll-On technique suitable to cover a long profile. The electrode spacing was of 0.5 m and the profile was in dipole-dipole configuration. The direction of the profile is west-east. The results are shown in Figure 5.14. On the right side of this figure, the black rectangular shows evidence for the existence of the bed of an ancient wadi, today not visible anymore on the surface. The existence of this wadi, which divided in ancient times the Lower Town in a roughly north-south direction (Figure 5.6) was already suggested after the 2016 magnetometer survey and later confirmed by a hydrological analysis ("Channel Network") conducted in QIGS-SAGA (Radner et al., 2017a). Final proof for its existence came from the excavation in 2018 of three geo-archaeological trenches, named GA43-44-45 that revealed the fluvial accumulation of the ancient

wadi (Radner, 2019c, 16 Fig. A3). The ERT results from profile 17 represent additional evidence for the existence of such a wadi and add information about the depth of its bed.

On the left side of profile 17, we can observe a different situation. This is where the profile crosses some structures visible in the magnetogram. Here the profile shows regular artificial features that become visible at a depth of about 3 m, highlighted in black circles in Figure 5.14. In the figure, the black circle on the left shows a linear anomaly that probably runs parallel to the profile. The black circle to the right shows another regular feature that seems to run perpendicularly to the profile. The features are around 2.5 m high but the exact width of them is not clear, because for calculating it more precisely we need to know their exact direction angle with respect to the profile. These regular anomalies which are shown in the black circles of Figure 5.14 do not correspond to the features visible in the magnetogram. The reason is that the magnetometer prospection is adapted for archaeological purposes to trace archaeological features no deeper than 2-3 m beneath the ground. For simple physical laws, structures from deeper parts of the soil become blurred and indistinct; moreover, the magnetic intensity is diminished by the factor $1/r^3$ (r = distance from object to magnetometer). On the other hand, the ERT allows us to reach greater depths. Therefore, the magnetogram shows the archaeological features of the Iron Age period belonging to the Dinka Settlement Complex, which do not reach depths greater than 2-3 m, while the regular features highlighted in the ERT profile 17 represent older structures located below the Iron Age ones. Due to their regularity and resistivity value we interpret them as remains of mudbrick buildings.

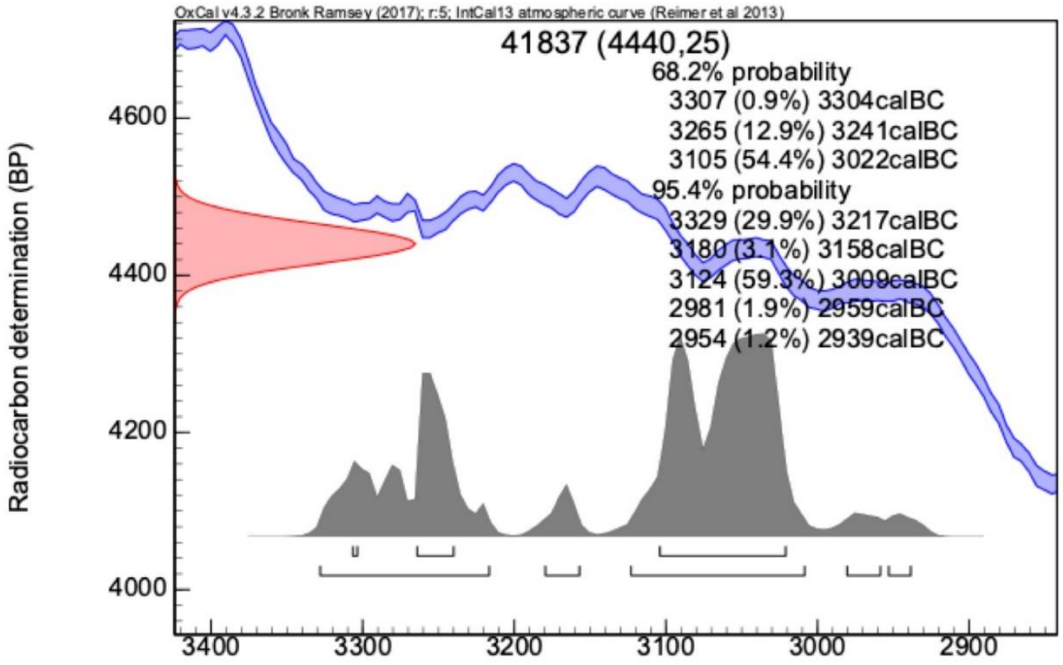

Figure 5.15. Calibrated radiocarbon dates from the charcoal sample collected at a depth of 55 cm from Core C36, taken in the Lower Town of the Dinka Settlement Complex. Calibration software OxCal v. 4.3.2.

Currently, we have no direct evidence for dating these structures that the ERT profile has showed, as no excavation was conducted; however, a hint to its dating is given by a charcoal sample coming from Core 36 (C36) taken about 10 m south of the western extremity of profile 17 (Figure 5.6). This core, described in detail below (Table B2.1 available at (Eckmeier, 2020)), reached a depth of about 3 m and yielded, among other things, a charcoal sample radiocarbon dated to 3329 - 2929 calBC (95.4 % probability, see Figure 5.15)[2]. The charcoal was found at a depth of about 55 cm below the ground, but it could well have originated from a much deeper level. It yielded a date that indicates that it must have originated from structures older than the Iron Age phase. We suggest that the deep mudbrick structure highlighted in profile 17 may date to the

[2] This part was done by a collaborating partner.

older phase from which the charcoal of Core 36 (C36) originated. Further investigations by means of ERT and coring are necessary to further explore this phase older than the Iron Age in the Dinka Settlement Complex. Nevertheless, the existence of archaeological phases below the Iron Age features is also supported by the results of the pottery survey conducted in 2013 by J. Giraud, which identified Late Chalcolithic and Early Bronze Age pottery across the Dinka Settlement Complex (Giraud, 2016). Also, the discovery of a Chalcolithic kiln in the operation DLT3 (Chapter I available at (Squitieri et al., 2020)) supports this.

5.7. The ERT profiles on the western slope of Qalat-i Dinka

Two ERT profiles, named profiles 12 and 13, were measured on the western slope of Qalat-i Dinka, south of the trench called QID2, which was excavated in 2018 (Figure 5.16). In this trench a large stone feature, measuring about 2 x 7 m, was unearthed characterized by a 30 % slope. It was interpreted as a glacis, which is a sloping structure with defensive purposes (Hashemi, 2019). The aim of profiles 12 and 13 was to verify whether the glacis continued south of trench QID2. The two profiles (Figures 5.17 and 5.18) were measured from east to west (from right to left in the figures), they are parallel to each other with the distance of 1 m, with 0.5 m electrode spacing. Here we present the ERT results of the dipole-dipole configuration. The total length of each profile is 30 m. At the middle of both profiles, we can see a feature that could confirm the existence of the glacis with a width of around 2 m, whose existence was already proposed from the excavation results. In Figure 5.17, the black circle to the left, that is on the east side of the glacis, shows the position of a wall with the depth of around 1 m. We cannot calculate the exact width of the wall, as we need more information about the direction of the wall and the angle of the profiles with respect to the wall. Profile 13 (Fig. 5.18) also shows the glacis, highlighted by a black circle. Hence, the two profiles demonstrate that the glacis structure excavated in QID2 continues towards the south for about 6.5 m, and they support the existence of a wall next to the glacis (Radner and Kreppner, 2019).

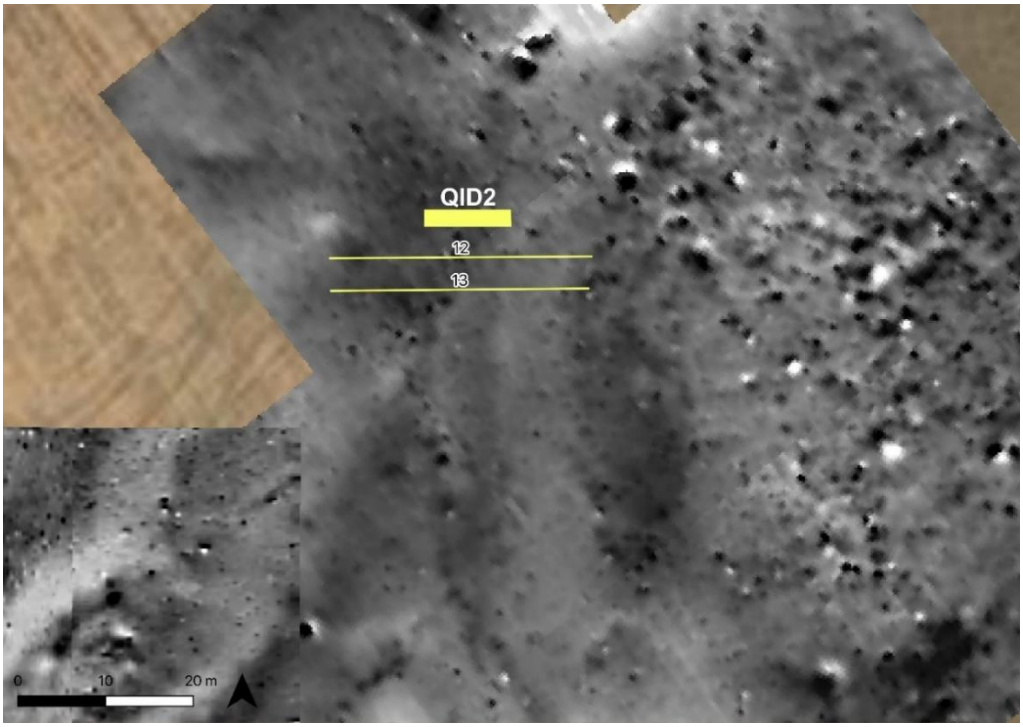

Figure 5.16. The 2015 magnetogram of the western slope of Qalat-i-Dinka (see Fassbinder/Ašandulesei 2016), overlaid by trench QID2 excavated in 2018 (yellow rectangle) and the two ERT profiles measured in 2019 (yellow lines). Prepared by Andrea Squitieri.

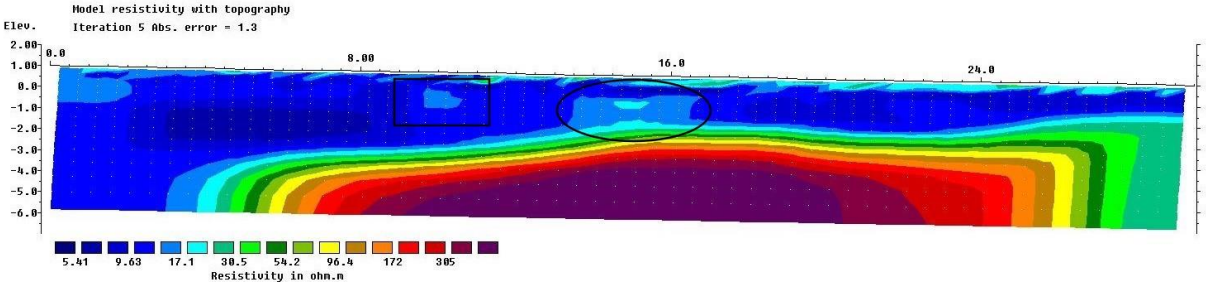

Figure 5.17. ERT Profile 12, measured in east-west direction with dipole-dipole configuration and 0.5 m spacing. The black circle shows a feature that matches the glacis structure excavated in trench QID2. The black rectangle shows a wall. Prepared by Mandana Parsi.

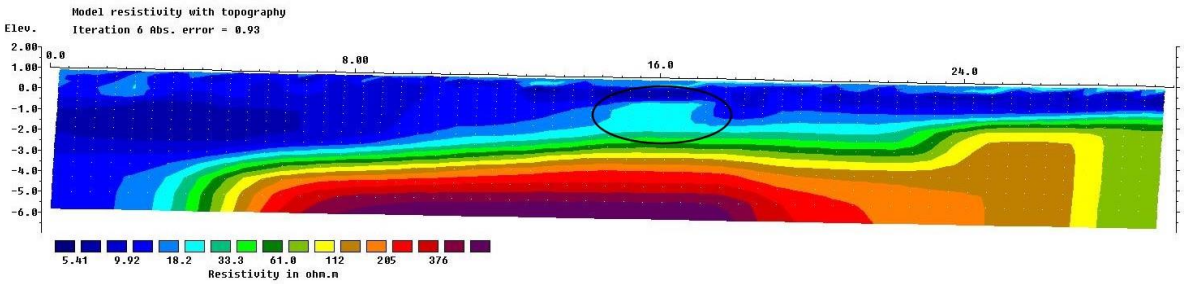

Figure 5.18. ERT Profile 13, measured in east-west direction, yielding similar results as in Profile 12. Prepared by Mandana Parsi.

5.8. Discussion and conclusions

The ERT measurement survey carried out in spring 2019 had two aims: first, to investigate the qanats of the Bora Plain, and second, to obtain additional information about the archaeological features of the Dinka Settlement Complex.

As to the first objective, we presented in §5.4 the results from the ERT profiles measured in the southeastern part of the Bora Plain, where the openings of qanat shafts are still visible on the ground and one qanat tunnel is still used today to supply water to a modern fish farm. The results obtained from Profile 8 revealed the possible presence of closed shafts, at a depth of around 1.7 m. In section §5.5, we discussed the results of the ERT profiles measured close to the Lower Town of the Dinka Settlement Complex, where artificial anomalies that may represent remains of archaeological structures were detected, although it is not clear if they belonged to buildings. We suggest that these anomalies represent artificial structures standing next to some elongated features, which could be the accumulation of coarse gravel and can be interpreted as pavement or floor.

In regard to the second objective, we discussed the results of Profile 17 in section §5.6. This profile crosses the magnetogram of the Lower Town, supplying additional evidence for the existence of an ancient wadi that once crossed the settlement in a roughly north-south direction. This profile also revealed that below the Iron Age structures of the Lower Town there are older structures, perhaps belonging to the Chalcolithic/Early Bronze Age periods. These will be further investigated in fieldwork

scheduled for spring 2021, for which funding from the Gerda Henkel Foundation has already been procured (grant AZ 42/V/20). Finally, we discussed the results from two ERT profiles measured on the western slope of Qalat-i Dinka. Here, a structure was identified that we interpret as the continuation of the glacis structure unearthed during the 2018 excavations in trench QID2. The results proved that the structure continues south of QID2 for at least 6.5 m, and showed the existence of a wall or palisade next to it.

6 Looking beneath Yeha (Ethiopia): A 3D model of a multi-layered substructure with Electrical Resistivity Tomography (ERT)

(The following chapter (Parsi et al., in preparation) is under preparation for the submission on a geophysical journal and with some alterations is accepted and in the process of the publication as an article in "„Forschungen am nördlichen Horn von Afrika - Research at the northern Horn of Afrika“, Archäologische Forschungen in Afrika 2 (from DAI – scheduled year of publication: 2023).)

Abstract

A 3D Electrical Resistivity Tomography (ERT) study was conducted at the Ethio-Sabaean settlement of Yeha in northeastern Ethiopia (Tigray region). The aim was to investigate, verify and complement images of the underground substructures and the extension of the cities from Pre-Aksumite and Aksumite times (early 1st millennium BC – 8th century AD), which we previously detected by magnetic measurements, in more detail and to provide additional arguments for the concept of the application for UNESCO world heritage site. The geophysical surveys started with a magnetometer prospection already in 2018. Magnetometry has several advantages; however, in Yeha some problems such as field boundaries that are characterized by highly magnetic anomalies, Basaltic rocks, modern infrastructures and shallow inclination due to the geomagnetic equator complicated the interpretation. ERT prospection helped to verify features that were not visible or only vaguely detected by the magnetometer measurements and provided depth information of the archaeological features.

Furthermore, we conducted several measurements with the Time Domain Reflectometry instrument, which has been done to monitor the moisture, temperature and conductivity of the topsoil. Based on the result of the magnetograms and the results of previous excavations, we chose a suitable and applicable test area for ERT prospection to reach the main archaeological purpose. To obtain more detailed information we generated two 3D models based on the ERT data. These 3D models revealed multi-layered interconnected stone walls with a height of 60 - 120 cm and proved the continuation of this substructure adjacent to the excavation. On the basis of these facts, the site of Yeha was extended by the area of Shilanat and was announced as a cultural heritage area by local administrations.

6.1. Introduction

6.1.1. Historical and Geological Background

Yeha is located 35 km northeast of the UNESCO world heritage site Aksum, one of the most prominent archaeological sites in Ethiopia, at an altitude of 2150 m above sea level (Figure 6.1). Yeha was the political and religious center of the Ethio-Sabaean community Dia'mat. The Ethio-Sabaean entity of Dia'mat is one of the Pre-Aksumites communities (existed before the Aksumite period) and developed after the migration of the Sabeans to the northern part of today's Ethiopia and the southern part of today's Eritrea and the acculturation with the indigenous culture. Since 2009 it has been under investigation by an Ethiopian-German team (Gerlach, 2017).

Compared to the Sabaean Kingdom and its territory in South Arabia (Yemen) with highly complex irrigation systems and economy, which was based on the trade with incense and myrrh, the economy in Ethiopia was characterized by agriculture in the temperate highlands and extensive animal husbandry in the savannah. Environmental conditions in Yeha were ideal for rain-fed farming and it had adequate water for humans and cattle breeding. Natural resources for building materials such as wood and high-quality stones (volcanic and sandstone) are mostly from this area.

The best-preserved Ethio-Sabaean buildings are the Great Temple (7^{th} century BC), which was dedicated to the main Sabaean god of Almaqah and the palatial building

Grat Be'al Gibri (8th century BC). Figure 6.2 illustrates these two monumental buildings. The Great Temple, which is a sacred place and the symbol of national pride and identity for Ethiopians, is a rectangular 18.5 by 15 m building with a maximum height of 14 m. It was built on a hilltop using the dry masonry construction technique with the block of stones, each up to 3 m long. Based on the Baptisteries, which are found inside of the temple, it was concluded that this temple was converted to a monastery in the 6th century AD.

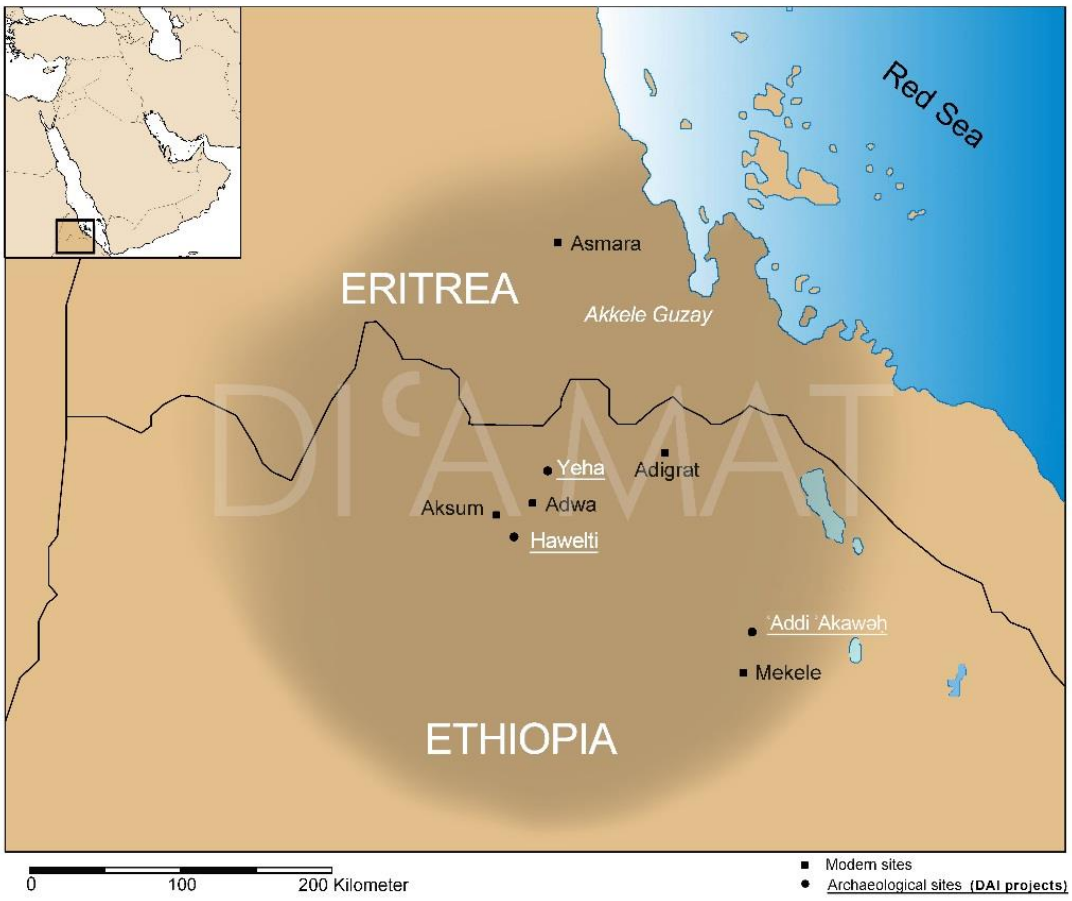

Figure 6.1. An overview of the Tigray region in Ethiopia. The dark-shaded area illustrates the position of the Ethio-Sabaean entity of Di'amat (After Gerlach, 2017).

Figure 6.2. The best-preserved Ethio-Sabaean buildings: Grat Be'al Gibri (left) and the great temple of Yeha (right).

The second monumental building in this area, Grat Be'al Gibri, is an axial symmetric 60 by 60 m multi-storey palace with a maximum height of 27 m, which is known as the largest ancient wood-stone construction in East Africa and South Arabia. It has been archaeologically verified that a devastating fire destroyed the monumental buildings in Yeha (Gerlach, 2017; D'Andrea et al., 2008).

There is not so much information available on the dispersion, structure and extension of the civilian settlements for this period. Therefore, different types of investigations such as geological, geomorphological-pedological, botanical and geophysical surveys have been undertaken in the framework of the research and restoration project of the German Archaeological Institute (DAI).

6.1.2. Geophysical Background

Archaeological geophysics provides us with a large range of tools suitable for tracing and mapping archaeological features and monuments beneath the ground in a non-destructive way. In modern archaeology, excavation projects ideally start with prior geophysical prospection to minimize destruction and to optimize the project (Scollar et al., 1990; Papadopoulos et al., 2010; Fassbinder, 2017; Getaneh et al., 2018).

The geophysical part generally starts with a large-scale prospection. For this purpose, we use a magnetometer, Ground Penetrating Radar (GPR) and/or Resistance Meter.

These methods provide information on the bulk physical properties of the subsurface and hence, the underground structures and features (Trinks et al., 2013).

In most cases, the GPR data contain information about the depth; however, in the case of the presence of the clay, due to the high electrical conductivity of the soil, the GPR signal is attenuated and consequently, it prevents us from conducting a successful GPR measurement.

We should consider the fact that the archaeological features show more variety in shape and are more complex in comparison to conventional geological structures, and they are located at different depths (Scollar et al., 1986).

Electrical Resistivity Tomography (ERT) is one of the most prevalent methods to image underground structures particularly concerning soil conditions. It provides information about the depth and the electrical resistivity values, which will be interpreted in terms of the geological or archaeological materials. The ERT is designed in such a way as to cope with a complex topography (Yi et al., 2001). In this method, we emit direct current (DC) into the ground and measure the voltage to map the resistivity distribution of the underground (Günther et al., 2006; Papadopoulos et al., 2006; Schmidt, 2013; Thiesson et al., 2014). The final images are created by the inversion of several hundred or thousands of the collected data sets (Loke & Barker, 1996a; Loke & Barker, 1996b). The application of ERT is getting more and more important, particularly in the last 20 years, to enhance and complete the information retrieved by other methods, such as magnetometry (Parsi et al., 2019). In addition to archaeology, this equipment is used to solve problems in different scientific areas such as environment, geology and engineering (Rogers & Kean, 1980; Atzemoglou et al., 2003; Caglar & Duvarci, 2001; Dahlin et al., 1994; Van et al., 1991).

It is possible to trace the electrical resistivity with considerable accuracy, illustrating the stratigraphic composition of underground layers. For this purpose, we use professionally designed computer software, which triggers the multi-channel setup and it automatically switches pairs of electrodes into a number of pre-programmed 4-point configurations (Tsokas et al., 2012).

However, ERT is a time-consuming method, as in this method setting the layout for each section takes longer compared to other methods (such as magnetic) and the number of the data points are vastly more than previously mentioned methods, therefore, it allows us to focus on the smaller areas. To understand different archaeological and geological layers we can use both 2D or 3D measurements.

ERT method, as a part of integrated geophysical methods, can serve as an ideal tool to trace archaeological features and it provides a detailed image of the subsurface electrical resistivity distribution, which helps us to detect substructure features. Above all, ERT and resistivity prospection is an active geophysical prospecting method and the main advantage of these methods in this area is that they are not disturbed by modern buildings or other technical installations nearby as is the case for magnetometry. Ground Penetrating Radar (GPR) prospecting could be an alternative, but the first trial of the method, which was done in Yeha by the DAI in 2011 failed. Uneven ground and the coverage of the topsoil with rough and irregularly shaped stones and pebbles prevented a successful survey of the area.

The aim of this research was to use magnetometer and 3D ERT prospection to combine, compile and compare the result of the two methods to make a visual image of the subsurface of this area. Moreover, we desired to investigate the extension of Yeha in ancient times to the south and to make 3D models of the substructures as a guide for future probable excavations.

6.2. Geophysical survey

6.2.1. Magnetic Data Acquisition and Processing

Magnetometry is one of the most used methods to find archaeological features and ancient activities, as it provides information about the remanent magnetization, such as kilns and fireplaces, as well as the induced magnetizations due to the enrichment of ashes and magnetic minerals in pits and ditches (Le Borgne, 1955). In this survey, we used the Scintrex Smartmag SM4G-Special and the Geometrics G-858 Caesium total field magnetometers in the so-called duo-sensor configuration to reach a high sensitivity and a maximum speed of the prospection (Becker, 1999); with a sampling

rate of 0.1 s and a traverse interval of 50 cm, we gain a spatial resolution of 25 x 25 cm. The diurnal variation near the geomagnetic equator was comparatively low and allowed us to reduce it to the mean value of all data of each 40 x 40 m grid (Fassbinder & Gorka, 2009). We fixed the probes on a wooden frame and carried them around 30 cm above the surface. Depending on the magnetic contrast, this method allows visualization of archaeological features to a maximum depth of 3 m but it hardly provides the information on the depth of an object or feature. Moreover, in the presence of a multi-layered substructure, with this method, it is rarely possible to distinguish multi-layered archaeological features (Fassbinder, 2015). Further difficulties for the application and archaeological interpretation of magnetic anomalies arise due to geographical and geomagnetic conditions near the geomagnetic equator (Fassbinder & Gorka 2011; Hahn et al., 2021 (in preparation)).

6.2.2. ERT Data Acquisition, Prospecting and Visualization

The ERT instrument, used for this research, is 4-point light 10 W, by Erich Lippmann (Lippmann Geophysikalische Messgeräte, Germany) (Figure 6.3). For ERT measurements, we conducted surveys with 40 electrodes for each 2D measurement and the interval spacing of 0.5 x 0.5 m to gain a high spatial resolution for archaeological interpretation.

The ERT measurements can be done by different electrode configurations. Each of these configurations has its advantages and disadvantages. Some factors, such as target structure, sensitivity to background noise, signal to noise ratio and the penetration depth play a role in choosing the suitable configuration (Aber & MeshinChi Asl, 2010). The Wenner and dipole-dipole arrays have a higher signal to noise ratio, in comparison to other arrays and are the most popular configuration in archaeological geophysics. The dipole-dipole configuration is more sensitive to lateral variation and is suitable to detect features such as walls and cavities. The Wenner array covers a greater depth and is more sensitive to vertical variation (Griffiths & Barker, 1993). In this research, due to the conditions and the anomalies that we were expecting, we applied the dipole-dipole configuration.

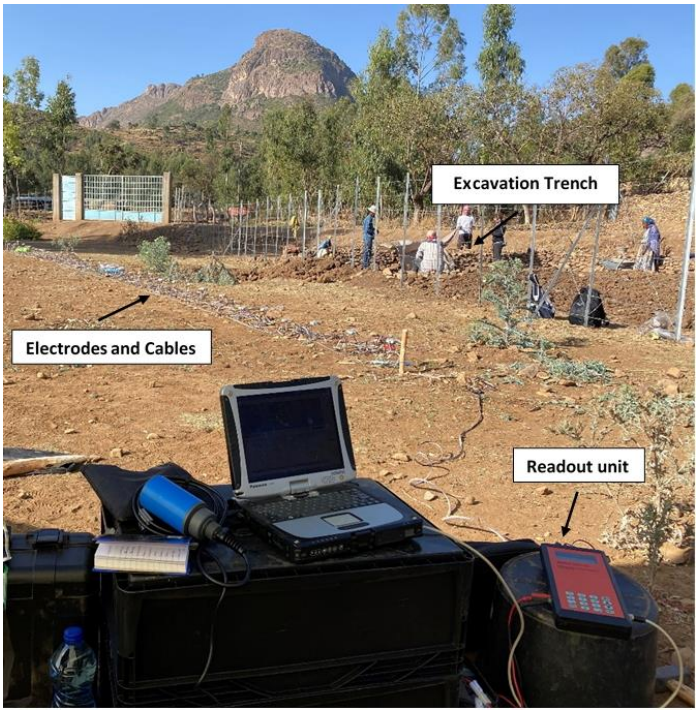

Figure 6.3. General field conditions during the ERT measurement in the Shilanat area of Yeha with the 4-point light 10 W instrument.

In 2D modelling, the result shows the resistivity distribution in a vertical two-dimensional plane. However, underground substructures are in 3D shape, therefore, a 2D image can lead to a wrong interpretation. Consequently, a 3D model is suggested to generate the best and most accurate underground image. In this research, the software for data processing is “RES2DINV” and “RES3DINV” and for further 3D data visualization, “Voxler” is used. To obtain the most accurate model from the substructures, we applied both the smoothness-constrained and robust inversion. The smoothness-constrained inversion tends to detect the smoothest variation in the resistivity values and the robust inversion method minimizes the absolute changes in the resistivity values and therefore, produces a model with sharp interfaces. Analyzing data sets based on both inversion methods benefit us to obtain a better understanding of the shape and the material of the underground anomaly. The forward resistivity calculations were based on the finite-element method (Loke & Dahlin, 2002; Constable et al., 1987; Getaneh et al., 2018).

6.2.3. TDR Measurements

Due to occasional rainfalls during our expedition in Yeha, we decided to assure the stability of ERT data and the contact resistance. To check this stability we used Time Domain Reflectometry (TDR), which measures moisture, temperature and the conductivity of the topsoil. This instrument is based on radar technology with an electromagnetic TDR impulse of 1 GHz, it is fast in measuring and its principle is based on the transmission of a short voltage pulse between the two probes (Linck and Fassbinder, 2014).

6.3. Results

Prior to ERT prospecting, a large-scale magnetometry prospection has been done in Yeha (in total 31 40 x 40 m grids were measured) to get an idea of the extension of the ancient settlements. Figure 6.4 shows an overview of Yeha, with the exact positions of all of the magnetograms (shown with white frames) and the magnetogram of the Shilanat area at the south. Due to the presence of several disturbances, such as modern buildings, metal installations, pipes and field boundaries that are highly magnetic, the magnetic interpretation became a challenge (Ostner et al., 2019). These problems highlight the importance of the necessity of the combination of multiple prospecting methods.

A careful selection of the study area for ERT measurement was performed. After analyzing magnetograms, inspecting archaeological documents, examining old and new excavation reports and considering the feasibility of applying the ERT method in all possible parts, the area of Shilanat was chosen for further prospection.

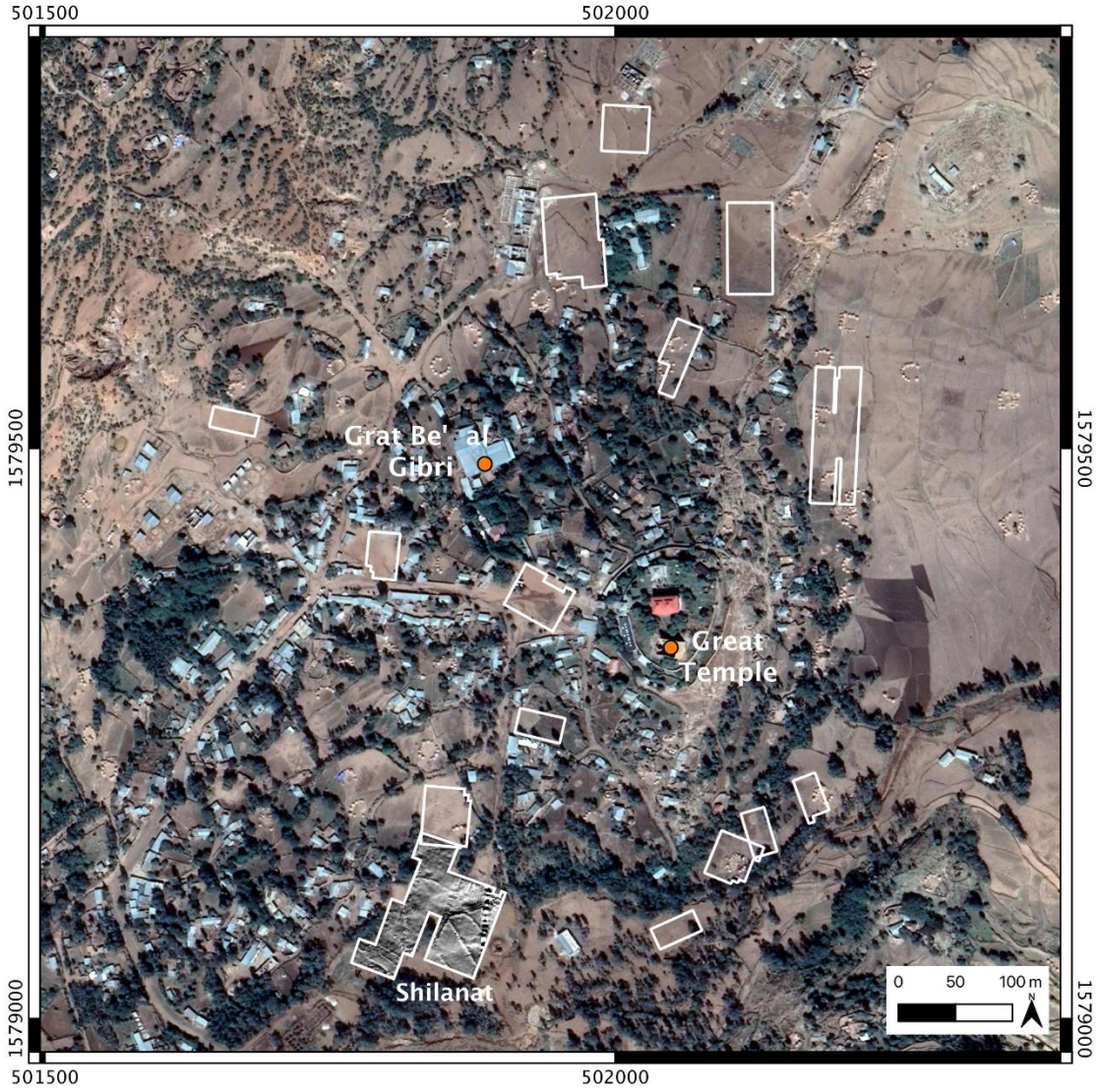

Figure 6.4. Overview of Yeha with the positions of magnetograms (shown with white frames) over it.

In the result of the magnetograms of the Shilanat area (Figure 6.5), we could detect the presence of a multitude of pits as well as some further vague features that could be interpreted as stone walls. Moreover, Shilanat was an interesting area for archaeological excavations as the survey showed several ancient pottery sherds scattered on the ground and the residents reported ancient findings.

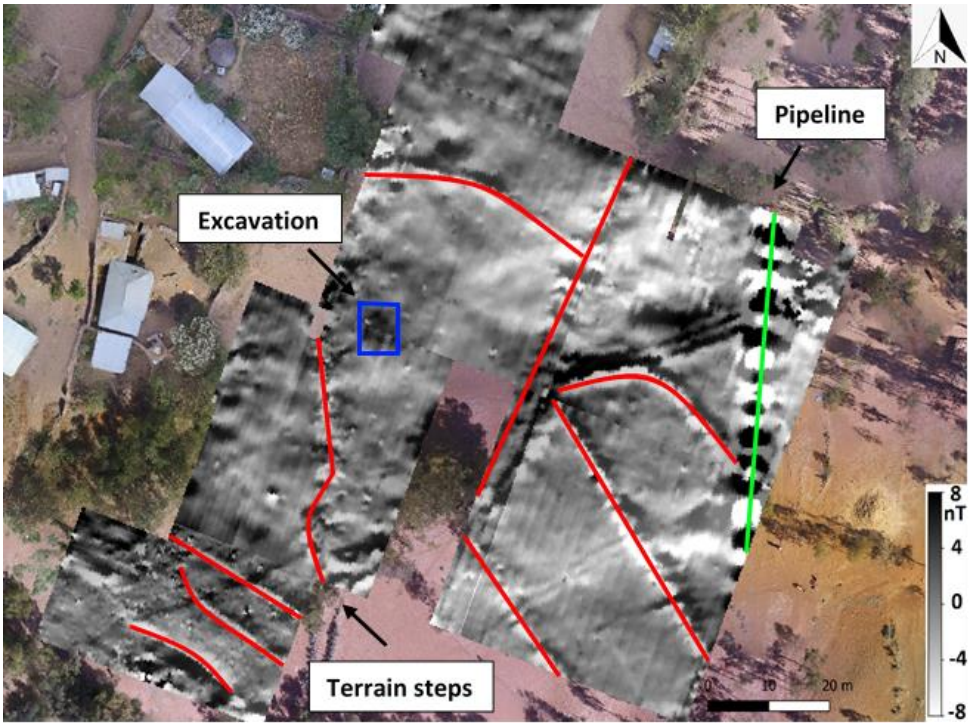

Figure 6.5. Magnetogram of a part of the Shilanat. The green line illustrates a pipeline, the red lines show terrain steps and the blue rectangle indicates the position of the excavation (trenches II-IV).

Figure 6.6 shows a picture of the old excavation trench (it is now refilled) from a multi-layered substructure (layers are shown with numbers inside of the Figure). The walls are made of stone rubble consisting of at least three different types of rocks (according to the susceptibility measurements). The pottery found in this trench, are dated to the Aksumite and Pre-Aksumite period. The stratigraphy of the trench points to a mixed surface layer followed by Aksumite settlement layers with architectural remains and house inventory. The lowest layer reached, presents the surface of a wall structure and might belong to the Pre-Aksumite period, which has to be verified. We chose to create a 3D model of the ERT data next to the excavation, to check if the excavated structure continues to the east side of it and to examine the possibility of the existence of further substructures in addition to this structure.

Figure 6.6. Excavated trench (which is now refilled) directly next to the chosen place for ERT measurement. The top part of this picture is toward the north. (Photo from DAI archive)

The 3D measurement method we chose for modelling is via measuring parallel 2D survey lines and collating them afterwards. For this purpose, for the first 3D modelling, we measured 12 parallel 2D lines. Each of them was laid in the north to south direction, with 0.5 m x - spacing with a total length of 20 m (for each section we used 40 electrodes). The first survey line of these parallel lines was 0.5 m away from the refilled excavation trench and 5 m away from the open trench.

As we expected to detect walls in the shallow depth, we applied the dipole-dipole configuration for our purpose. We measured the parallel lines with 0.5 m y - spacing in the east of each of the previous lines.

As these sections were measured in different hours during three days, we conducted sets of TDR measurements in parallel to our daily measurements, to monitor moisture percentage, soil temperature and topsoil conductivity. This allows us to check the consistency of resistivity values compared to changes in temperature, moisture and conductivity of the topsoil.

The TDR measurements reveal a maximum change in the moisture of the soil of 1.2 %, a maximum temperature change of 12.3 °C and a maximum change in the conductivity of 0.37 dS/m during the measurement time with the instrument measurement error of ± 2 %. By measuring these values, the concern is to check if the resistivity values are significantly affected by these changes and, if necessary, to correct the data. By checking maximum, minimum and the trend of the resistivity values of all of these sections, we can observe that these variations in temperature, moisture and the conductivity of the topsoil did not affect the data. Therefore, we could process our data without any major correction.

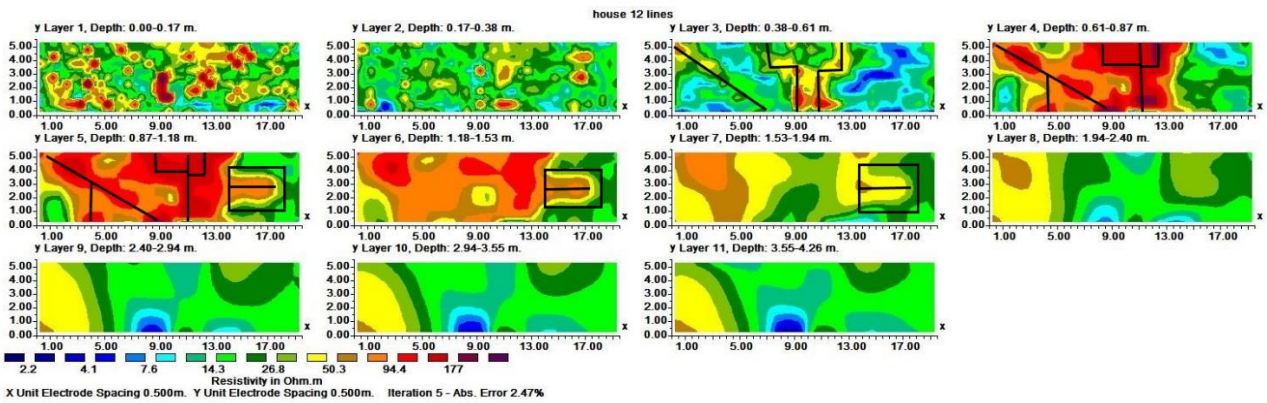

Figure 6.7. 3D model of the ERT data in the first area of a multi-layered substructure. The x-axes show the length of the survey line, each panel (from layer 1 to 11) shows the x-y plane in different depths (from the surface to a depth of 4.26 m ± 10 cm) and each colour represents a resistivity value. The black lines (starting from depth layer 3) show the positions and the lineation of the anomalies, which can be man-made (at a depth of around 40 cm deep and continuing for 2 m). Rectangles (starting from depth layer 5) show the position of the second layer of the anomaly, which appeared at a depth around 1 m.

The result of the 3D-modelled ERT data of this area, calculated from 12 parallel survey lines, is shown in Figure 6.7. In this Figure, each colour represents a specific resistivity value and it is plotted from the surface to a depth of 4.26 m ± 10 cm in eleven depth layers. Two layers of higher resistive anomalies (in the range between 80 and 170 Ωm), possibly of man-made origin, one starting at around 40 cm and the

other one at around 1 m, are appeared in the results. The data misfit for this data set with 5 iterations is 2.47 %.

To have a better understanding of the anomaly, we plotted a vertical cross-section view of the same data set with the same measurement conditions (Figure 6.8). This Figure demonstrates the model in x-z planes in every 0.5 y - spacing in eleven planes, in which we can observe the same higher resistive anomaly (between 80 and 170 Ωm), which is surrounded by lower resistive anomalies.

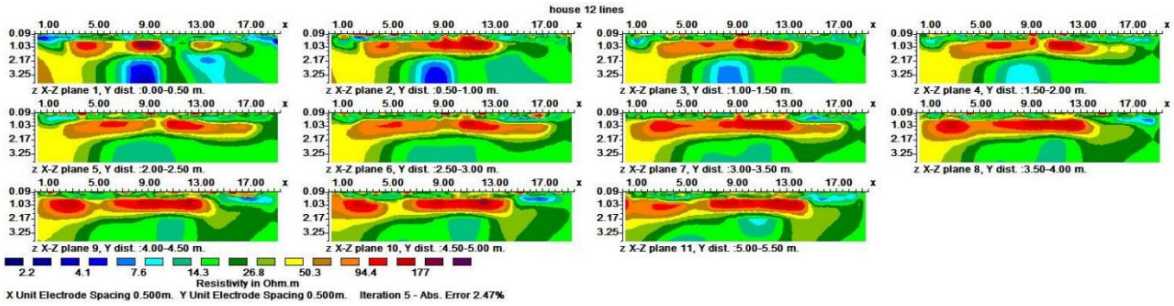

Figure 6.8. 3D model of the first area based on the ERT data. The x-axes show the length of the section and vertical axes show the depth. This Figure shows the result in x-z planes in every 0.5 m y - spacing.

After creating the first successful 3D model based on ERT data in this area and discovering some underground structures, we measured the second set of ERT 2D measurements, in the same area at the northeast of the first place to develop a new 3D model to better comprehend the underground substructure and its extensions. For this survey, we applied the same measuring condition as before but with a smaller number of parallel 2D survey lines. We measured six parallel north to south 20 m sections with 0.5 m electrode spacing and dipole-dipole configuration. Figure 6.9 illustrates the 3D model of this result based on ERT data. The data misfit for this data set for 4 iterations is 3.63 %. In this Figure, each colour represents a resistivity value and the resistivity values, which are in the range between 40 and 80 Ωm (Shown by black lines in the Figure), can be a man-made anomaly.

Similar to the first model, additionally, we plotted the vertical model of the ERT data of this area (Figure 6.10). The Figure visualizes the results in x-z planes in every 0.5 m y - spacing.

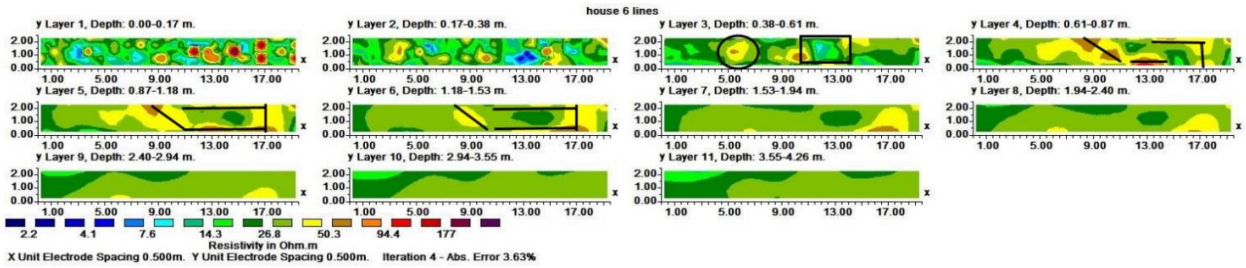

Figure 6.9. 3D model of the second area based on the ERT data. The x-axes show the length of the survey lines and each panel (from layer 1 to 11) shows the x-y plane at a different depth. The black lines (starting from layer 3) indicate the position and direction of possible substructures in different depths.

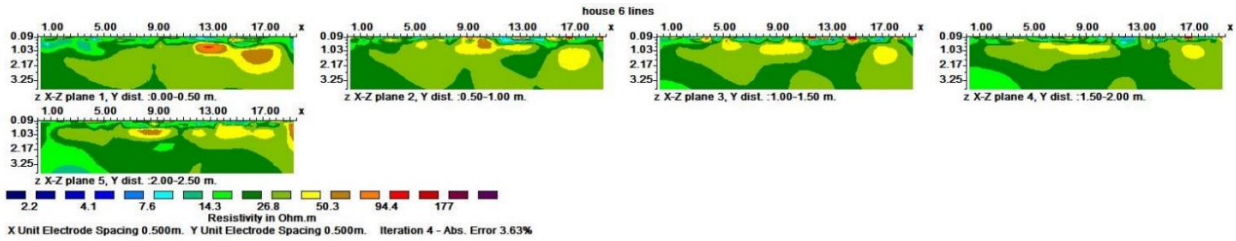

Figure 6.10. 3D model of the ERT data in the second area. The x-axes show the length of the sections and the vertical axes show the depth. This Figure shows the result in x-z planes in every 0.5 m y - spacing.

6.4. Integrated Data Interpretation

In the first area (Figures 6.7 and 6.8), based on the shape of the higher resistive anomalies and their positions with respect to each other, we can assume that the anomalies represent walls. By considering the resistivity values of this substructure, which were in the range between around 80 and 170 Ωm, and comparing it with the periphery soil, we can conclude that the material used for the walls can be made from gravels (or other larger sized rock fragments).

Based on the material of these walls, their lineation and elongation with respect to the refilled and open trench excavations, we deduce that it is probable that this anomaly belongs to the east extension of walls that appeared in the excavations. Similar to the excavations, we observe two layers of substructure, one starting at around 40 cm (shown by lines in Figure 6.7) and the second layer starting at around 1 m (shown by a rectangle in Figure 6.7). The presence of the second layer in the deeper part verifies that we mapped a multi-layered structure.

Moreover, the blue anomaly, which appears at around 2.20 m depth, can be a representation of highly saturated soil, as the ERT measurement time was right after the rain season, and consequently, it is expected to have higher underground water, which supports our assumption.

In the second area (Figure 6.9 and 6.10), the higher resistivity values (shown in brown, orange and red), in the range between around 40 and 80 Ωm, presumably for the same reasons as the previous data sets are walls.

Since this part of the area was limited from one side with a fence and had a sudden depression on the other side, the maximum possible number of parallel survey lines that we could measure was six. Therefore, the final map is not large enough to detect the exact pattern of the substructure. However, we can recognize the presence of some walls from the anomalies in both horizontal and vertical models. The material, of which these walls were made, can be either baked-bricks or gravel (or other larger sized rock fragments).

The anomaly values of areas 1 and 2 do not completely match. This could be because either we are plotting two different substructures or we detected one substructure but it is completely or partly made of different materials.

After the first interpretation, in order to have a better view of these probable walls and their positioning under the surface, we plotted them in an iso-surfaced model based on a constant resistivity value in 3D volume. For this purpose, we generated a custom

colour scale to demonstrate the anomaly in the best way. Figure 6.11 shows this visualization from different views for both areas 1 and 2. The chosen resistivity value for area 1 is 70 Ωm and for area 2 is 31 Ωm.

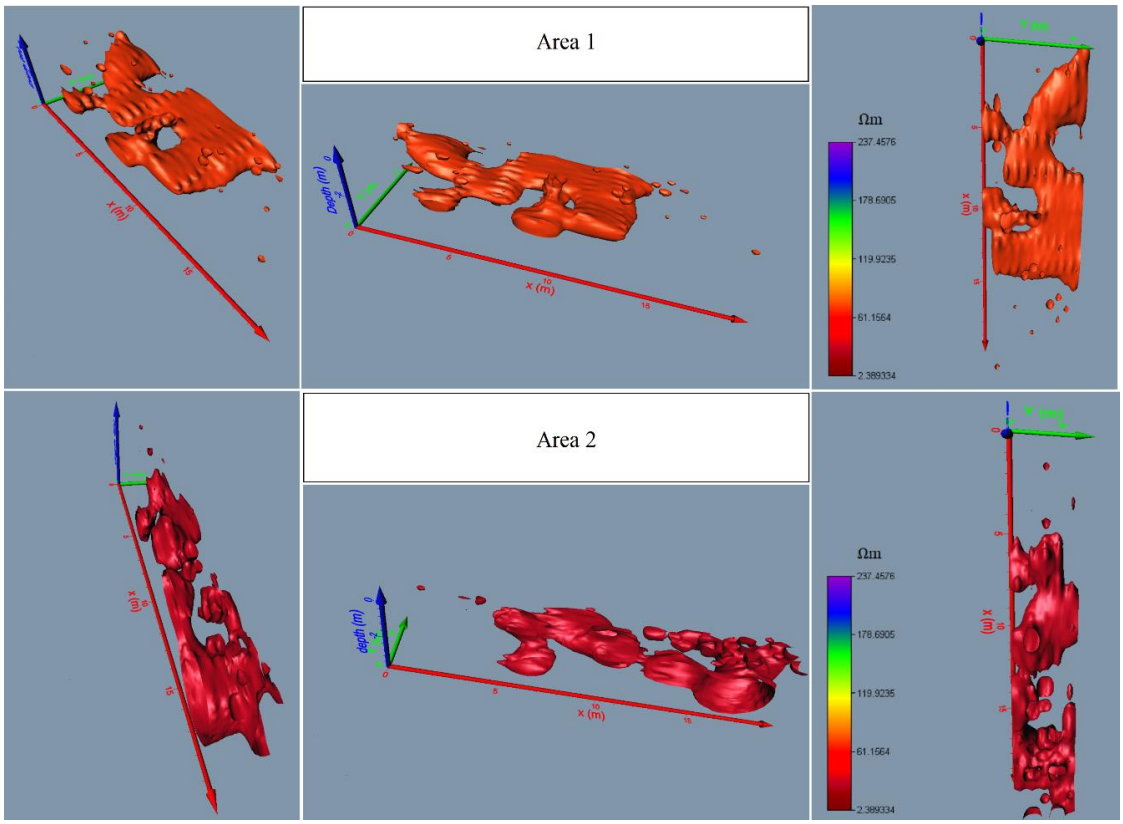

Figure 6.11. 3D iso-surfaced model of the substructure of area 1, with the resistivity value of 70 Ωm and area 2 with the resistivity value of 31 Ωm.

As a final step, we overlaid the 3D ERT models on the magnetogram to compare the results of both prospecting methods (Figure 6.12) and to discover similar patterns for other probable man-made anomalies. Figure 6.12a demonstrates layer three (from Figures 6.7 and 6.9) of the 3D model over the magnetogram and the shallower layer of the multi-layered structure (from 0.38 to 0.61 m). Figure 6.12b shows layer five (from Figures 6.7 and 6.9) of the ERT model over the magnetogram and illustrates the deeper layer (from 0.87 to 1.18 m) of the interconnected walls. The blue lines in this Figure point out some of the underground features that we see in both magnetic and 3D ERT. Although we could not conclude from the magnetic results whether these features have geological or archaeological properties, by analyzing the ERT results of different

layers from different directions and due to their shape, we suggest that these features have an archaeological origin. The archaeological interpretation and the function of these features are still under debate.

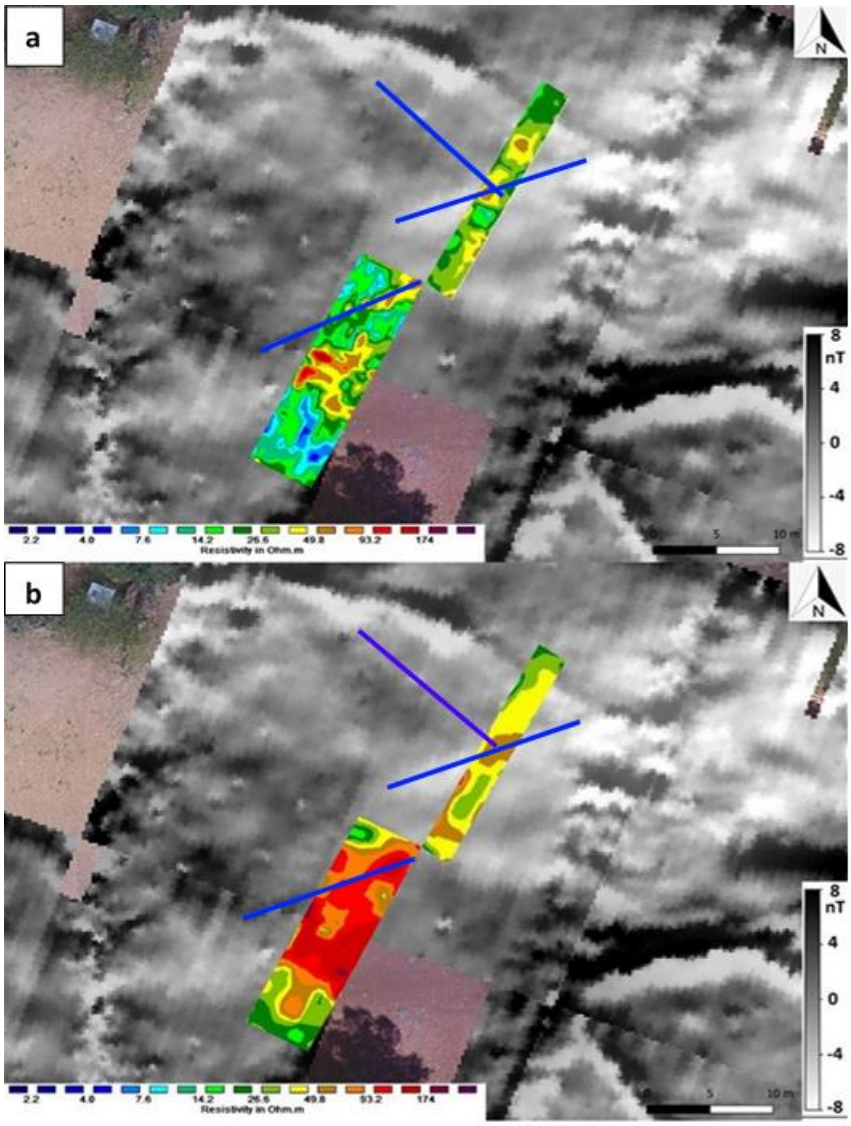

Figure 6.12. 3D modelled ERT data overlaid on the magnetogram. Blue lines illustrate the archaeological base substructures, which are detected by both methods. Part "a" illustrates depth layer three (from 0.38 to 0.61 m) and part b illustrates depth layer five (from 0.87 to 1.18 m).

6.5. Discussion and Conclusion

There are several constraints, which limited and complicated the magnetic prospection. In this area, mostly just small measuring grids for magnetometry were available and the presence of modern infrastructures such as modern houses, pipelines and electrical power cables disturbed our magnetic measurement.

Moreover, the presence of plenty of highly magnetic rocks over the surface, volcanic geology, field boundaries that are highly magnetic (visible on the magnetogram) and prospecting near the geomagnetic equator, which provoked some problems due to shallow inclination and low total magnetic field intensity (around 30,000 nT), majorly complicates the magnetic interpretation. Consequently, the magnetic prospection was not sufficient for the full interpretation of this area.

GPR prospection, which was conducted as a test measurement in 2011 by the DAI, was not fully successful because of the uneven surface and the occurrence of rocks and gravels that cover the surface. These rocks are spread over the ground to save the field from heavy rains and avoid moisture evaporation from the soil. However, having enough moisture in the soil provides a suitable situation for ERT prospection.

One of the challenges we faced in this area is the fact that the building material used in this site in recent years can be similar to the material used in ancient times. Therefore, knowing the depth of the substructure can help us to distinguish modern structures from ancient ones. Although magnetic prospection is one of the most used methods in archaeological prospection, it does not provide information about the depth of the substructure.

In the TDR results, as the first measurement was conducted in cloudy weather, the moisture percentage was rather high. From the second measurement, the sun was out and therefore, in the result of the second measurement we observed a drop in the soil temperature, which was caused by the evaporation. Our interpretation of the TDR data is proof of the fact that small-daily events do not change the ERT results and therefore, there is no need to correct the data for the final modelling.

Although our work was done in the relatively dry season (with some occasional short rainfalls), we were able to present high-resolution ERT results. Both 3D models of the ERT data illustrate underground structural walls in two different layers. The first 3D model was 5 m away from the open excavation trench and 0.5 m away from the back-filled excavation trench, which proves the continuation of the unearthed structures on the east side of the excavation. Therefore, the shallower layer of the model could be from the Aksumite period and the deeper layer from the Pre-Aksumite period.

The second set of parallel 2D sections was measured to make a new 3D model in the northeast part to check the possibility of the extension of this substructure toward the northeast. A comparison of the resistivity values of each depth layer of both measurements shows a low probability of the connection of these substructures. Due to the condition of the field and the limitation of time, it was not possible to measure larger areas and to perform further investigation.

According to the resistivity values in the first area, our measurements reveal that the walls are made of stone, mostly gravels (or other large-sized rock fragments) and in the second area they are made of either baked-bricks or gravels (or other large-sized rock fragments). The height of the walls (depending on the structure) is between 60 and 120 cm.

Two assumptions as the reason for having this height of the walls will come up. It either can be because of the low preservation of the stone walls or because of the wood-stone structure that is common in some of the buildings in this area, in which the wood is rotted and just the stones remained. As these houses are assumed to be for the common people, and therefore, are made of pure rubble, the first hypothesis is more probable and the low preservation was caused by natural erosion and stone robbery. The archaeological site around the temple and the palace have been occupied for 3000 years and it is densely overbuilt by modern houses. For these houses, stones of the previous buildings of the settlements are reused.

In this paper, we showed that resistivity tomography prospection allowed us an easy detection of stone-built underground features and showed the extension of the ancient

city to the south and gave us valuable information about the depth of each one of the features. Furthermore, this instrument helped us to verify the existence of some features that were detected vaguely by the magnetometer measurements. However, more research is needed to get more information on these features.

As an additional point, it is important to highlight that the minimum distance between the electrodes and metal fences, which were already there to construct a tourism bus station, is 4.5 m (nine times more than electrode spacing), which is one of the reasons for not observing the disturbance of fences in ERT data sets. To build this bus station, the local people have made several unsupervised diggings, which led to the seeming destruction of parts of the archaeological substructures in Shilanat. Putting the bus station in operation and its maintenance also would risk a further loss of important archaeological knowledge. With ERT results, we offered detailed information and confirmed the proof on the extension of the Aksumite and Pre-Aksumite city in the area, especially wall structures and provided sufficient reasons to the local administration to stop the further modern constructions in this part of the city to save archaeological underground structures and the accompanying knowledge on the settlement history of Yeha. After this research, in 2021, the Shilanat area of Yeha was announced as a cultural heritage area.

Acknowledgements

The research of the ancient cultural area of Yeha is in the foreground of the Ethiopian-German joint project of the Sanaa branch of the Orient Department of the German Archaeological Institute and the Friedrich Schiller University Jena in cooperation with the Authority of Research and Conservation of the Cultural Heritage (ARCCH) and the Tigray Culture and Tourism Bureau (TCTB). The German Research Foundation (DFG) has been funding the project as part of a long-term project since 2016.

Moreover, Mandana Parsi greatly appreciates the funding of her short-term scientific mission (STSM) in the Institute for Mediterranean Studies-FORTH in Greece by the European Cooperation in Science and Technology (COST) under the number

CA17131 and thanks to the IMS-FORTH lab for being a great host to help her learn more about the 3D modelling of ERT data sets.

7 Venice in the desert: Archaeological geophysics on the world's oldest metropolis Uruk-Warka, the city of King Gilgamesh (Iraq)

(The following chapter (Fassbinder et al., 2019) is in a slightly altered form published on New global perspectives on archaeological prospection: International Conference on Archaeological Prospection, 13:197-200.)

7.1. Historical Background

Uruk-Warka, UNESCO-world heritage site together with Ur and Eridu, can be claimed to be the world's oldest megacity. Here the invention of handwriting and the scene of action of the oldest epic of humankind, the famous "Epic of Gilgamesh", took place. The inner city covers an area of c. 555 ha and was populated by c. 40,000 people already in BC 3000. The diameter of the enclosed city is 4-5 km; the city wall has a length of c. 9 km and is up to 8-25 m wide. Uruk was inhabited for nearly 5000 years till the 3rd century AD. Its occupation ended when the Euphrates River changed its way towards west and since this time the site remained untouched as a huge heap of adobe mudbricks with a Ziggurat on top (Figure 7.1). Magnetometer measurements revealed a sophisticated water canal system, which provided access to the different city quarters, but also protected the inhabitants from the danger of annual flooding.

7.2. Prospecting Method

Magnetometer prospecting was initiated in 2001 and continued in 2002, resumed in 2016 and carried out for a larger area in 2018 and 2019 (Figure 7.2). For the survey, we applied three different types of magnetometers: a caesium Scintrex Smartmag SM4G-

special, the caesium Geometrics G-858G magnetometer (both applied as total field magnetometers in a so-called duo-sensor configuration) and a Foerster Ferex 4.032 fluxgate gradiometer in a so-called “quadro-sensor” configuration. Ground conditions are of soft and muddy, or dusty and salty soil. To get further information about the depth of the canals and the adobe city wall, we applied an ERT (4-point light 10W) system with 60 active electrodes (ActEle), which allows spacing of 0.5m to 5m.

Figure 7.1. Uruk. Panorama view of the city center with the Ziggurat.

7.3. Results

Our magnetometer prospection now covers an area of c. 70ha and revealed a network of waterways, ship canals, harbours and moles, water gates and landing places that gave access to different city quarters. The water network crosses the city from north to south, provides water for the irrigation of gardens inside the enclosed city, and protects the inner city from floodwaters (Figure 7.2).

The magnetometer surveys focus on the south-western part of the city inside and close to the city wall. The magnetometer results reveal one of the main canals, coming from the north gate and leading to a large harbour in the western part of the city, passing settlement areas in the east of the “Sinkashid” palace and a settlement area southwest of the palace (Becker et al., 2013). In the south, this harbour is limited by a mole and a water gate, obviously to regulate a junction to another branch of the canal. This branch reaches towards the south-east direction, connecting another settlement area,

which due to archaeological field survey results, can be dated into Obeid and early Uruk-period (Finkbeiner, 1991). Further to the south the main canal leads to a spacious agricultural field system with a complex network of irrigation canals.

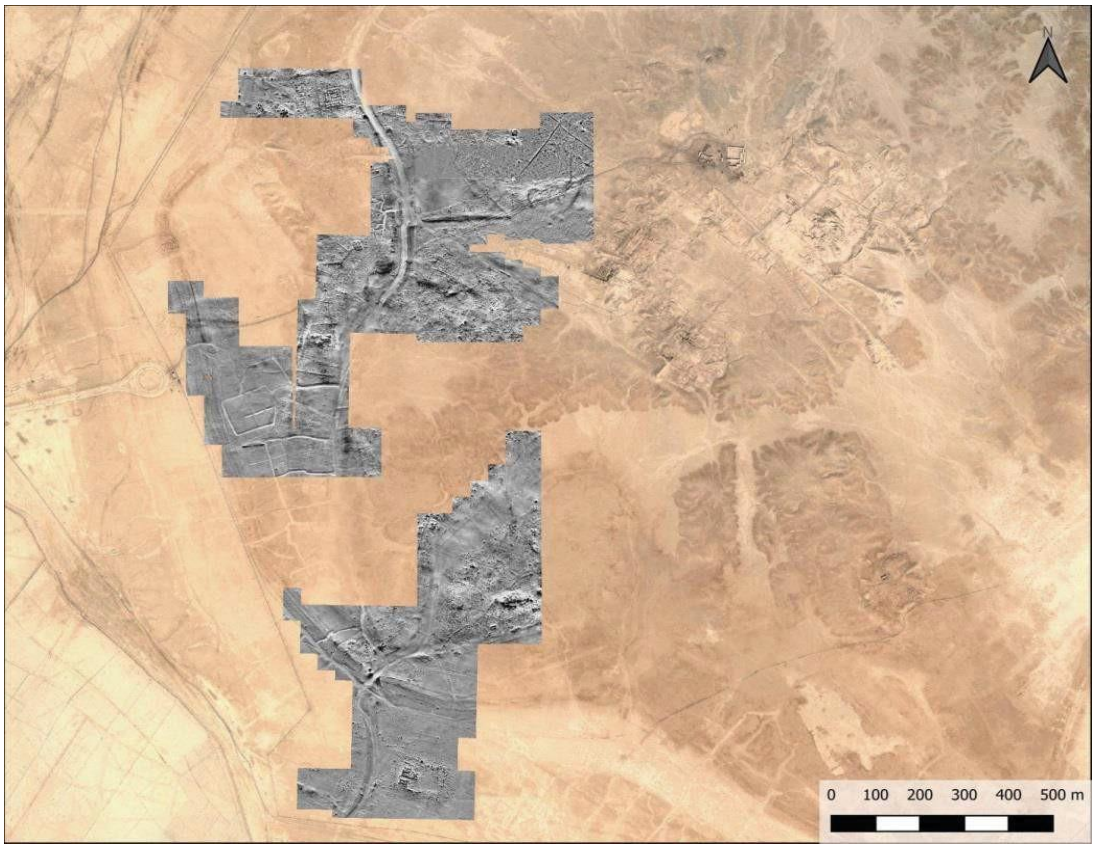

Figure 7.2. Magnetogram of the survey areas 2001-2019. Caesium-magnetometers Scintrex SM4G-Special and Geometrics G-858, both in duo-sensor configuration, dynamics ±25 nT in 256 greyscales, spatial resolution 25 cm x 50 cm. The average total Earth's magnetic field intensity in Uruk increased from 2001 to 2019 from 45,180 ±20 nT to 46,000 ±20 nT.

A second large area was measured at the southern city, bringing to light the detailed structures of the city wall with bastions that are described in the Gilgamesh Epic. In the south, the city wall and a canal crossing itcan be seen. Here, the course of the city wall and, at regular intervals, its bastions, known from previous excavations and doc-

umentation elsewhere in the city, are clearly visible. The data moreover seems to indicate that parts of the wall on its inner and outer faces are made of fired bricks; a detail that was not known before (Fassbinder et al., 2005).

Excavations undertaken in late March 2019, however, furnished the proof that these adobe bricks were tempered by pottery debris and thus behaved magnetically like burned bricks. It is also apparent that the wall was made out of several separate layers that were previously unknown and that the canal that circled the city ran just outside it. The entire wall complex was nearly 20 - 40 m wide. The wall itself, with its inner and outer shells of tempered bricks, is some 9 m thick, an observation that corresponds with the excavation results. Further details about Uruk's structure are provided by the magnetogram of the southwest gate, which is nearly 15 m wide and can be interpreted as a floodgate, where the inner city's large east, west and central canals flowed out through the wall. On the outside, the gate was flanked by towers and strengthened very probably with fired bricks. In front of the floodgate at a distance of 240 m, a small side canal branches off to the southeast, expanding roughly midway in front of a large building of fired bricks into a small harbour- like structure.

7.4. ERT Measurements

In spring 2019, for the first time, we applied complementary ERT measurements on a range of selected profiles in order to get some additional information on the construction details of the city wall and the construction of the canal. One profile crosses the western canal (Figure 7.3). The results clearly provide us with the evidence that this canal was an anthropogenic construction and not a natural riverbed. Moreover, the ERT method illustrated the sedimentation inside of this canal. The magnetogram already indicates an edging of the canal with burned mudbrick. Now the ERT measurements clearly confirm this assumption.

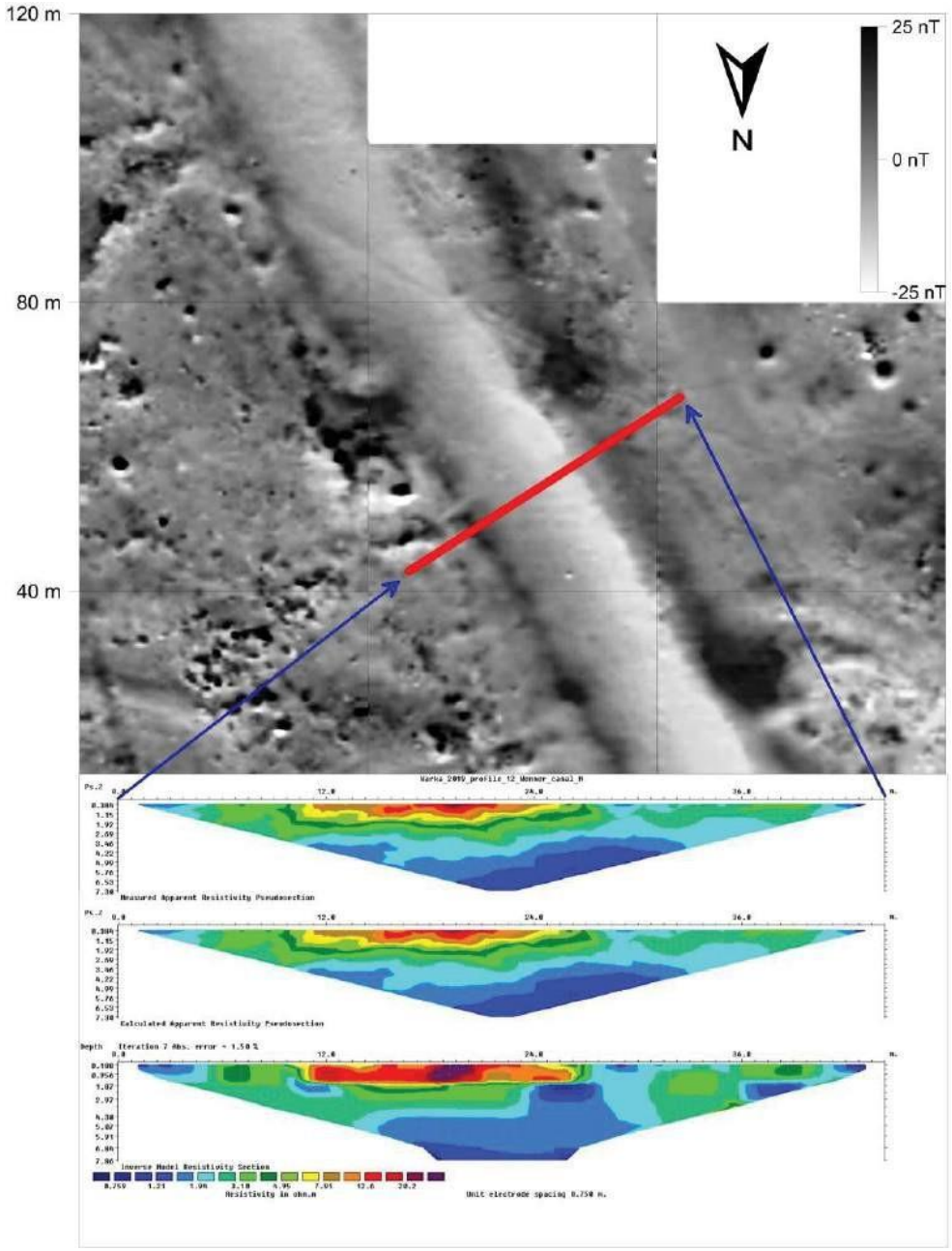

Figure 7.3. At the top: Magnetogram extract of the main canal near the "Sinkashid" palace, the location of the 45 m ERT - profile is marked in red. Below: ERT profile across the canal (0.75 m electrode spacing, Wenner configuration).

7.5. Conclusion

All in all the magnetometer measurements gave insight into settlement areas of different occupations, the western part of the city, has a length of c.1500 m. It is up to

15 m wide and c. 3 m-4 m deep. At several points, slightly smaller canals branch off for the irrigation of fields. Left and right of the bordered canal, we find little landing stages, settlement areas, harbours and moles.

Detailed analysis of the magnetograms, complemented by rock magnetic analysis and further ERT measurements, the topographical information, as well as the available archaeological data, will possibly allow closer insights into the development, structure and function of the city and will support future excavations. The magnetometer survey hopefully will be continued soon and will offer a comprehensive picture of the structure of Uruk through time. Magnetometer prospecting is supposed to be carried out in all accessible areas of the city. Excluded from large scale prospections are the central district of Uruk and the Ziggurat, where already extensive excavations took place during the last 100 years.

8 Conclusion and Outlook

In the framework of this dissertation, the resistivity data of different features and structures made of different constructional material in several countries has been analyzed and modelled. As there was no previous solid research on the detection of mudbrick features with the ERT method and these were also hardly detectable by other geophysical prospecting methods, the main focus of this research was the detection of mudbrick features with ERT.

One of the most spectacular outcomes of this dissertation was in Ur, in which I was able to detect a Neo-Babylonian mudbrick house with the ERT method. Although the resistivity value of the mudbrick features and the periphery soil were quite similar, by using the smoothness-constrained inversion method I was able to distinguish mudbrick features, as I could map the smoothest changes in the resistivity values and model the structure in 3D form.

This detection was a new start and one of the most important results in the recent researches in the discovery of mudbrick features with the ERT method and led me to our main project entitled “Achaemenid residences and their paradises”, which was focused on the Achaemenid Empire and its impact on the historical, political and the monumental architecture in the Caucasus region. In this study, I conducted several dense parallel 2D survey lines in order to collate the data in 3D form and as mudbrick walls were made of highly similar material to the background anomaly, based on the mathematical proportion proved in the paper, I focused on the higher density of the mudbrick walls, which causes a slightly higher resistivity value compared to the periphery soil. After modelling the data, I observed that resistivity values that I could refer to as the structural walls were varying in a wide range. The conclusion was that the structure is presumably partly burnt and this is the reason that at some parts the resistivity value is quite close to the background anomaly and at some parts is as high

as baked-bricks. This conclusion was supported and verified by the result of the excavation. The research on the mudbrick features highlights the fact that to analyze the data in more advanced form, applying different types of data processing is necessary. Moreover, I showed that the ERT method is an ideal tool to detect the Achaemenid buildings and structures, especially in the Southern Caucasus region.

Additionally, by the examples in Uruk, Kurdistan and Ur I showed the applicability of this method for the detection of harbours, qantas and canals, not only by detection of the shape and depth of these features, but also by illustrating the gradual sedimentation in them over time. In the harbour detected in Ur, I could reveal the initial depth of the harbour, as well as the gradual sedimentation that happened within the time of its usage and the final depth, in which they used this harbour for a longer time. Next to this harbour, I detected a baked-brick wall, which I suggested was the main wall of this harbour.

In the case studies in Kurdistan and Yeha, I showed the effectivity of the ERT method in the detection of multi-layered structures and the possibility of analyzing each one of the layers in detail. The ERT result in Kurdistan was one of the first proofs of the presence of a deeper archaeological layer in this area. A radiocarbon dating of a charcoal sample collected from a drill core in this part, pottery survey and a discovery of a Chalcolithic kiln in the area supported the suggestion of the presence of this deeper archaeological layer (probably mudbrick) based on ERT results. These results initiated a new research project with Gerda-Henkel Stiftung to obtain further information about this deeper settlement layer.

In Yeha, based on the ERT result, I verified the extension of the ancient city (Aksumite and Pre-Aksumite), proved the multi-layer stratigraphy and provided adequate reason to the local administration to stop any further modern construction in the area. Based on this research, this part of Yeha was announced as a cultural heritage area.

Another important result of this dissertation was concluded from the results of the Peiting project, which was derived from the comparison between the robust and the smoothness-constrained inversion method. This comparison let one to observe that

some walls were destroyed or removed through time and with the smoothness-constrained inversion method it is possible to detect the remnant of the densification that happened due to the pressure of these walls (at the time of their presence) on the soil beneath them. In archaeological geophysics, such remnants are defined as “ghost features”, since they are visible by geophysical prospection and cannot be detected by traditional archaeological excavations. Therefore, to model the initial shape of the underground structures, as they are not necessarily fully preserved through time, operating the ERT method and the combination of different geophysical methods is necessary. Moreover, I showed that the 3D ERT results are as detailed as the GPR results; therefore, in the cases that the usage of the GPR is not applicable, ERT is a trustable substitution.

Although the ERT method is a time consuming method, and therefore, the measurement area is generally smaller compared to large-scale prospecting methods, I showed that it is a powerful and practical method for the detection of structures made of different type of materials in various areas and countries. Depending on the type of the inversion method used for the data, one can obtain results with different focuses, which can help to model a more realistic map of the initial shape of the underground structure.

Future Perspective

In this study, I collected several thousand data points and provided a data bank with a high variety of prospections on different locations and over different materials, which creates a unique opportunity for further researches.

A future resourceful addition would be using data collected from excavations for numerical modelling and comparing its results with the outcome, which was modelled from the measurement data collected in the field. By these means, we can calculate the exact deviation of the result of our measurements with respect to the position of these features and consequently calculate the exact error of this method for each one of the materials.

It is known that the moisture content percentage of the soil can play a role in the resistivity results; therefore, big events such as changing seasons can slightly change the results. A future research goal is to check the effect of the different seasons on the resistivity results. We can seasonally or monthly, if it is applicable, measure one specific survey line, on one already investigated site, compare the results with each other and with the numerically modelled data to have a better and deeper understanding of the deviation of the results with respect to each month and each event. Moreover, with the TDR instrument, we can monitor the soil moisture percentage to compare it with the resistivity result of each month and/or season and finally we can have beneficial information for more advanced interpretations.

In the detection of the mudbrick, I proved mathematically and practically that the ERT method is capable of detecting these features; however, we can take one-step further and produce in laboratory mudbricks with different soil contents and different densities and finally we measure the resistivity values of each one of these bricks. This process helps us to compare the density and its exact relation to the resistivity value and finally we can calculate the exact proportionality between these two parameters.

9 Further Publications and Conference Presentations

In previous chapters, I published some of the main papers, in which I authored or co-authored. In the following is the list of other papers of mine, which are not published in this dissertation:

a) Fassbinder JWE, Becker F, Hahn S, Parsi M. 2021. Archaeological Geophysics: Case Studies from Bronze Age/Iron Age Sites in the Alazani and Shiraki Plain, Kakheti, Georgia. In the Caucasus: Bridge between the urban centres in Mesopotamia and the pontic steppes in the 4th and 3rd millennium BC / Der Kaukasus Brücke zwischen den urbanen Zentren Mesopotamiens und der pontischen Steppe im 4. und 3. Jahrtausend v. Chr., Scriften des Archäologischen Museums Frankfurt am Main, 34: 333-340. ISBN: 978-3-7954-3439-7.
b) Fassbinder JWE, Hahn S, Parsi M., Becker F, Wolf M, Gagošidze I, Kaniuth K. 2021. Persian Residences in the Southern Caucasus: Latest Discoveries in the Periphery of the Achaemenid Empire. Revue d'archéométrie, 45: 117-127, doi: 10.4000/archeosciences.8404.
c) Hahn S, Parsi M, Fassbinder JWE, Bobokhyan A, Kunze R. 2021. The Ecstasy of Gold: Magnetometer Prospection for the Ushkiani Project in Armenia. Revue d'archéométrie 45: 67-70. doi: 10.4000/archeosciences.8544.
d) Hahn S, Parsi M, Fassbinder JWE. 2021, December. Shallow Inclination in Archaeological Magnetometer Prospection-Theory and Case Examples of the two Ethio-Sabaean Sites Yeha and Melazo (Ethiopia) at an inclination of 15°. In AGU Fall Meeting 2021. AGU.
e) Linck R, Fassbinder JWE, Becker F, Parsi M, Eitel M. 2021. Bodenradaruntersuchung liefert neue Erkenntnisse zur Villa rustica am Kreuther Weg in Peiting. Das Archäologische Jahr in Bayern 2020: 180-182. ISSN: 0721-2399.

f) Linck R, Schönemann L, Fassbinder JWE, Parsi M, Issifu F. 2021. Römische Streuhofvilla mit „Bellevue“ am Hopfensee. Das Archäologische Jahr in Bayern 2020: 177-180. ISSN: 0721-2399.
g) Fassbinder JWE, Linck R, Becker F, Parsi M. 2019. Viereckschanze mit "Außenposten": Magnetometerprospektion im Wald bei Walpertskirchen. Das Archäologische Jahr in Bayern 2018: 160-162. ISSN: 0721-2399.
h) Ostner S, Fassbinder JWE, Parsi M, Gerlach I, Japp S. 2019. Magnetic prospection close to the magnetic equator: Case studies in the Tigray plateau of Aksum and Yeha, Ethiopia. New Global perspectives on Archaeological prospection, 13: 180-183. doi: 10.32028/9781789693072.
i) Thiesson J, Gondet S, Fassbinder JWE, Becker F, Scheiblecker M, Ostner S, Parsi M, Espèron SB, Kaniuth K. 2019, August. Magnetic signal prospecting in a former Achaemenid ‘palace’: the example of Gumbati (Georgia). New Global perspectives on Archaeological prospection, 13: 193-196. doi: 10.32028/9781789693072.

Moreover, I have given presentations in the following conferences:

a) American Geophysical Union (AGU): 2021
b) International Conference of Archaeological Prospection (ICAP): 2021
c) Near Surface Geophysics Group (NSGG): 2021
d) Eurasien-Abteilung des deutschen Archäologischen Instituts (DAI): 2020
e) International Conference of Archaeological Prospection (ICAP): 2019

References

Aber H, MeshinChi Asl MS. 2010. Present a proper pattern for choosing the best electrode array based on geological structure investigating in geoelectrical tomography in order to get the highest resolution image of the surface, the 1st international applied geological congress, Islamic Azad University. 26-28.

Aitken M J. 1958. Magnetic Dating-I. Archaeometry, 1: 16–20. doi: 10.1111/j.1475-4754.1958.tb00204.

Aitken MJ. 1974. Physics and archaeology, 2nd edition. Oxford: Clarendon Press, 286 pp.

Altaweel M. 2017. Electrical resistivity tomography investigations of the qanat system, 2016-2017, Peshdar plain project publications, 2: 33-34.

Altaweel M, Marsh A. 2016. Landscape and geoarchaeology of the Bora Plain. Peshdar Plain Project Publications, 1: 23-28.

Archie GE. 1942. The electrical resistivity log as an aid in determining some reservoir characteristics. Trans, A.I.H.E., 146: 54-67.

Atzemoglou A, Tsourlos P, Pavlides S. 2003. Investigation of the tectonic structure of the NW part of the Amynteon Basin (NW Greece) by means of a vertical electrical sounding (VES) survey. Journal of the Balkan Geophysical Society, 6: 188–201.

Becker H. 1999. Duo- and quadro-sensor configuration for high-speed/high resolution magnetic prospecting with caesium magnetometer. In: Archaeological Prospection. Fassbinder JWE, Irlinger WE, (eds). Arbeitshefte des Bayerischen Landesamtes für Denkmalpflege München, 108: 100–105.

Becker, H., van Ess, M. and Fassbinder, J.W.E. 2013. Uruk: Urbane Strukturen im Magnet- und Satellitenbild. In Vorderasiatisches Museum Berlin and Reiss Engelhorn Museum Mannheim (ed.). Uruk: 5000 Jahre Megacity. Begleitband zur Ausstellung "Uruk - 5000 Jahre Megacity". Petersberg. 355-361.

Burkart U, Günther T, Rücker. 2008. Electrical resistivity tomography methods for archaeological prospection. International Conference on Computer Applications and Quantitative Methods in Archaeology, 35: 1-7.

Caglar I, Duvarci E. 2001. Geoelectric structure of inland area of Gökova rift, south-west Anatolia and its tectonic implications. Journal of Geodynamics, 31: 33–48.

Carey AM, Paige GB, Carr BJ, Dogan M. 2017. Forward modeling to investigate inversion artifacts resulting from time-lapse electrical resistivity tomography during rainfall simulations. Journal of Applied Geophysics, 145: 39-49.

Carson HH. 1962. A seismic survey at Harpers Ferry. Archaeometry, 5: 119-122.

Chambers JE, Kuras O, Meldrum PI, Ogilvy RO, Hollands J. 2006. Electrical resistivity tomography applied to geologic, hydrogeologic, and engineering investigations at a former waste-disposal site. Geophysics, 71: B231-B239.

Constable SC, Parker RL, Constable CG. 1987. Occam's inversion: a practical algorithm for generating smooth models from electromagnetic sounding data. Geophysics, 52: 289–300.

Conyers LB. 2013. Ground-penetrating radar for archaeology. AltaMira Press.

Dahlin T, Johansson S, Landlin O. 1994. Resistivity surveying for planning of Infrastructure. Proceedings of Symposium on the Application of Geophysics to Engineering and Environmental Problems 27–31 March, Boston, Massachusetts. 509–528.

D'Andrea AC, Manzo, A, Harrower MJ, Hawkins AL. 2008. The Pre-Aksumite and Aksumite settlement of NE Tigrai, Ethiopia. Journal of Field Archaeology, 33: 151-176.

Dolphin LT. 1981. Geophysical methods for archaeological surveys in Israel. Stanford Research International, Menlo Park, Calif..

Eckmeier E. 2020. Remote sensing and soil analysis in the Bora Plain: Soils and sediments in the Dinka Settlement Complex and the surrounding Bora Plain: sampling and new data from 2019, Peshdar Plain Project Publications, 5: 37-43.

Edgerton HE. 1972. Underwater archaeology-Sonar surveys in Greece: MASCA (Museum Applied Science Center for Archaeology, University of Pennsylvania, Philadepphia) Newsletter, 9: 3.

Fassbinder JWE. 2015. Seeing beneath the farmland, steppe and desert soil: Magnetic prospecting and soil magnetism, Journal of Archaeological Science, 56: 85-95. doi:10.1016/j.jas.2015.02.023.

Fassbinder JWE. 2017. Magnetometry for Archaeology. In: Encyclopedia of Geoarchaeology, Encyclopedia of Earth Sciences Series. 499-514. doi: 10.1007/978-1-4020-4409-0.

Fassbinder JWE, Becker H, van Ess M. 2005. Prospections magnétiques à Uruk (Warka). La cité, du roi Gilgamesh (Iraq). Dossiers Archéologie, 308: 20-25.

Fassbinder JWE, Gorka TH. 2009. Beneath the desert soil - archaeological prospecting with a ceasium magnetometer, in New technologies for archaeology. Multidisciplinary investigations in Palpa and Nasca, Peru, First, Natural Science in Archaeology, Reindel M and Wagner GA (eds), Springer, Berlin, Heidelberg: 49-69. doi:10.1007/978-3-540-87438-6_4, ISBN: 978-3-540-87437-9.

Fassbinder JWE, Gorka TH. 2011. Magnetometry near to the geomagnetic Equator, in Archaeological Prospection - 9th International Conference, M.G. Drahor and M.A. Berge (eds), 9: 45-48. ISBN: 978-605-396-155-0.

Fassbinder JWE, Ašandulesei A. 2016. The magnetometer survey of Qalat-i Dinka and Gird-i Bazar, 2015. Peshdar Plain Project Publications, 1: 36-42.

Fassbinder JWE, Ašandulesei A, Scheiblecker M. 2017. Magnetometer prospection at the Dinka Settlement Complex and Gawr Miran, 2016. Peshdar Plain Project Publications, 2: 18-32.

Fassbinder JWE, Ašandulesei A, Scheiblecker M. 2018. The 2017 magnetometer survey of the Dinka Settlement Complex. Peshdar Plain Project Publications, 3: 20-30.

Fassbinder JWE, Ostner S, Scheiblecker M, Parsi M. 2019. Geophysical prospection campaign 2019: Magnetometry and Earth Resistance Tomography (ERT) at the archaeological site of Ur, Iraq (Unpublished report, Directorate of Antiquities, Iraq).

Fassbinder JWE, Ostner S, Scheiblecker M, Parsi M, Van Ess M. 2019. Venice in the desert: Archaeological geophysics on the world's oldest metropolis Uruk-Warka, the city of King Gilgamesh (Iraq), New Global perspectives on Archaeological prospection, 13: 197-200. doi: 10.32028/9781789693072.

Fassbinder JWE, Hahn S, Parsi M., Becker F, Wolf M, Gagošidze I, Kaniuth K. 2021. Persian Residences in the Southern Caucasus: Latest Discoveries in the Periphery of the Achaemenid Empire. Revue d'archéométrie, 45: 117-127. doi: 10.4000/archaeosciences.8404.

Fassbinder JWE, Becker F, Hahn S, Parsi M. 2021. Archaeological Geophysics: Case Studies from Bronze Age/Iron Age Sites in the Alazani and Shiraki Plain, Kakheti, Georgia. In the Caucasus: Bridge between the urban centres in Mesopotamia and the pontic steppes in the 4th and 3rd millennium BC / Der Kaukasus Brücke zwischen den urbanen Zentren Mesopotamiens und der pontischen Steppe im 4. und 3. Jahrtausend v. Chr., Scriften des Archäologischen Museums Frankfurt am Main, vol. 34, edited by Svend Hansen Liane Giemsch: 333-340, Schnell & Steiner. ISBN: 978-3-7954-3439-7.

Finkbeiner U. 1991. Uruk Kampagne 35-37, 1982-1984. Die archäologische Oberflächenuntersuchung (Survey). Mainz.

Furtwängler A, Knauß F, Egold A. 1995. Gumbati. Archäologische Expedition in Kachetien 1994. Eurasia Antiqua, 1: 177–211.

Furtwängler A, Knauß F, Egold A. 1996. Gumbati. Archäologische Expedition in Kachetien 1995. 2. Vorbericht. Eurasia Antiqua, 2: 363–380.

Gamkrelidze IP .1997b. Geology of Georgia. In: Encyclopedia of European and Asian regional geology. 256–261.

Gerlach I. 2017. Neue Forschungen zur äthio-sabäischen Kultur, in: Steffen Wenig - Burkhard Vogt (Hrsg.), In kaiserlichem Auftrag: die Deutsche Aksum-Expedition 1906 unter Enno Littmann. Ethnographische, kirchenhistorische und archäologisch-historische Untersuchungen, Forschungen zur Archäologie außereuropäischer Kulturen, 3: 355–390.

Getaneh A, Haile T, Sernicola L. 2018. Three-dimensional modelling of a pre-Aksumite settlement at the archaeological site of Seglamen, Aksum, northern Ethiopia using integrated geophysical techniques. Archaeological Prospection, 25: 231–241. doi: 10.1002/arp.1705.

Giraud J. 2016. Surface survey of the Dinka Settlement Complex, 2013-2015. Peshdar Plain Project Publications, 1: 29-35.

Griffiths DH, Barker RD. 1993. Two-dimensional resistivity imaging and modelling in areas of complex geology: Journal of Applied Geophysics, 29: 211–226. doi:10.1016/0926-9851(93) 90005-J.

Günther T, Rücker C, Spitzer K. 2006. Three-dimensional Modelling and Inversion of DC Resistivity Data Incorporating Topography-II. Inversion. Geophys. J. Int., 166: 506–517.

Hahn S, Parsi M, Fassbinder JWE. 2022. Challenges and results of the magnetometer surveys in Yeha and Melazo, Ethiopia (In preparation).

Hashemi Z. 2019. The excavations in QID2. Peshdar Plain Project Publications, 4: 59-62.

Hulin G, Maneuvrier C, Tabbagh A, Vincent JB. 2018. What exists beneath the place where Conrad Schlumberger carried out the first (1912) electrical prospection experiment: the Val-Richer Abbey. Near Surface Geophysics, 16: 445-460.

Knauß F. 2000. Der Palast von Gumbati und die Rolle der Achaimeniden im transkaukasischen Iberien. Archäologische Mitteilungen aus Iran und Turan, 32: 119-130.

Knauß F. 2006. Ancient Persia and the Caucasus. Iranica Antiqua Journal, 41: 79-118. doi: 10.2143/IA.41.0.2004762.

Knauß F, Gagoshidze I, Babaev I. 2013. Karacamirli: Ein persisches Paradies. ARTA 2013.004: 1-28.

Le Borgne E. 1955. Susceptibilité magnétique anormale du sol superficiel. Ann. Geophys., 11: 399-419.

Leicher J. 2018. Die Villa Rustica von Peiting: Die Chronik der Wiederauferstehung eines antiken Landgutes.

Lightfoot DR. 1996. Syrian qanat Romani: history, ecology, abandonment. Journal of Arid Environments, 33: 321-336.

Linck R, Fassbinder JWE. 2014. Determination of the influence of soil parameters and sample density on ground-penetrating radar: a case study of a Roman picket in Lower Bavaria. Archaeological and Anthropological Sciences, 6: 93-106.

Loke MH, Barker RD. 1996a. Practical techniques for 3D resistivity surveys and data inversion: Geophysical Prospecting, 44: 499–523.

Loke MH, Barker RD. 1996b. Rapid least-squares inversion of apparent resistivity pseudo-sections using quasi-Newton method: Geophysical Prospecting, 44: 131–152.

Loke MH, Dahlin T. 2002. A comparison of the gauss–Newton and quasi-Newton methods in resistivity imaging inversion. Journal of Applied Geophysics, 49: 149–162. doi: 10.1016/S0926- 9851(01)00106-9.

Loke MH, Chambers JE, Rucker DF, Kuras O, Wilkinson PB. 2013. Recent developments in the direct-current geoelectrical imaging method. Journal of Applied Geophysics, 95: 135-156.

Melikadze G, Jukova N, Todadze M, Vepkhvadze S, Kapanadze N, Chankvetadze A, Jimsheladze T, Vitvar T. 2014. Evaluation of recharge origin of groundwater in the Alazani-Iori basins, using hydrochemical and isotope approaches. Journal of Georgian Geophysical society, 17: 53-64.

McGhee MS, Luyendyk BP, Boegemen DE. 1968. Location of an ancient Roman shipwreck by modern acoustic techniques-A critical look at marine technology. Proceedings of the Marine Technology Society, 4th Annual Conference, Washington, D.C..

Ostner S, Fassbinder JWE, Parsi M, Gerlach I, Japp S. 2019. Magnetic prospection close to the magnetic equator: Case studies in the Tigray plateau of Aksum and Yeha, Ethiopia. New Global perspectives on Archaeological prospection, 13: 180-183. doi: 10.32028/9781789693072.

Papadopoulos NG, Tsourlos P, Tsokas GN, Sarris A. 2006. Two-dimensional and Three-dimensional Resistivity Imaging in Archaeological Site Investigation. Archaeological Prospection, 13: 163–181. doi: 10.1002/arp.276.

Papadopoulos NG, Yi M-J, Kim J-H, Tsourlos P, Tsokas GN. 2010. Geophysical investigation of tumuli by means of surface 3d electrical resistivity tomography. Journal of Applied Geophysics, 70: 192-205.

Parsi M, Fassbinder JWE, Papadopoulos NG, Scheiblecker M, Ostner S. 2019. Revealing the Hidden Structure of the Ancient City Ur (Iraq) with Electrical Resistivity

Tomography, New Global perspectives on Archaeological prospection, 13: 206-208. doi: 10.32028/9781789693072.

Parsi M, Fassbinder JWE. 2020. Remote sensing and soil analysis in the Bora Plain: The 2019 Electrical Resistivity Tomography (ERT) survey, Peshdar Plain Project Publications, 5: 24-37.

Parsi M, Linck R, Fassbinder JW, Eitel M. 2021. Highlighting the Potential of 3D ERT by Comparing its Results with GPR and the Excavation Map of a Roman Building. Revue d'archéométrie, 45: 183-186. doi: 10.4000/archaeosciences.9485.

Piro S, Ceraudo G, Zamuner D. 2011. Integrated geophysical and archaeological investigations of Aquinum in Frosinone, Italy. Archaeological Prospection, 18: 127-138. doi: 10.1002/arp409.

Radner K. 2019c. The Peshdar Plain Project in its fourth year: The 2018 work programme. Peshdar Plain Project Publications, 4: 13-20.

Radner K, Kreppner FJ, Squitieri A. 2017a. Conclusions and future lines of research. Peshdar Plain Project Publications, 2: 176-180.

Radner K, Kreppner FJ. 2019. Conclusions and perspectives. Peshdar Plain Project Publications, 4: 156-159.

Rogers RB, Kean WF. 1980. Monitoring ground water contamination at a fly ash disposal site using surface resistivity methods. Ground Water, 18: 472–478.

Sancisi-Weerdenburg H. 1990. The Quest for an Elusive Empire. In: H. Sancisi-Weerdenburg & A. Kuhrt (eds.), Centre and Periphery: Proceedings of the Groningen 1986 Achaemenid History Workshop. Achaemenid History 4 (Leuven: Peeters, 1990), 4: 263-274.

Sarris A. 2012. Multi+ or Manifold Geophysical Prospection?. Computer applications and Quantitative methods in Archaeology, University of Southampton, in the Conference on Computer Applications and Quantitative Methods in Archaeology, 40: 761-770. e-ISBN: 978-90-4852-728-1.

Schleifer N. 2004. Ghost features: a proposal for appropriate management and a forum for discussion. Newsletter of the International Society of Archaeological Prospection. Bradford, 1: 6–8.

Schlumberger C. 1912. Premières expériences. Carte des courbes équi- potentielles, tracées au courant continu Val-Richer (Calvados). Août- Septembre 1912. Ref 4717, Musée de Crèvecoeur en Auge, Calvados, France.

Schmidt A. 2013. Earth resistance for archaeologists. AltaMira Press (Lanham, New York, Toronto, Plymouth, UK).

Scollar I, Weinder B, Segeth K. 1986. Display of archaeological magnetic data. Geophysics, 51: 623–633.

Scollar I, Tabbagh A, Hesse A, Herzog I. 1990. Archaeological prospecting and remote sensing. Cambridge University Press (Cambridge, New York, Port Chester, Melbourne, Sydney)

Squitieri A, Altaweel M, Amicone S, Herr J-J, Pietsch S, Rohde J. 2020. A Chalcolithic kiln in the Bora Plain, Peshdar Plain Project Publication, 5: 190-200.

Tabbagh A. 2017. Electrical resistivity and electromagnetism. In: A.S. Gilbert, P. Goldberg, V.T. Holliday, R.D. Mandel and R.S. Sternberg (eds.), Encyclopedia of geoarchaeology, 211-219. doi: 10.1007/978-1-4020-4409-0.

Thiesson J, Kessouri P, Schamper C, Tabbagh A. 2014. Calibration of frequency-domain electromagnetic devices used in near-surface surveying. Near Surface Geophysics, 12: 481-491. doi: 10.3997/1873-0604.2014012.

Thiesson J, Gondet S, Fassbinder JWE, Becker F, Scheiblecker M, Ostner S, Parsi M, Bourgois-Esperon S, Kaniuth K. 2019. Magnetic signal prospecting in a former Achaemenid 'palace': the example of Gumbati, 13TH Int. Conf. on Archaeological Prospection Sligo – Ireland. Archaeopress, Oxford, 13: 193-196, doi:10.32028/9781789693072.

Trinks I, Larsson L, Gabler M, Nau E, Neubauer W, Kucera M, Söderberg B, Thoren H. 2013. Large-Scale archaeological prospection of the Iron Age settlement site Uppakra-Sweden. Advancing large-scale high-resolution near-surface geophysical prospection, 183-187.

Tsokas GN, Van de Moortel A, Tsourlos PI, Stampolidis A, Vargemezis G, Zahou E. 2012. Geophysical survey as an aid to excavation at Mitrou: A preliminary report. Hesperia, 81: 383-432.

Tsourlos P, Papadopoulos N, Yi M-J, Kim J-H, Tsokas G. 2014. Comparison of measuring strategies for the 3-D electrical resistivity imaging of tumuli. Journal of Applied Geophysics, 101: 77-85.

Van PV, Park SK, Hamilton P. 1991. Monitoring leaks from storage ponds using resistivity methods. Geophysics, 56: 1267–1270.

Wesenberg B. 1971. Teil III: Die Vorgeschichte der Ionischen Säulenbasis. Beihefte der Bonner Jahrbücher, 32: 87-145.

Woolley CL. 1934-1976. Ur Excavations, vol. 2-10. Oxford University Press.

Wynn JC. 1986. A review of geophysical methods used in archaeology. Geoarchaeology, 1: 245-257.

Yi M-J, Kim J-H, Song Y, Cho S-J, Chung S-H, Suh J-H. 2001. Three-dimensional imaging of subsurface structures using resistivity data. Geophys. Prospect., 49: 483-497.

Acknowledgments

First of all, I want to thank my supervisor, Jörg Fassbinder, who introduced me to this highly exciting topic, guided and supported me through my PhD and trusted my opinion on new ideas. I am very grateful for all the opportunities that he gave me to participate in different conferences and meetings and for all personal growth that I achieved due to our vast number of travels and team works. I have learnt how to collaborate peacefully with several different groups and I am appreciating all of these lessons in my PhD journey.

I want to deeply thank Nikos Papadopoulos, who welcomed me to the institute of IMS-FORTH lab in Greece to teach me about the method, supported me since then, and patiently answered all of my questions in these years. Moreover, I am thankful to the COST action SAGA, which supported me financially for this visit.

I further want to thank Kai Kaniuth, who despite of his busy schedule was always available whenever I had questions, trusted my opinions, vastly helped me to understand the archaeological ideas behind our work and supported me financially.

I would like to thank the Eurasien Abteilung of the German Archaeological Institute (DAI), especially Prof. Svend Hansen, who awarded me with the DAI scholarship, as the first geophysicist who was honored with this scholarship and supported my studies.

I want to especially thank Sandra Hahn, who was my harshest and the most favorite critic and at the same time the best colleague and friend, someone can have. We went through so much together and we grew together. My time during PhD would not be the same if she was not there.

I thank Michael Eitel for all of his helps, brainstorms and proof reads and for being the best office mate someone can imagine. Moreover, I am thankful for all my friends and colleagues, who made my days in the institute more pleasant.

I highly thank my parents, who never doubted the way I took and always supported me. And finally, very special thanks to my fiancé Vincent, for his continuous and unconditional love and support over the last years.